METAL-OXIDE ENRICHMENT AND GAS-PHASE CHARACTERIZATION OF SULFOPEPTIDES USING FOURIER TRANSFORM ION CYCLOTRON RESONANCE MASS SPECTROMETRY

by

Katherine E. Hersberger

A dissertation submitted in partial fulfillment
of the requirements for the degree of
Doctor of Philosophy
(Chemistry)
in The University of Michigan
2012

Doctoral Committee:

Associate Professor Kristina I. Håkansson, Chair
Professor Phillip C. Andrews
Professor Mark E. Meyerhoff
Assistant Professor Brandon T. Ruotolo

To life, love and the pursuit of happiness

ACKNOWLEDGMENTS

This dissertation would not be possible without the help of some of the best scientists, colleagues and friends whom I have met here at the University of Michigan. I would first like to thank Dr. Kristina Håkansson for her mentoring and encouragement throughout this process. I made a very unconventional decision to join her lab at the end of my third year, and I am extremely grateful for her guidance over the past four years to help me achieve my dream. I would also like to thank my committee members, Dr. Brandon Ruotolo and Dr. Phil Andrews for offering their expert advice and ideas for my final project and especially Dr. Mark Meyerhoff for being their every step of the way to help me transition from my previous research environment.

I have had the pleasure to work with so many wonderful people both past and present. First, I would like to thank the former and current members of the Håkansson research group, especially Dr. Natasa Kalli and Dr. Hangtian Song. Dr. Kalli has been a wonderful friend through research and has provided me with guidance and enduring friendship these past years and hopefully many more years to come. Dr. Hangtian Song has been an invaluable colleague and friend for whom it is safe to say that without his help I would not have the hope of earning a doctoral degree. Secondly, I would like to

thank Dr. Masato Koreeda for many, many hours of his advice regarding a slew of synthetic organic reactions that I pursued, some successfully and others not-so-successfully. Finally, I would like to thank Dr. David Clemmer and Dr. Ted Widlanski at Indiana University for their motivational support and academic friendship from my undergraduate to graduate years.

I would also like to thank my friends who have come and gone from the University of Michigan but still remain very close to me. Members of the 2005 incoming class of analytical students (Dr. Laura Zimmerman, Dr. Anna Clark, Dr. Kate Dooley, and Dr. Chris Avery) were and still are the best friends I have ever had. I am not sure where I would be without our Killa-Joules softball team, frequent trips to Wendy's for a midday chocolate Frosty, our freshman lunch hour in the Parisian café (located on the bottom floor of the chemistry building with the "street lamps" and "park benches" as I saw them), and the hours and hours of game nights that formed the backbone of our friendship. Their ongoing support during the good times and the bad offers me a pleasant reminder of how much I value these friends. I especially thank Dr. Kate Dooley for helping me format my thesis and the rest of the 2005 incoming cohort for their continued encouragement and words of wisdom.

As I venture out into the real world of heavily structured work hours and less impromptu beverage breaks, I must also thank those who have given me the opportunity to develop as a teacher. In the past ten semesters of teaching, I have had the pleasure to work with Dr. Nancy Kerner, Dr. Dotie Sipowska, Dr. Amy Gottfried, Dr. Stephen

Maldonado, Dr. Sunil Dourado, Dr. Jian Peng, Dr. Mark Meyerhoff, Dr. Michael Morris, and my advisor Dr. Kristina Håkansson. I especially thank Dr. Meyerhoff and Dr. Morris for their special guidance as I grow more familiar with teaching as a lifelong occupation.

Last but not least, I would like to thank my family and close friends outside the department for their love, patience, and acceptance of me during this difficult period in my life. I am blessed to have my parents, grandparents, sister, and brother cheering me on from start to finish. I am excited to be the first Ph.D. in my immediate and extended family, and I know that my paternal grandparents and love ones who could not see this accomplishment are somewhere smiling down on me. Finally, I would like to thank someone very dear to me who has seen me through the toughest part of my life and still stood by me despite the anxiety, frustration, and the roller-coaster ride that graduate school was for me. Dr. Achilleas Anastasopoulos was my best friend for the past four years, and I will always appreciate the time that we spent together.

Ever since I began graduate school, I thought that the end would never come. Undoubtedly, this was the most trying period of my life, both emotionally and intellectually. I hope that from this moment forward, I can make the best of my experience at the University of Michigan and take pride in who I am and who I have become.

TABLE OF CONTENTS

LIST OF FIGURES

LIST OF TABLES

LIST OF ABBREVIATIONS

3', 5' ADP	Adenosine 3', 5'-diphosphate
ACN	Acetonitrile
ANSA	4-Aminonaphthalene Sulfonic Acid
ApoMb	Apomyoglobin
APTD	Atmospheric Pressure Thermal Dissociation
BSA	Bovine Serum Albumin
CAD	Collision Activated Dissociation
CCK	Cholecystokinin
CCKS	Sulfonated Cholecystokinin
CRL	Caerulein
DEAE-D	Diethylaminoethyl Dextran
DHB	Dihydroxybenzoic acid
DTT	Dithiothreitol
ECD	Electron Capture Dissociation
EDC	1-Ethyl-3-(3-Dimethylaminopropyl)carbodiimide
EDD	Electron Detachment Dissociation
ESI	Electrospray Ionization
ETD	Electron Transfer Dissociatioin
eV	Electron Volt

FT ICR-MS	Fourier Transform Ion Cyclotron Resonance Mass Spectometry
GAGs	Glycosaminoglycans
GPB	Gas Phase Basicity
GPCR	G-Protein Coupled Receptors
GST	Sulfonated Human Gastrin II
HIR	Sulfonated Hirudin
IPA	Isopropanol
IRMPD	Infrared Multiphoton Dissociation
IT MS	Ion Trap Mass Spectrometry
LHRH	Leutinizing Hormone Releasing Hormone
LC	Liquid Chromatography
MAD	Metastable Atom-Activated Dissociation
MALDI	Matrix-Assisted Laser Desorption Ionization
MS	Mass Spectrometry
MS/MS, MS^n	Tandem Mass Spectrometry
m/z	Mass-to-Charge ratio
NETD	Negative Electron Transfer Dissociation
niECD	Negative Ion Electron Capture Dissociation
PAPS	3'-phosphoadenosine-5'-phosphosulfate
PTM	Post-Translational Modification
QIT	Quadrupole Ion Trap
Q MS	Quadrupole Mass Spectrometry

QQQ, QqQ	Triple Quadrupole
RF	Radio frequency
SORI-CAD	Sustained Off-Resonance Irradiation CAD
TEA	Triethylamine
THF	Tetrahydrofuran
TOF MS	Time-of-Flight Mass Spectrometry
TPST	Tyrosylprotein Sulfotransferase

ABSTRACT

METAL-OXIDE ENRICHMENT AND GAS-PHASE CHARACTERIZATION OF SULFOPEPTIDES USING FOURIER TRANSFORM ION CYCLOTRON RESONANCE MASS SPECTROMETRY

by

Katherine E. Hersberger

Chair: Kristina I. Håkansson

Though not as well studied as phosphopeptides, sulfopeptides are important for many biological processes, including proper endocrine function and extracellular signaling. The discovery of sulfopeptides dates back to the 1920s; however, their enrichment and characterization have only recently become of broader interest. With a limited toolbox for analyzing sulfopeptides, we employ several chemistries to develop robust enrichment and characterization methods. At the heart of each method lies Fourier transform ion cyclotron resonance mass spectrometry, a gas-phase detection method with the power to differentiate even the slightest mass differences, such as phosphate vs. sulfonate.

First, Lewis acid-base characteristics inherent to transition metal oxides are examined for the selective interaction and enrichment of sulfopeptides in the presence of mixtures of competing poly-oxyanions. Careful control of the binding and elution pH with an optimized amount of sulfopeptide loaded onto the metal oxide surface can enhance enrichment selectivity of sulfopeptides up to 97% relative abundance compared to as low as 4% prior to enrichment.

Second, the utility of gas-phase activation methods for structural characterization of sulfopeptides is investigated. The sulfonate post-translational modification (PTM) is extremely labile at low pH, high temperature, and during gaseous collisional activation. This fragility has challenged researchers to discover new techniques for analysis of intact sulfonated biomolecules. As recently as 2011, authors have accepted that the sulfonate modification is lost during mass spectrometric analysis. We have found that a combination of different activation techniques can elucidate sulfopeptide sequence while keeping the labile sulfonate residue intact, allowing for unambiguous localization of this PTM. In particular, negative ion electron capture dissociation was found to yield >50% fragmentation efficiency with complete sulfonate retention.

Finally, ideas are explored for improving fragmentation efficiency in electron detachment dissociation, which commonly leads to extensive neutral loss from carboxylic acids, precluding efficient backbone fragmentation and subsequent structural elucidation. To block carbon dioxide loss, chemical derivatization and anion adduction were employed. We found that chloride adduction to acidic peptides improves the

fragmentation efficiency and provides nearly complete sequence coverage for several peptides. In addition, N-acetylation was shown to alter observed fragmentation pathways, presumably through changes in peptide gas-phase structures.

CHAPTER I

Introduction

1.1 Protein Sulfonation

1.1.1 Biochemistry of Sulfopeptides and Sulfoproteins

Sulfonation is the most prevalent post-translational modification (PTM) for tyrosine amino acid residues[1] and is found in all eukaryotes.[2] A wide variety of molecules such as hormones, xenobiotics, carbohydrates, lipids, and proteins can be O-sulfonated,[3] which refers to the transfer of a sulfonate group (SO_3H) to a hydroxyl acceptor.[4]

Specifically, protein tyrosine sulfonation occurs on up to 1% of all tyrosine residues in eukaryotes.[5] It is one of the last PTM events to occur in the Golgi apparatus in cells.[1] In all animal species analyzed to date, this process is highly regulated by two membrane-associated enzymes: tyrosylprotein sulfotransferase (TPST) 1 and 2 that catalyze the transfer of a sulfonate group from a specific donor molecule (3'-phosphoadenosine-5'-phosphosulfate, PAPS) to a tyrosine residue, as shown in Figure 1.1.[3-4, 6-7*] In animals TPSTs are trans-membrane proteins that are located near the trans-

[*] This transfer is often misconstrued in the literature as the transfer of a sulfate group (SO_4^{2-}), and the substrate is considered "sulfated." For the sake of consistency and accuracy, this thesis refers to the presence of SO_3H/SO_3^- on peptides as the chemically accurate sulfonate group and the modified peptides are referred to as sulfonated peptides or sulfopeptides.

Golgi network.[8-11] Furthermore, the active site of the TPSTs is directed toward the lumen within the Golgi apparatus,[8] which may explain why precursors to sulfonated species must be closely

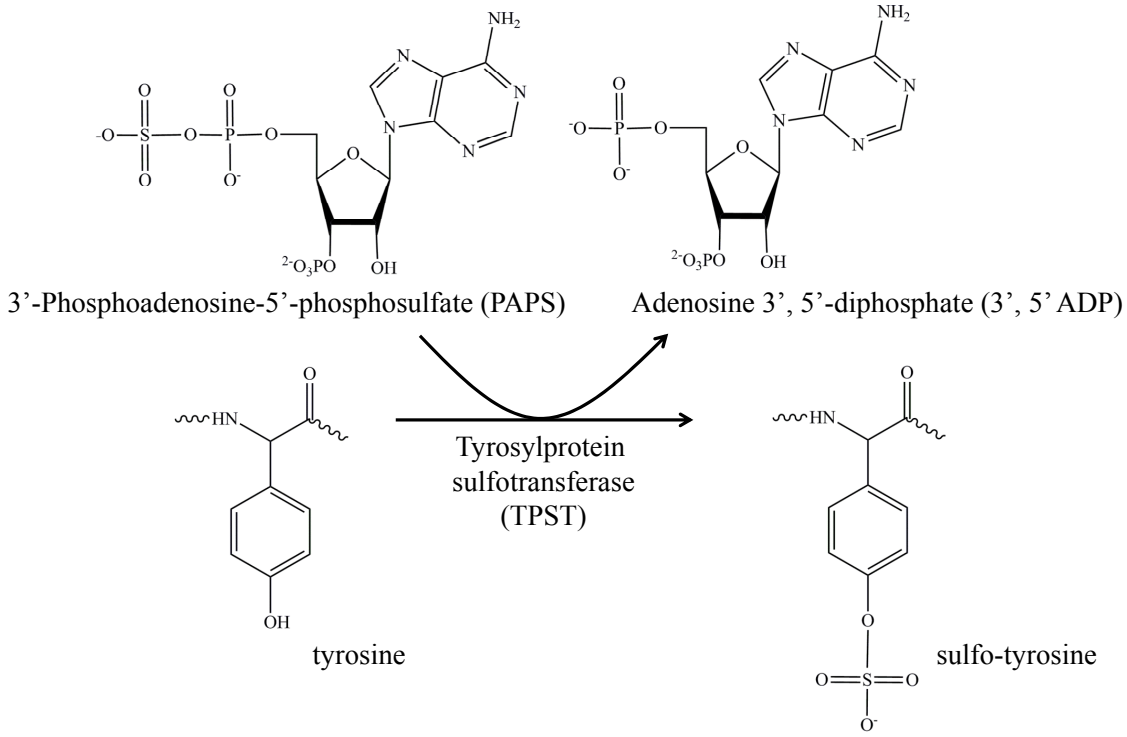

Figure 1.1. Enzyme-mediated tyrosine sulfonation of peptides and proteins. Image modified and recreated from Corbeil and Huttner[12] and Stone, et al.[13]

associated with this organelle. The Golgi apparatus, specifically the trans-Golgi network, acts as a post-translational processing, sorting and packaging center that receives and processes proteins and peptides synthesized in the rough endoplasmic reticulum then sorts and sends the processed biomolecules to their final destinations. Transportation throughout the cell is provided by secretory granules that deposit few sulfonated biomolecules within the cell or through the cell membrane while transporting the majority of sulfonated species into the extracellular matrix. These sulfoproteins and sulfopeptides are membrane or secretory in nature[7, 14] with the latter kind accounting for

approximately 65–95% of the total protein tyrosine sulfonation.[1, 15] Furthermore, proteins and peptides destined to be sulfonated for membrane-related or secretory function must originate from the rough endoplasmic reticulum in order to pass through the trans-Golgi network in close proximity to the TPST enzyme and sulfonate donor molecule PAPS. It has been proposed and observed experimentally that cytoplasmic, nucleoplasmic, as well as mitochondrial proteins and peptides are not sulfonated *in vivo*.[1, 14] TPSTs are also thought to be strictly localized to the trans-Golgi network, except for a single case in which TPST was found in human saliva.[16]

1.1.2 Vertebrate Sulfopeptides and Sulfoproteins

The very first sulfonated protein, fibrinogen, was discovered by Bettelheim in 1954.[17] Other sulfonated species began to surface in the literature throughout the 1960s.[18-22] However, it was not until 1982, nearly three decades after the initial sulfoprotein discovery, that the potential biological significance of sulfonation was first suggested by W. B. Huttner in his *Nature* report describing that tyrosine sulfonation is a widespread modification found in all tissues of all multicellular organisms examined.[23] Since this monumental discovery, researchers have found that the biological activities of sulfonated proteins and peptides are quite diverse despite the theorized limited localization for these species as mentioned above. Moore has compiled a comprehensive list of over sixty tyrosine-sulfonated proteins and peptides from seventy-five different sources, suggesting that the functional role(s) of tyrosine sulfonation for the majority of the identified sulfonated species are currently unknown.[7†] In this reference, the author categorizes sulfonated proteins and peptides by either a similar functional role, in the case

[†] This lack of knowledge may be due to the fact that there are little or no available non-sulfonated analogs for which to compare the function or loss-of-function of a particular species *in vivo*.

of G-protein-coupled receptors (GPCRs), or a similar localization such as matrix proteins. Several sulfonated proteins and peptides, such as cholecystokinin, gastrin and caerulein from the gastrin family[21, 24-28 29-32 18, 20, 22, 33] as well as hirudin[34-35] have been studied extensively for decades and are very well characterized. Several sulfoproteins and peptides have been characterized in hemostasis,[34, 36-40] inflammatory response,[41-43] protein-protein interactions,[36, 44-45] as well as hormone regulation[24-25] and certain diseases.[46-49]

1.1.3 Invertebrate Sulfopeptides and Sulfoproteins

From the 1980s–2000s, sulfopeptide discoveries in plants, insects, and other invertebrates suggest that sulfonation is not just a widespread PTM present in vertebrate animals. Some of these invertebrate sulfopeptides include phytosulfokine from asparagus (*Asparagus officinalis*) and rice (*Oryza sativa*),[50-51] pherophorins from green algae (*Volvox carteri*),[52-53] sulfakinins[54-55] and vitellogenins[5, 56] from fruit flies (*Drosophila melanogaster*), leucosulfakinins from cockroaches (*Leucophaea maderae*)[57-58] and CCK/gastrin homologs from roundworms (*Caenorhabditis elegans*)[59] among other discoveries from crustaceans and insects.[60]

Functional characterization of sulfonated peptides from invertebrates suggests a wide variety of functions similar to those of vertebrate-derived sulfopeptides. In the first report of sulfonated plant hormones, Matsubayashi and Sakagami showed that sulfonated tyrosine residues in the doubly-sulfonated phytosulfakinin-α and –β promote rapid growth of asparagus mesophyll cells.[50] These rather short sequences (penta- and tetra-peptide sequences, respectively) do not strictly follow the suggested guidelines for sulfonation observed in animal species,[1, 61-64] perhaps indicating a different mechanism

for sulfonation in plants. Other examples of sulfopeptides that promote growth include the pherophorins and a membrane glycoprotein from green algae. During green algae embryogenesis, differentiation of the indeterminate embryo into somatic and reproductive cells (asexual, male or female spheroids) occurs at the 32-cell division upon which a specific pheromone "sexual inducer" influences the further differentiation of reproductive cells into egg and sperm.[52-53] It was postulated by Wenzl and Sumper[65] that a cell-surface component was needed to provide information to the cells regarding the embryo's stage of division. In their later work, this group discovered the sulfonated membrane glycoprotein SSG-185[66] that may control cell-cell interactions during embryogenesis but prior to differentiation.[52] Lee, et al.[67] have shown that rice produces a sulfonated peptide near the N-terminus of a large protein called Ax21 (activator of gene XA21-mediated immunity). The active peptide axY^{S}22 requires tyrosine sulfonation for immunity against the bacterium *Xanthomonas oryzae*.[67] Sulfopeptides from the cholecystokinin (CCK)/gastrin family, which includes the sulfakinins found in fruit flies and cockroaches and the CCK/gastrin homologs found in roundworms, share a common C-terminal active sequence motif with CCK and gastrin and, thus, exhibit a similar function.[5, 57-59] More importantly, tyrosine sulfonation is critical for optimal activity of these peptides.

Another recent discovery from Medzihradszky, et al.[68] marks the first observation of serine- and threonine-sulfonated peptides from invertebrates. The identification of HTTNV[I/L]SMFR (sulfonation site not indicated) from myosin light chain and LAGLQDEIGS(SO_3H)LR, both from an intermediate filament protein digest from the nerve axoplasm of the freshwater snail *Lymnaea stagnalis*, as well as RIEVALT(SO_3H)K from the *Plasmodium falciparum* malaria parasite suggests that sulfonation may be more

widespread than originally thought.[23] This finding opens up a once-narrow field that focused only on tyrosine-sulfonated species and poses many unanswered questions about the production and biological function of these peptides.

Not until recently did researchers understand how plant hormones were sulfonated. Matsubayashi, et al.[69] reported the first plant TPST, which shares no sequence homology with animal TPST-1 or TPST-2. The newly discovered TPST from *Arabidopsis thaliana* (mouse-ear cress) contains acidic amino acids in close proximity to the tyrosine residue, which is thought to be indicative of tyrosine sulfonation.[1]

1.1.4 Cholecystokinin/Gastrin

The Cholecystokinin/Gastrin family of proteins includes caerulein[20, 22] as well as the namesake sulfoproteins gastrin[18, 24, 32] and cholecystokinin[21, 25] plus cionin.[70‡] Each of these proteins contains a similar pentapeptide sequence at the C-terminus of the active peptide. This common pentapeptide C-terminal sequence (GWMDF-NH_2) is critical for proper biological activity and has been conserved over 500 million years,[71] having descended from coelenterates.[72-73] Cholecystokinin and gastrin are involved in regulation of enzyme secretion and stimulation of growth in the adult gastrointestinal system.[46, 74] As regulators of growth, gastrin and cholecystokinin have also been associated with cancer progression. For an extensive review on this subject, see Rehfeld et al.[46] as well as Rozengurt, et al.[75] and references therein. Another interesting development in this area suggests that cholecystokinin could play an important role in satiation and, thus, appetite

‡ The sulfakinins as well as FMRF-amide neuropeptides are not included in this family due to differences in the conserved pentapeptide sequence observed compared to that of the gastrin/cholecystokinin family. For more details, please refer to Johnsen and Rehfeld, Cionin: a disulfotyrosyl hybrid of cholecystokinin and gastrin from the neural ganglion of the protochordate *Ciona intestinalis*. In *J. Biol. Chem.*, 1990; Vol. 265, pp 3054-3058. However, others consider the sulfakinins part of the gastrin/CCK family due to similar responses from sulfakinins to gastrin/CCK antisera. See Nachman, Holman, Haddon and Ling, Leucosulfakinin, a sulfated insect neuropeptide with homology to gastrin and cholecystokinin. In *Science*, 1986; Vol. 234, pp 71-73.

suppression.[76-78] Thirty years ago, Kissileff, et al. showed that intravenous administration of the active N-terminal region of the cholecystokinin peptide (CCK-8) in man resulted in decreased food intake up to nearly 20%.[76] Follow-up analyses of the satiation effects of CCK-8 and its potential use as a supplement have been discussed,[77] but to our knowledge, there have been no recent developments for treatment of this kind to be used by consumers.

For this particular family of sulfonated hormones, the presence of sulfonation is required for proper biological activity. For instance, non-sulfonated CCK exhibits significantly lower hormonal activity than its sulfonated counterpart[56, 79] while desulfonated caerulein does not properly inhibit acid secretion in the presence of gastrin nor does it stimulate gallbladder contraction to the same degree as its sulfonated counterpart.[80-81] Of the aforementioned sulfopeptides, cionin is the only doubly-sulfonated species with back-to-back sulfonated tyrosines,[70] which is observed for only one other sulfopeptide found in the white shrimp *Litopenaeus vannamei*.[82] The function of cionin is similar to that of CCK and gastrin, though it is reported to exhibit activity more closely related to CCK,[83-84] while the biological significance of two sulfonation sites in a single active peptide is still unknown.

1.1.5 Hirudin

Hirudin is a naturally-occurring, 65-amino acid polypeptide extracted from the salivary glands of the leech *Hirudo medicinalis*.[34, 85-89] It was first reported in the late 1800s that a compound contained in medicinal leeches (later known as hirudin) acts as an anticoagulant.[90-91] Since then, researchers have been able to propose a mechanism for preventing blood coagulation with hirudin as an inhibitor. Markwardt, et al. reported that

hirudin binds to and inhibits thrombin,[91-93] a serine protease responsible for the enzymatic digestion of fibrinogen into fibrin. Though the full hirudin sequence is over 60 amino acids long, not all of the sequence is required for biological activity. In fact, the acidic residues of the C-terminal sulfonated dodecapeptide are critical for binding hirudin to thrombin.[86, 88] Specifically, when hirudin residues 59-65 or more (up to 22 residues in total) were eliminated by enzymatic digestion, there was a reduction in the inhibition of clotting activity by up to 90%.[86] If the acidic C-terminal region of this polypeptide is included in its native form, the activity is unaffected. The author concludes that this acidic region is important for facilitating binding to the recognition site of thrombin. Interestingly, this article also reports that sulfonation is not required for this interaction, but total thrombin inhibition activity decreased by a factor of two without tyrosine sulfonation.[86]

1.1.6 Methionine- and Leucine-Enkephalin

Another distinct family of peptides is the enkephalins, which are found in the brain and gastrointestinal tract of a variety of species as well as in the skin of amphibians.[94] Satoh, et al. first suggested that the endogenous "morphine-like" agonist, later known as enkephalin, could be an inhibitory neurotransmitter.[95] These particular peptides bind to opioid receptors in the brain in a similar way as morphine and other opioid drugs to regulate pain and pleasure.[96-101] Extensive reviews on this subject are available from Erspamer[94] and Amiche, et al.[102]

1.1.7 Recent Discoveries in Sulfopeptide and Sulfoprotein Characterization

Within the past ten to fifteen years, exciting discoveries regarding the function of sulfonated GPCRs[103-106] and chemokine receptors[47, 107-111] have reinvigorated research in

functional characterization of sulfonation. GPCRs are transmembrane hormone-binding receptors that contain a large ectodomain with one or more sulfonated tyrosine residues.[13] It has been shown in several cases, regardless of the final function of the signaling event, that sulfonated tyrosines are critical for the binding of the agonist to its receptor.[104-106] Sulfonated chemokine receptors bind small, secreted proteins called chemokines that mediate the movement of leukocytes and the immune system response to viral infection.[36, 112] In the past fifteen years, several authors report that the tyrosine-sulfonated chemokine receptor CCR5 with help from the CD4 glycoprotein binds HIV-1 protein gp120 (a 120 kDa glycoprotein in the HIV envelope), allowing the virus to enter cells.[107-109, 113] More recently, Kwong, et al. published the structures of the unbound and bound sulfonated CCR5 to gp120,[110] elucidating the sulfonation site through a conserved binding pocket in the V3 loop of gp120. Though these specific results illustrate how structure and function are related, the majority of the reports cited here do not present a complete story. This lack of finality further highlights the need to continue efforts for sulfonated protein and peptide structural and functional characterization.

1.1.8 Trends for Identifying Potential Sulfonation Sites on Peptides and Proteins

Following the structural characterization of many sulfonated proteins and peptides, much attention was focused on how to predict whether a protein or peptide will be sulfonated in a biological system. Figure 1.2 shows several well-known sulfopeptides from the CCK/gastrin family that share a common C-terminal pentapeptide sequence. Striking similarities such as these and others prompted further investigation. In the 1980s-1990s, the existence of consensus features for detecting sulfonated proteins and peptides was a hotly debated area,[1, 61-64] in which no true consensus features were ever

discovered but trends were suggested to explain observations of sulfonation events. With the discovery of more sulfonated proteins and peptides from a variety of plant and animal

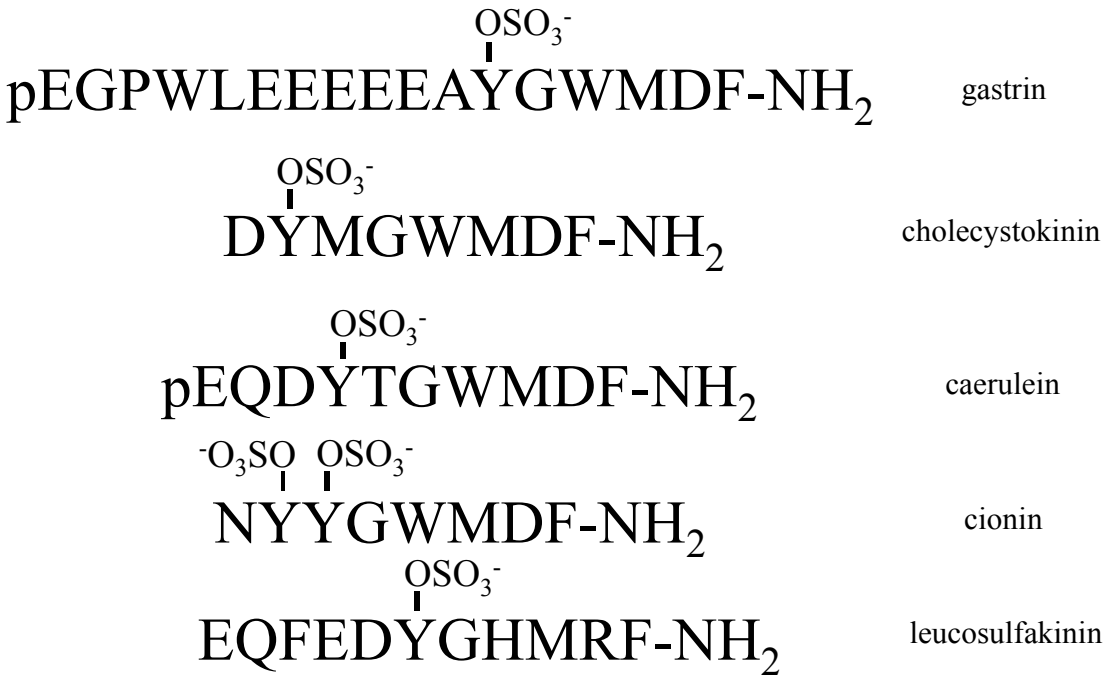

Figure 1.2. Sequences of cholecystokinin-related sulfonated peptides.

sources throughout the 1990s[5, 50, 54, 57-58, 70, 99, 114] and most recently in 2009,[67] it is clear that there are still no definitive consensus features that aid in identifying *all* sulfonated peptides/proteins. However, there are several guidelines, widely accepted though also disputed, for suggesting which tyrosine residue(s) may be sulfonated. In 1986, Hortin, et al.[63] laid the foundation for the major trends observed for a short list of common sulfonated peptides. His investigation utilized computational algorithms to predict sulfonation sites. Hortin and many others have since concluded that no single trend could stand alone to predict sulfonation sites but the combination of these features would lead to the most accurate prediction. In later years, several researchers refined, questioned,

and further extended these trends. Several structural features that may promote tyrosine sulfonation are summarized in the text below. It is important to note that the amino acid positions within a given peptide are relative to the site of sulfonation, which is assigned as position 0. All residues N-terminal and C-terminal to position 0 are assigned -1 to -x and +1 to +y, respectively, where x, y are the total number of residues away from the sulfonation site in either direction.

Acidic amino acid residues are common but not required in the region from -5 to +5. Most but not all sulfonated peptides contain acidic amino acid residues in the region from -5 to +5. In many cases, there is either an aspartic or glutamic acid residue directly N-terminal to the site of sulfonation at position -1. This trend is seen for all sulfopeptides in the cholecystokinin/gastrin family with the exception of doubly-sulfonated cionin. Initially, Hortin, et al. reported that acidic residues were required at position -1 or -2 and there should be three or more acidic residues from -5 to +5 with only a few exceptions lacking Asp/Glu at -1 or -2 but complying elsewhere.[63] Four years later, this assertion was rebuked with the discovery of cionin[70] as it contains only one aspartic acid at position +4/+5 to the sites of sulfonation (see Figure 1.2 for sequence information.). However, the experimental support for the original hypothesis[115] suggesting the importance of acidic residues and their position relative to the sulfotyrosine residue appeared a few years later in 1992.[61] Lin, et al. have shown that removal of acidic residues at various positions relative to the sulfonation site from cholecystokinin, complement C_4, heparin cofactor II, and α_2-antiplasmin decreases the peptide substrate's affinity for the TPST enzyme by up to 22-fold.[61] These authors further reported that TPST interacts with more than 4-5 residues on either side of the sulfotyrosine, and

specifically, positions -1 and +1 are important for determining the peptide's affinity for TPST. Furthermore, site-directed mutagenesis of human gastrin has shown that replacing a neutral or acidic residue at position -1 with a basic residue completely inhibits sulfonation.[62] Thus, one important aspect has remained unchallenged. There have been 0-1 basic residues and a low occurrence of hydrophobic residues (Ile, Leu, Phe, Val) observed within five residues of the sulfonation site.[1]

Turn-inducing amino acid residues are observed near the sulfonation site. Initially, turn-inducing amino acid residues such as proline or glycine can be observed near the sulfonation site as long as the sulfonation site is accessible to TPST, sulfonation can occur.[63] That is, the residues in close proximity to the sulfonation site do not induce a complex secondary structure that may sterically hinder TPST's access to the tyrosine residue. This hypothesis was later refined by Huttner, who suggested that either one turn-inducing Pro/Gly or at least two moderate turn-inducing Asp/Ser/Asn residues should be included from -2 to -7 and from +1 to +7 relative to the sulfonation site.[1] He proposed that turn-inducing amino acids could possibly enhance exposure of the nearby tyrosine to TPST.

No PTMs that may induce steric hindrance are found near the sulfonation site. Along the same theoretical lines as with turn-inducing amino acids mentioned above, PTMs such as cysteine disulfide bond linkages and N-linked glycans may alter the secondary structure near the tyrosine sulfonation site.[1] These modifications, however, are not observed. Because these PTMs are incorporated in the protein sequence prior to sulfonation, they may act to sterically hinder TPST access to nearby tyrosine residues.

Recent computational efforts to predict sulfonation sites have shown promise in this area. SulfoSite[116] as well as Sulfinator[117] and a new nearest neighbor algorithm from Niu, et al.[118] provide up to 90% prediction accuracy. Though the development of computational models for predicting sulfonation sites is a step in the right direction, a prediction accuracy of 90% may result in missed or incorrectly assigned sites. Furthermore, one fact remains: sulfonation site prediction alone cannot validate the occurrence of tyrosine sulfonation. Other methods for isolation and identification of sulfopeptides from biological systems are thus needed.

1.1.9 A Chemical Juxtaposition: Sulfonation vs. Phosphorylation

Post-translational modifications such as phosphorylation ($R\text{-}OPO_3H_2$) and sulfonation ($R\text{-}OSO_3H$) are critically important for the proper function of proteins, metabolites, sugars, and other biomolecules. Although phosphorylation and sulfonation are negatively-charged PTMs with an identical nominal mass (80 Da), there is not much else in common between them from a chemical and biological standpoint.[119] The sulfonate group consists of a single sulfur atom and three oxygen atoms, two of which participate in π-bonding to the sulfur atom. Consequently, sulfonates can exhibit only one negative charge from the single sulfur-oxygen σ-bond at a pH value greater than its pK_a value of 1.5[4] while phosphonate groups have two ionizable protons with pK_a values of 1.5 – 1.9 and 6.3 – 6.8 depending on the character of the variable substituent.[120]

Sulfonation has also been found to be less stable than phosphorylation in solution-phase reactions[17] and gas-phase electrospray ionization tandem mass spectrometry (ESI-MS/MS) reaction conditions.[103] The sulfonate group is cleavable in 1 N HCl[17] or with >90% TFA at high temperatures.[121] Furthermore, sulfonation can be accidentally

hydrolyzed during sulfopeptide synthesis following common deprotection steps which require acid.[103] Careful control of the reaction conditions during peptide deprotection can minimize the amount of sulfonate hydrolysis that occurs.[121] Phosphorylation, on the other hand, is much more chemically resilient to highly acidic, solution-phase conditions and is removed primarily with phosphatases or alkali hydroxides.

From a biological standpoint, sulfonation is an irreversible PTM which is conferred on a peptide/protein sequence as one of the last events to occur in the trans-Golgi network prior to transport out of the cell.[122] Phosphorylation, on the other hand, is a reversible modification added to peptide/protein sequences and functions primarily inside the cell. Given the differences in origin and localization of these PTMs in multicellular organisms, one can postulate that their functional paths are divergent. Indeed, phosphorylation is implicated in regulation of intracellular cytosolic and nuclear protein activities while sulfonation is involved in extracellular protein-protein interactions.[103]

1.1.10 Challenges of Peptide/Protein Sulfonation Analysis

The identification and characterization of sulfonation in biological systems is hampered by the following: 1) sulfonate instability to heat and low pH, 2) low concentration of sulfonated species present only outside the cell, and 3) the isobaric mass of sulfonate compared to phosphorylation. Since the discovery of the first sulfonated protein in the 1950s,[17] there have been reports indicating that the sulfonate group is hydrolyzed above 90 ^{o}C under acidic conditions.[121, 123] This lability presents a problem as many enzymatic digestion procedures for bottom-up proteomics approaches require high temperatures ($\geq$90 ^{o}C) to effectively denature the wide range of proteins present in a

given sample. Furthermore, some derivatization procedures such as methyl esterification[124] require concentrated, strong acids or produce them as a by-product of the reaction. If sulfonation is present on the peptides or proteins of interest, alternative derivatizations must be used to prevent SO_3 loss. At present, no published reports suggest to what degree the sulfonate group is lost from the original biomolecule at milder temperatures and slightly less acidic pH values.

Secondly, sulfonated peptides and proteins are mainly found outside of the cell as secreted species,[1, 125] rendering common cellular fractionation approaches and cell lysate profiling improbable for determining the degree of sulfonation in biological systems. Despite these adverse conditions, scientists have been able to identify sulfonated peptides, proteins, and glycans in plasma[78, 126] and in the retina.[127-128] For example, Young, et al. quantified the amount of endogenous sulfonated cholecystokinin in hamster plasma and used their immunoprecipitation-based liquid chromatography method to monitor the changes in basal levels of CCKS after administering a high-fat diet.[78]

Perhaps the most difficult task is differentiation of sulfonated and phosphorylated species by mass. Mass spectrometry (MS) is a powerful tool that measures mass-to-charge ratios of gaseous ions. Due to the isobaric nature or identical nominal mass of 80 Da for the sulfonate group compared with the more widely characterized phosphate group, misidentifications are possible with relatively low mass resolution instruments.[129] These PTMs differ only slightly by mass, specifically less than a one-hundredth of an atomic mass unit ($\Delta m = 0.0095$ Da).[130] This narrow difference arises from the mass difference between a hydrogen atom plus a phosphorous atom for phosphorylation (HPO_3^-, 79.9663 Da) versus a sulfur atom for sulfonation (OSO_3^-, 79.9568 Da). It may be for these several

reasons that sulfonation is less studied by the scientific community at large in favor of the more accessible, more widely characterized, and chemically resilient phosphorylation.

1.1.11 Qualitative and Quantitative Methods for Determining Sulfonation without the use of Mass Spectrometry

In the past 60 years since the first sulfopeptide was discovered, there have been only a few non-MS-based methods for sulfonation analysis, including both qualitative and quantitative approaches. In the mid-20th century, radioactive labeling with ^{35}S provided the only option for direct determination of tyrosine sulfonation in specimens from biological systems for many years and is still widely used today. Once incorporated, the labeled sulfo-tyrosine residues are separated from other proteins and carbohydrates by a lengthy procedure involving a series of fractionation steps prior to phenol extraction, SDS-PAGE, and detection by autoradiography.[123] A few problems with this approach include the difficulty and cost of conducting cell culture labeling methods *in vitro* as well as the number of complicated steps required to effectively separate and detect ^{35}S-labeled sulfopeptides. Also, direct localization of the tyrosine sulfonation site is not possible with this method.

Perhaps the most promising method for determining sites of sulfonation on proteins, peptides, and other biomolecules without the use of mass spectrometry involves using anti-sulfo-tyrosine antibodies to selectively bind sulfo-tyrosine residues. Initially, sulfopeptides of greater than 10 amino acid residues were needed to raise high-quality antibodies.[131] However, because these antibodies cannot be produced in most animals due to the animal's lack of an immune response to the common sulfo-tyrosine PTM, alternative methods have been suggested. Recently, two reports indicate that anti-sulfo-tyrosine antibodies raised from *in vitro* phage display methods have shown high

selectivity over phospho-tyrosine residues.[132-133] However, these two approaches require both time and a considerable amount of money to generate these specialized antibodies. Furthermore, these aforementioned methods cannot measure the accurate mass of large, complex sulfonated biomolecules, nor can these methods precisely determine the location of the sulfonate group in the protein or peptide sequence. For these reasons, mass spectrometry holds much promise for the complete characterization of sulfonated biomolecules.

1.2 Mass Spectrometry

1.2.1 Mass Spectrometry as a Method for Detection of Sulfopeptides

Mass spectrometry (MS) is a technique that measures the accurate mass-to-charge (m/z) ratios of gas-phase ions. The first mass spectrometer (known at the time as a parabola spectrograph) was built in 1912 by J. J. Thomson to measure the m/z values of various diatomic and low molecular weight gases with mass resolution of ~13 m/Δm.[134] This effort was soon followed by A. J. Dempster's 180^{o} magnetic sector instrument equipped with an electron ionization source developed in 1918, at which time the mass resolution was 100 m/Δm.[135] As technology developed rapidly in the 1950s and 1960s and electrospray ionization was later introduced in the 1980s,[136] mass spectrometers paved the way for analyzing larger molecules—from mass-to-charge ratios ranging from a few Daltons to greater than 20,000 Da over 20 years ago. Today, the largest attainable mass resolving power ($m/\Delta m_{FWHM}$) is obtained with Fourier transform ion-cyclotron resonance mass spectrometry (FT ICR-MS), e.g., 8,000,000 at a mass of ~8600 Da.[137] Another recent report from Nikolaev, et al. shows that a redesign of a traditional FT ICR trapped ion cell involving segmentation of the cylindrical surface of the ICR cell can

produce a resolving power ($m/\Delta m_{FWHM}$) of 24,000,000 for reserpine at m/z 609.[138] This improvement in resolving power was due only to the redesign of the ICR cell and not due to an increase in magnetic field strength.

Current mass spectrometers contain three essential regions following sample introduction: an ionization source, a mass analyzer, and a detector. Samples can be introduced into the gas-phase from either the liquid phase (as in electrospray ionization or ESI)[136] or the solid phase (as in matrix-assisted laser desorption/ionization or MALDI).[139] Analytes must be ionized to be guided through the instrument for detection. MS instruments operate at very low pressure compared to atmosphere (10^{-3} to 10^{-10} mbar) in order to transfer ions to the detector, avoiding collisions and possible subsequent fragmentation events. Many MS instruments including quadrupole MS (Q MS), time-of-flight MS (TOF MS), and ICR MS differ in how ions are separated and subsequently detected. Briefly, Q MS and ICR MS require time-varying electric fields or a static magnetic field, respectively, to manipulate and thus differentiate ions with varying mass-to-charge ratios while TOF MS requires a field-free drift region for ions of identical kinetic energy to be separated based upon individual m/z values. Current instrumentation in mass spectrometry varies quite widely for the intended application and desired instrument attributes. High mass accuracy, high mass resolution, high sensitivity, large dynamic range, and fast detector response time (duty cycle) are all desirable features of mass spectrometers. Unfortunately, all of these advantages cannot be realized simultaneously in a single instrument; thus, a compromise must be met. Quadrupoles, for example, are inexpensive, relatively fast-scanning mass analyzers that are commonly used for single ion monitoring as well as collision-activated fragmentation events, but

these mass analyzers typically have an upper m/z limit of approximately 4000 and provide only unit resolution of 1 Da,[140] which cannot differentiate phosphorylation and sulfonation ($\Delta m = 0.0095$ Da). TOF MS instruments, on the other hand, have no m/z limit, very high sensitivity and extremely fast detection[140] but also cannot provide a mass resolution great enough to routinely differentiate sulfonation and phosphorylation. Furthermore, ion trap mass spectrometry (IT-MS) and TOF-MS instruments are usually equipped to perform only collision activated dissociation (CAD) fragmentation, which leads to sulfonate loss in both positive and negative ion modes.[§] A few instruments that provide the best combination of attributes for differentiating sulfonation from phosphorylation occurrence in biological samples are Orbitrap™ and FT-ICR MS instruments. The latter instrument provides the highest mass accuracy and highest mass resolution of any mass spectrometer that is now commercially available. These two attributes enable accurate and intact mass differentiation between isobaric phosphorylation and sulfonation, which cannot be attained with other MS instruments. Additionally, FT-ICR MS instruments are capable of performing a variety of fragmentation techniques, which allows for further investigation of the structural properties of sulfonated peptides. These techniques are discussed in detail in Sections 1.2.4 and 1.2.5.

1.2.2 Fourier-Transform Ion Cyclotron Resonance Mass Spectrometry

Ion cyclotrons were first used in the early 20th century to accelerate elementary particles such as protons in order to investigate physical properties of the nucleus.[141] E.

[§] It is important to note that while CAD is the most common fragmentation technique for IT and TOF-MS instruments, some IT-MS instruments can now be modified to incorporate the ion-ion fragmentation technique of electron-transfer dissociation in positive (ETD) and negative (NETD) ion mode. These techniques are discussed in more detail in Section 1.2.5.

O. Lawrence first reported that protons introduced into a magnetic field could be accelerated to kinetic energies in excess of $1x10^6$ eV without the use of high voltages. In fact, he applied high frequency oscillations (requiring no more than 4000 V) to opposing electrodes positioned normal to an applied magnetic field in order to accelerate ions multiple times as they repeatedly passed by these electrodes on an orbit bent into a circular path by the magnetic field.[141] The applicability of ion cyclotron resonance (ICR) to mass spectrometry was first realized in 1949 by Sommer, et al.,[142] and the first application of Fourier transformation in ICR MS was presented in 1974 by Comisarow and Marshall.[143] Even then, the impact of this technique was not immediately realized due to the high cost and complicated yet required electronics. However, there has been a steady growth in the interest of using ultra-high mass resolution FT-ICR MS instruments. As mentioned above, two clearly advantageous benefits above all other MS instruments are the high mass accuracy and high mass resolution. A 7 Tesla (T) FT-ICR instrument that offers a resolution of 1,000,000 at m/z 400 can separate a mass-to-charge ratio of 400.0000 from 400.0004. Furthermore, the resolution increases with the strength of the magnetic field,[144] which can range from as small as 3 T to as large as 25 T. The high mass accuracy of this instrument results from precisely measuring the frequencies of ion motion in the cyclotron region. A detailed explanation of this phenomenon is included in the following section.

In FT-ICR MS, ion motion and subsequent ion separation is influenced by both a magnetic field and an electric field. A magnetic field is used to measure ion orbital frequency for mass-to-charge ratio determination while an electric field is used to trap the ions axially in the detection region. The total force exerted on an ion is equal to the sum

of the forces exerted by the magnetic and electric fields (Equation 1.1). To calculate the magnetic field component, we consider an ion placed in a magnetic field. The ion will move perpendicular to the magnetic field and experience a Lorentz force** perpendicular to both its direction of motion (i.e., its velocity vector) and the direction of the magnetic field as shown in Figure 1.3 and represented in Equation 1.2.[144] Thus, its motion will be

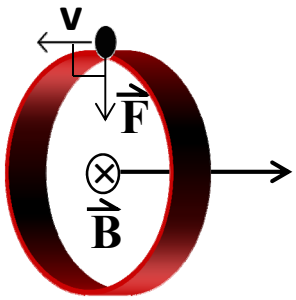

Figure 1.3. Cartoon representing motion of a negative ion in a magnetic field. The ion is shown as a black circle while its orbit is a red and black circle with the Lorentz force, magnetic field and velocity indicated. Note that motion of a positive ion will be reversed.

"bent" into a circular path, and it will orbit at a specific frequency (cyclotron frequency) which can be very accurately measured. For a stable ion trajectory with a circular orbit, the force exerted by the magnetic field must also be equivalent to Equation 1.3. By equating these expressions and substituting an expression for angular frequency (Equation 1.4), we find that the frequency at which an ion orbits in a magnetic field depends only upon the magnetic field and the mass-to-charge ratio (Equation 1.5). The departure from velocity dependence differentiates ICR-MS from all other MS-based techniques and offers ICR-MS an upper hand on mass accuracy—so long that ions of the

** Note that the Lorentz force is a downward force toward the center of the ICR cell and is the centripetal force in this cyclic motion.

$$\vec{F}_{total} = \vec{F}_E + \vec{F}_B = q\vec{E} + q(\vec{v} \otimes \vec{B})$$

Equation 1.1

$$F_B = qvB$$

Equation 1.2

$$F_B = \frac{mv^2}{r}$$

Equation 1.3

$$\omega_c = \frac{v}{r}$$

Equation 1.4

$$\omega_c = \frac{q}{m} B$$

Equation 1.5

same or similar cyclotron frequency are detected simultaneously. From this equation, we can also see that the angular frequency is inversely proportional to the m/z of a particular ion. Thus, ions with smaller m/z ratios will orbit at a higher frequency in the cell compared to larger m/z ratios. Because the lighter and the heavier ions have different cyclotron frequencies, they will resonate with different applied excitation frequencies. This resonance is discussed in more detailed later in this section.

The second component of the total force in Equation 1.1 belongs to the force exerted by the electric field, which can be represented simply by the elemental charge multiplied by the electric field vector. This additional contribution to the force exerted on an ion also affects its motion. Ions in an ICR MS instrument have three types of motion simultaneously in the cell—axial oscillations, cyclotron motion and magnetron

motion.[145] First, axial oscillations correspond to the movement of ions back and forth along the axis of the magnetic field (z-axis) as influenced by the trapping potentials applied to the end plates of the analyzer cell (see Figure 1.4). As described earlier, cyclotron motion refers to the tight, circular orbit of ions influenced by the magnetic field in the ICR cell (Equation 1.5) while magnetron motion refers to the movement of ions about a central axis (z-axis) within the ICR cell due to combined electric and magnetic fields.[144] Specifically, the magnetron motion reduces the measurable cyclotron frequency due to electric field repulsion of the ion radially toward the outer edges of the analyzer cell. The outward force from the electric field directly opposes the inward Lorentz force

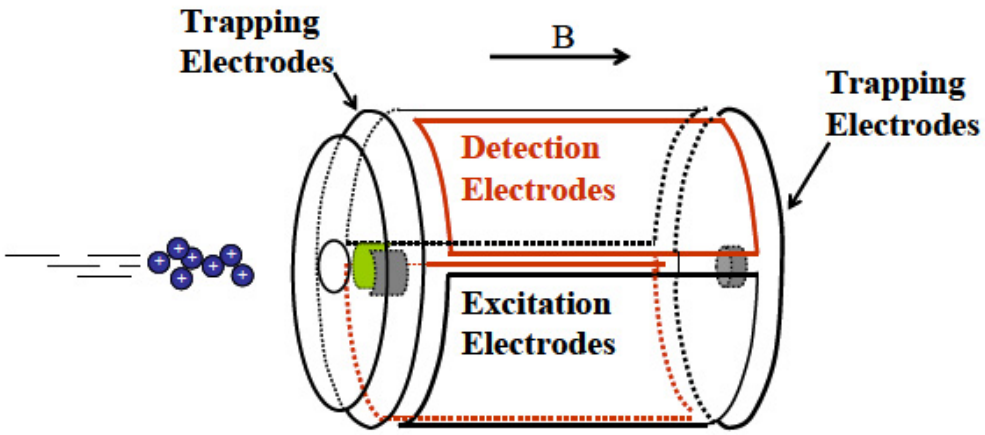

Figure 1.4. Illustration of a cylindrical ICR cell. Trapping plates are placed perpendicular to the axis of ion motion prior to ion entry into the cell. Detection and excitation electrodes are placed 180° out of phase (alternating) on the outer walls of the cell.

discussed earlier, thus generating an additional ion orbit about the z-axis of the ICR cell.[146] One way to imagine the combination of these ion motions is to compare them to the movement of the moon around the Earth and the Earth around the sun. Figure 1.5 shows how these motions are similar yet not the same. It is important to note that

experimentally, magnetron frequencies are much smaller compared to cyclotron frequencies (1–100 Hz vs. 5000–5 x 10^6 Hz, respectively). Because magnetron motion has no analytical utility,[144] reducing its influence on the cyclotron motion and subsequent ion detection is desirable to maintain high mass accuracy. When considering ion motion in a magnetic field, magnetron motion can cause a shift in the measurable cyclotron frequencies. For this reason, calibration is used to reduce the frequency shift caused by magnetron motion by taking into consideration the applied electric field voltage.[147] Another way to reduce magnetron motion is to reduce the axial displacement of ions upon entry to the analyzer by keeping the sidekick voltages as close to zero as possible and using the lowest possible electric field.

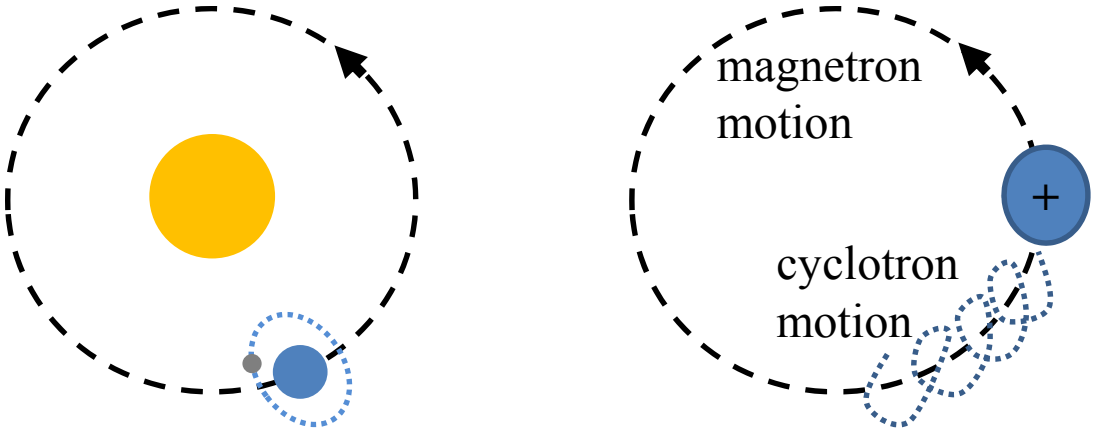

Figure 1.5. Cartoons representing the difference between cyclotron motion (blue dotted line) and magnetron motion (black dotted line) of ions in an ICR MS instrument. The cartoon on the left draws an analogy from the orbit of the moon (grey) around the earth (blue) and the orbit of the earth around the sun (yellow). It is important to note that the ratio of the orbits of magnetron motion to cyclotron motion is exaggerated here for visualization.

Experimentally, ions are introduced from either a matrix-assisted laser desorption ionization (MALDI) source under vacuum or an atmospheric pressure ionization source such as electrospray ionization (ESI), which is used exclusively in this thesis. In the ESI process, charged analyte droplets generated from the electrospray source undergo a

cascade of fission events due to Coulomb repulsion after solvent evaporation reduces the overall size of the droplets. The fission events continue until the smallest stable unit is achieved (i.e., a single analyte ion containing a single charge or multiple charges commonly from protons or the loss of protons) or until ion evaporation occurs from the droplets.[148]

Following ESI, gas-phase ions are guided through a hexapole-quadrupole-hexapole region prior to ion focusing and entry to the ICR cell (see Figure 1.6). Briefly, hexapoles contain six parallel rods in pairs of two while quadrupoles contain four parallel rods in two pairs of two. These pairs of rods are connected electrically by a direct current. A superimposed alternating current is applied 180^{o} out of phase to excite or resonate with ions of a chosen m/z ratio. The first hexapole serves as a focusing region to guide ions into the quadrupole, which can act as a highly selective mass filter or as an additional focusing region (radio-frequency [RF] only mode). The chosen m/z ratio will be guided through the quadrupole without energetic collisions whereas ions of other m/z ratios will have an unstable trajectory and will not be detected. The second hexapole can be operated as a focusing region or a collision cell, where ions fragment after colliding with an inert gas such as helium or argon of a higher pressure (10^{-3} mbar). This tandem mass spectrometry (MS/MS) fragmentation technique, referred to as collision activated dissociation (CAD),[149] is discussed in more detail in Section 1.2.4. Ions are then focused using a series of optical lenses and accelerated through the magnetic field into the ICR cell.

As mentioned earlier, ion motion is "bent" into an orbit around the magnetic field due to a balance of centripetal and centrifugal forces for stable ion trajectory. To detect

ions, radio frequencies in resonance with a large range of cyclotron frequencies (also known as a frequency sweep or "chirp") or a single frequency must be applied to excite ions to orbit closer to the detection plates positioned at the outer walls of the ICR cell. The RF voltage applied will provide resonant energy to a particular m/z ratio, causing the ion to orbit the cell in an increasingly larger radius until it can be imaged by a detector. The detector is composed of a pair of opposing electrodes which are offset by 90° from a pair of excitation electrodes. An image of the fast-moving ions is captured as a change in electrical current at the surface of the detection electrode as a function of time without relying upon collision of the ions into a detector.[††] This non-destructive method of detection, also used in Orbitrap™ instruments, allows for multiple rounds of excitation and detection, increasing the overall sensitivity of the instrument. The detection process is repeated for the entire m/z range of interest by scanning the range of radio frequencies appropriate for exciting ions in the ICR cell. The image signal, or transient, is the time-domain signal that results from the digital conversion of an analog signal corresponding to all the detected frequencies and their respective amplitudes.[144] A transient may contain from 32,000 data points (low resolution) up to 1.24 million data points (high resolution) acquired over fractions of a second or several seconds. To obtain frequency-domain data, the mathematical algorithm of Fourier transform (FT) is applied by instrument software to convert time-domain to frequency-domain signal, and the frequency data are converted to m/z values and displayed in a mass spectrum of ion abundance versus m/z.

[††] It is important to note that while ions in ICR-MS do not collide into a device for detection, they may undergo collisions with other ions, which will decrease the time-domain signal as a function of time. The average duration of a time-domain signal is on the order of seconds.

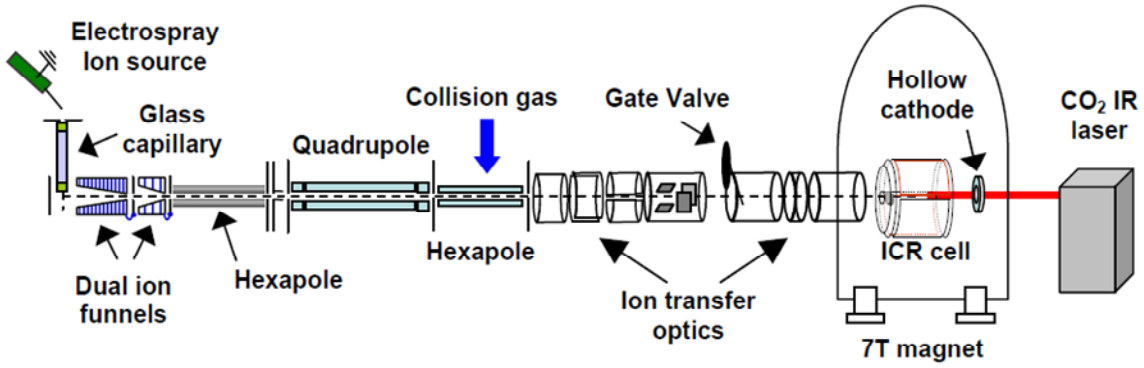

Figure 1.6. Schematic of Bruker APEX-Q™ FT-ICR MS instrument.

In this thesis, two commercially available FTMS instruments, the Bruker APEX-Q™ and Bruker solariX™, were used to collect all MS and MS/MS data. Figure 1.6 shows a schematic of the APEX-Q™ instrument, which is a 7T hybrid Q-h-FT ICR-MS instrument equipped with an Apollo II ESI source and a indirectly heated hollow dispenser cathode for generating electrons during ion-electron activation. The solariX™ is a newer, modified design similar to the APEX-Q™ but contains a split octopole prior to the quadrupole for allowing transfer of ion-ion activation reagents for negative- and positive-ion mode electron-transfer dissociation. Additionally, the ion transfer optics have been replaced by a transfer hexapole prior to ion entry to the ICR cell. The latter instrument is also equipped with a standard electrospray source as well as a hollow dispenser cathode for ion-electron reactions.

1.2.3 Tandem Mass Spectrometry

In single-stage mass spectrometry detection, intact mass-to-charge (m/z) ratios are measured without providing additional information regarding the primary structural identity of the ion. Tandem mass spectrometry (or MS^n, where n is the number of stages of subsequent mass spectral detection) allows the researcher to probe the primary

structure or sequence of the original ion. Each stage of mass spectrometric detection is preceded by a fragmentation event in order to whittle away at the analyte structure. There are several ways to fragment a biomolecule, but each of these falls into two widely recognized classes, vibrational activation and electronic activation. These two classes differ by how they induce dissociation of chemical bonds in the gas phase.

1.2.4 Vibrational Activation with CAD

Vibrational activation methods, such as low-energy CAD[149-150] and infrared multi-photon dissociation (IRMPD),[151] impart upon the ion a relatively low energy, which is then redistributed evenly amongst all bonds. This energy redistribution causes the bonds to vibrate until one or more of the weaker bonds becomes unstable and the ion dissociates. It is important to note that the vibrational activation process is thought to occur much faster than dissociation.[152] In CAD, the additional energy is imparted from collisions of the analyte ions with a relatively high pressure of inert helium or argon gas ($1 – 2 \times 10^{-3}$ mbar) whereas in IRMPD, an infrared laser irradiates the analyte ion, which absorbs a quantized amount of energy that is then redistributed amongst all bonds. When employing vibrational activation methods, the weakest bonds dissociate, which in positive ion mode peptide and protein activation correspond to amide backbone bonds. This fragmentation leads to formation of *b* and *y*-type ions with occasional fragmentation at specific amino acid side chains for positive ion mode CAD while negative ion mode CAD can be more complicated.[153-154] Figure 1.7 highlights the commonly observed cleavage points within the backbone of a peptide for different fragmentation techniques. For vibrationally activated fragmentation, my work utilized negative ion mode CAD only.

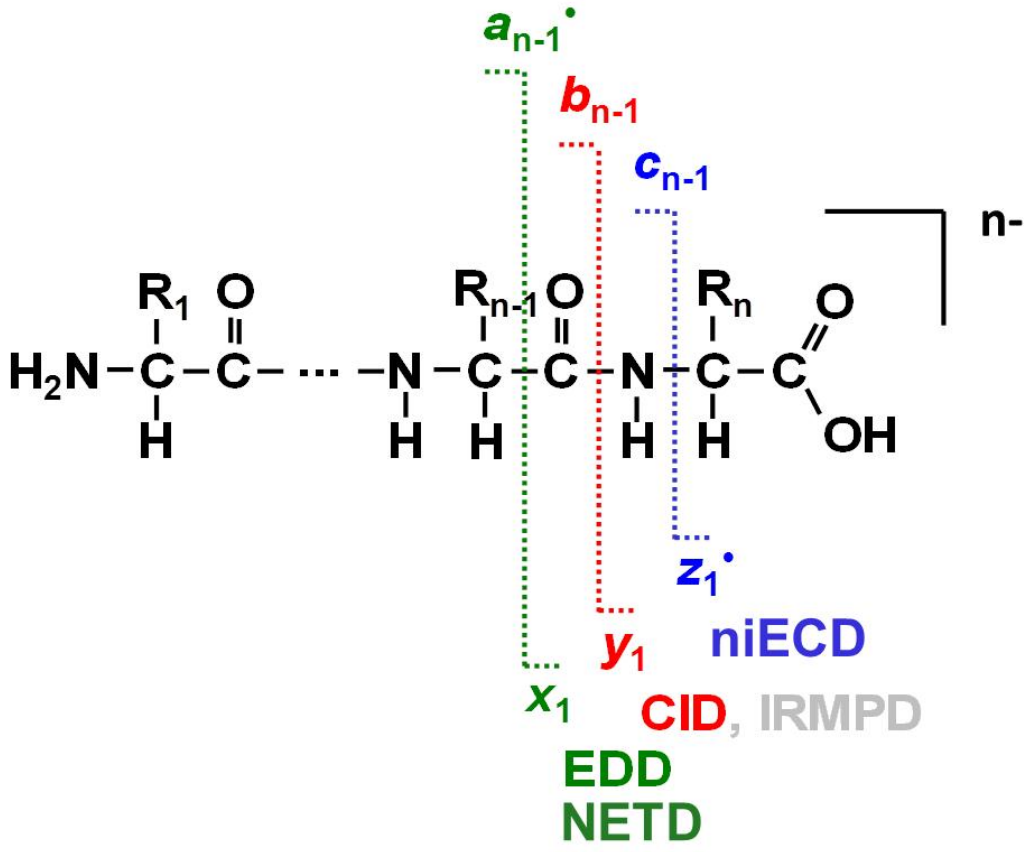

Figure 1.7. Illustration of a generic peptide sequence with dotted lines indicating the location and identity of product ions formed using various types of activation techniques. The acronyms given for these techniques are discussed in Sections 1.2.4 – 1.2.5.

Bond cleavage in negative ion mode peptide CAD is less predictable, and the fragmentation spectra are usually more complicated than in positive ion mode.[154] In fact, product ions corresponding to *a*, *b*, *c*, *x*, *y*, *z* and internal pieces of the precursor ions are observed in negative ion mode CAD[155] while positive ion mode commonly produces *b*- and *y*-ions only. Furthermore, dominant neutral loss from amino acid side chains can lead to reduced structural information. Out of the twenty amino acids naturally occurring in the human body, sixteen exhibit some form of neutral loss in negative ion mode CAD, making it difficult to interpret spectra.[154] Furthermore, there are several ways in which

backbone fragmentation can occur in negative ion mode. Bowie, et al. suggest that a mobile proton, which is important in positive ion mode fragmentation,[156] could also play a role in the formation of enolates to promote *b*- and *y*-ion formation in negative ion mode.[‡‡154] The important conclusions that can be drawn from these reports are the following: 1) backbone fragmentation most commonly results in C-terminal y-ions which may contain the negative charge at the terminal carboxylic acid;[154] 2) backbone cleavage at Asp/Glu[157] and Asn/Gln residues is very abundant and is frequently accompanied by neutral loss of H_2O and NH_3, respectively;[158] 3) amino acid side chain cleavage at Ser/Thr produces dominate neutral losses of CH_2O and CH_3CHO, respectively;[159] and 4) N-terminal loss of pyroglutamic acid resulting in a characteristic *y*-ion occurs for relatively short peptides (4 – 6 residues).[160]

As discussed above, side chain losses represent common, and sometimes very abundant, fragmentation pathways in negative ion mode CAD. Other side chains that could potentially be lost during CAD are acidic post-translational modifications such as sulfonation as well as CO_2 from carboxylic acids. Boontheung, et al. report that the sulfopeptide caerulein 2.2 [pEQDY(SO_3H)TGAHFDF-NH_2, where pE = pyroglutamic acid] electrosprayed in negative ion mode retains the sulfonate group during ESI yet not completely.[161] It is possible that this particularly labile group could be lost during ion transfer from a higher pressure region of the source to a lower pressure region, e.g., while passing through the nozzle, skimmers, or ion funnels. The fragmentation of ions in this region is referred to as "in-source" or "nozzle/skimmer dissociation."[162] To reduce in-source fragmentation and retain the sulfonate group, source conditions such as the

‡‡ These authors propose a new, yet confusing, notation for negative ion mode fragmentation pathways. Here, we will refer to the original notation first published by Biemann and Scoble, Characterization by tandem mass-spectrometry of structural modifications in proteins. In *Science*, 1987; Vol. 237, pp 992-998.

voltages applied to the first ion funnel and the second skimmer must be carefully tuned (personal findings). Of the sulfonate-retaining precursor ion peaks in MS mode, very few if any remain following CAD. Boontheung, et al. report that the most abundant fragment observed after CAD of the aforementioned peptide corresponds to the desulfonated caerulein 2.2 parent ion with a single backbone fragmentation peak observed.[161]

For acidic peptides, the likely sites of deprotonation are carboxylic acids in the side chains of aspartic and glutamic acids as well as the C-terminus.[163] Following CAD fragmentation of acidic peptides, cleavage is frequently observed at or near the site of negative charge,[164] which may lead to neutral loss of CO_2 if carboxylic acids are deprotonated. Ewing and Cassady observed abundant CO_2 loss following sustained off-resonance irradiation (SORI) CAD of triply- and quadruply-deprotonated peptide precursors.[155] These authors and others propose that sidechain carboxylates can promote fragmentation through cyclization of the precursor.[155, 164] Another interesting feature of CAD fragmentation is the influence of charge state on fragmentation efficiency. A particular trend of improved CAD fragmentation efficiency as a function of increasing charge state has been observed in positive ion mode for large proteins[165-167] as well as negative ion mode CAD of peptides.[155] Higher charge-state peptides and proteins should exhibit higher coulombic energy than lower charge-state peptides and, thus, require less applied energy for efficient dissociation.[155] It is important to note, however, that the location of the charge also plays a critical role in fragmentation efficiency. Summerfield and Gaskell reported that highly acidic groups such as cysteic acids can sequester the negative charge, thus driving CAD fragmentation away from the backbone and towards the amino acid side chain.[157] Despite these shortcomings, CAD remains the most

commonly used technique for fragmenting ions in tandem mass spectrometry albeit mostly in positive ion mode due to the fragmentation pattern predictability and compatibility with common liquid chromatography solvents used in high-throughput proteomic analyses.

1.2.5 Ion-Electron and Ion-Ion Activation Methods

Mass spectrometers that can perform vibrational activation methods such as CAD have been commercially available since the 1970s. However, a relatively new class of fragmentation methods employing ion-electron and ion-ion reactions is emerging. Figure 1.8 shows the different types of ion-electron and ion-ion reactions and organizes these by the charge state required for each reaction. In several cases, more than a single charge is inherently required for these particular fragmentation mechanisms to work. In general, *ion-electron* reactions require the irradiation of an ion of either positive or negative charge with electrons of varying energy whereas *ion-ion* reactions require a charge transfer of either an electron or a proton to an ion of positive or negative charge, respectively.

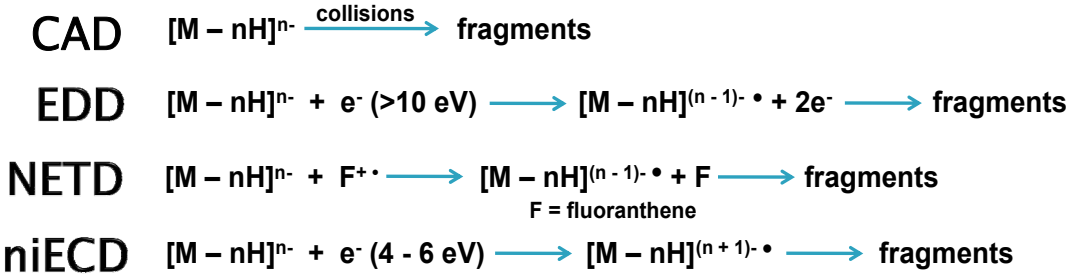

Figure 1.8. Vibrational, ion-electron, and ion-ion activation methods used for negative ion mode analysis.

In electron detachment dissociation (EDD), multiply charged anions interact with high-energy electrons (> 10 eV) to detach an electron from the analyte, producing an

odd-electron, charge-reduced species. This interaction forms a highly energetic, unstable radical ion which fragments, often at a backbone C_α–C bond N-terminal to the radical site,[168] to form $a^\bullet$ and *x* ions (Figure 1.9).[§§168, 170-172] The fact that an electron is detached from the analyte limits what charge states are compatible with EDD: only negative charge states of greater than 2^- can generate charged product ions. The first report of EDD by Budnik, et al.[170] shows that fragmentation of the doubly-deprotonated sulfonated peptide caerulein, which normally loses SO_3 in positive ion mode MS as well as in positive and negative ion CAD, resulted in SO_3 retention in most product ions. However, neutral loss of CO_2 and SO_3 was also observed.

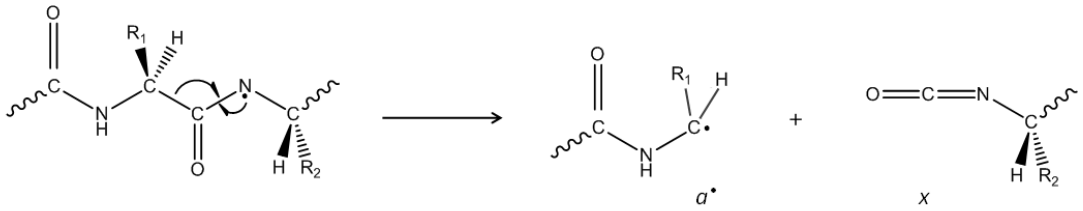

Figure 1.9. EDD fragmentation mechanism modified from References 168 and 170.

The proposed mechanism for this reaction suggests that the high-energy electron interacts with the negatively charged analyte to detach an electron and form a positively charged radical site. This site acts as a sink to which an electron can be transferred from a nearby location that has a low-energy electron, mostly from likely a deprotonated carboxylate[173] or a deprotonated backbone amide. Budnik, et al. suggested that electron irradiation is energetic enough that electron detachment could occur from carboxylates and/or a backbone amide as their ionization energies (3.3 eV, ~8.5 eV, respectively)[170, 174]

[§§] In the first reference in this series, the authors initially propose N—C_α bond cleavage due to observed *a*, *c* and *z*-ions. It was later shown by the same authors that C_α—C bond cleavage is the predominant cleavage in EDD. However, there are additional reports that suggest EDD is a radical-initiated yet charge-*remote* fragmentation process. For additional information, please refer to Laskin, Yang, Lam and Chu, Charge-remote fragmentation of odd-electron peptide ions. In *Anal. Chem.*, 2007; Vol. 79, pp 6607-6614. and references therein.

are much lower than the incident electron energy (> 10 eV).[170] The energy released from this recombination of the positively charged radical and the transferred electron ($\simeq$ 5 eV)[175] corresponds to the difference between the energy cost of forming the radical site and the electron affinity of the carboxylate that lost the electron. This amount of energy is more than sufficient to cause electronic excitation and subsequent fragmentation of the charge-reduced analyte ion. However, one caveat is that electron detachment at or near a carboxylate results in facile loss of CO_2,[168, 170-171] which is a low-energy pathway. This fragmentation behavior differs from electron capture dissociation (ECD) of protonated precursors in that one of the lowest energy pathways is loss of acidic sulfonation.[176] Because EDD occurs much faster than vibrational techniques such as CAD, the excess energy does not have time to dissipate throughout the peptide, thus leaving PTMs intact as is evidenced by sulfonation[170] and phosphorylation retention in peptide EDD fragments[168, 177] as well as sulfonate retention in fragments from oligosaccharides.[178] Recently, Ganisl, et al. have shown that top-down EDD can fragment large, intact acidic proteins of nearly 150 residues.[179] These reports suggest that there are many more possibilities for structural characterization using EDD.

In negative electron transfer dissociation (NETD), a multiply deprotonated analyte ion transfers an electron to a radical cation of high electron affinity to generate a charge-reduced, odd-electron radical anion which fragments into EDD-like $a^{\bullet}$ and x ions (Figure 1.10). In their initial discovery, Coon, et al. used xenon cations to withdraw electrons and promote radical formation for subsequent fragmentation.[180] These authors proposed that the resulting radical site following electron abstraction could be an acidic site such as a side-chain carboxylate that abstracts $H^{\bullet}$ from a nearby amide nitrogen

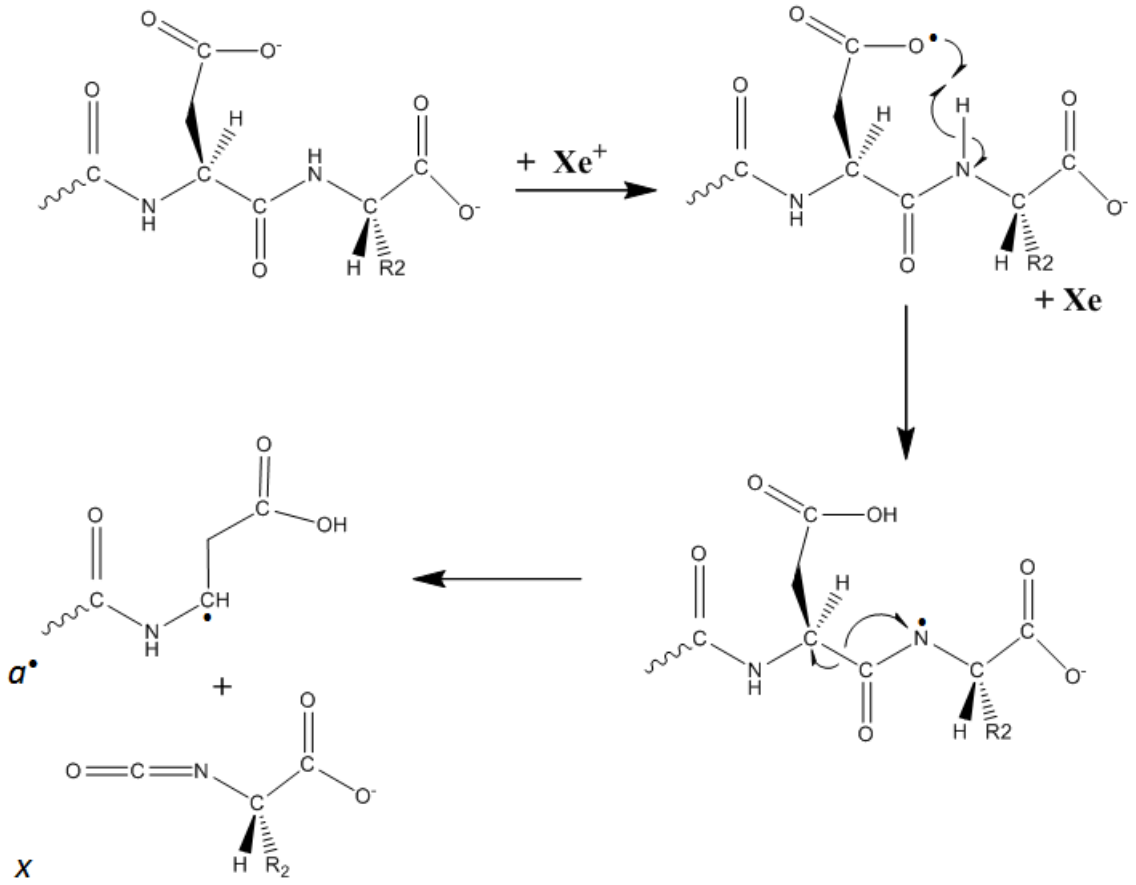

Figure 1.10. NETD mechanism modified from Reference 178.

to affect rearrangement into $a^{\bullet}$ and *x* ions. This mechanism is similar to EDD in that it involves charge reduction by electron abstraction at an acidic site on the peptide, whether that be part of a PTM, a side chain of an amino acid residue, or the C-terminal carboxylate. Also, both mechanisms suggest that these processes are charge-directed events in which cleavage of the C_{α}—C bond(s) is realized after proton transfer from the amide nitrogen to the neutral radical site.[168, 180] Because NETD proceeds through a similar mechanism as EDD with simply a different method for electron abstraction, similar neutral losses are expected. Indeed, loss of CO_2 is a dominant pathway in NETD; however, the difference in excess energy following ion activation is far less in NETD

than in EDD, allowing different reaction pathways to be realized.[180] Recently, Huzarska, et al. reported that the use of $Xe^{+\bullet}$ radical cations can impart too much energy from the electron abstraction (transfer) process, leading to neutral loss of CO_2 and H_3PO_4 from phosphopeptides.[181] These authors found that use of a fluoranthene radical cation ($C_{16}H_{10}^{+\bullet}$) with a lower electron affinity, thus a lower initial ionization potential for the corresponding neutral, than $Xe^{+\bullet}$ imparts less recombination energy for fragmentation (2.5–4.5 eV for $C_{16}H_{10}^{+\bullet}$ vs. 6.7–8.7 eV for $Xe^{+\bullet}$), allowing for less complex spectra due to reduced neutral loss.[181***] In other work, Wolff, et al. applied NETD to sulfonated glycans, specifically glycosaminoglycans (GAGs).[178] Both glycosidic and cross-ring cleavages were observed, albeit with some neutral loss of CO_2 and SO_3. Sulfonate loss could be reduced by using the gentler fluoranthene radical, fragmenting higher charge state ions, or adding sodium ions. The latter of these three suggestions is in direct contrast to the second recommendation and can reduce the overall signal in negative ion mode. These authors also reported that, despite the advantage of conducting NETD in an inexpensive ion trap, the relatively low mass resolution of an ion trap can preclude reliable interpretation of the MS/MS spectra.[178]

In negative ion electron capture dissociation (niECD), a negatively charged analyte ion captures a relatively low energy electron (4.5–6.5 eV) to form a charge-*increased* radical species which fragments at N—C_α bonds, producing c' and $z^\bullet$ ions analogous to those formed in positive ion mode ECD.[182] This seemingly improbable technique is believed to work for zwitterions of overall negative charge for m/z ≥1000.[182] What is particularly exciting about this m/z range is that it includes many acidic, post-

*** These authors also note that not all of the calculated excess energy is imparted to the analyte ion. Some of the energy will be carried off with the neutralized electron-transfer reagent.

translationally modified peptides such as phospho- and sulfopeptides, which are difficult to analyze in both positive and negative ion modes as discussed earlier. Furthermore, this is the first report of a negative ion-electron activation method that can actually increase the charge state of the fragment ions. Increased charge is of great interest for ion detection in ICR instruments because the generated image current is proportional to charge;[183] thus, there is enhanced signal for higher charge states and possibly a better chance of detecting low abundance product ions using this technique.

1.2.6 Primes and Dots: Keeping Track of Hydrogens and Electrons in MS/MS

Roepstorff and Fohlman devised the first and still most widely used nomenclature for peptide fragmentation.[184] In this report, they highlight the *b*- and *y*′-ion fragments which are the most frequently observed ions following positive ion mode CAD of peptides. As discussed above in Section 1.2.5, electronic activation methods provide highly complementary product ions to those observed following vibrational activation. Specifically, *a*, $a^{\bullet}$, *b* (to some degree), *c*′, *x*, *y*′, $z^{\bullet}$, and *z* – 2H ions can be observed in EDD, NETD, and niECD. Therefore, it is extremely important to keep track of the addition or subtraction of hydrogens and electrons in MS/MS product ions. Radical $a^{\bullet}$ ions differ from even-electron *a*-ions by one additional $H^{\bullet}$ (or hydrogen atom), making the radical ion ~1.00837 Da heavier than an even-electron ion. The primes (′) common in *c*′- and *y*′-ions indicate that the *c*- and *y*-ion contain an additional hydrogen atom, which does not confer a charge on the peptide.

In Figures 1.9 and 1.10, we can see that cleavage in ion-ion and ion-electron activation methods very closely resembles homolytic cleavage. Figure 1.11 shows product ion structures with the appropriate notation (including a prime for one additional

hydrogen atom or a dot for a single-electron radical site) for a hypothetical tripeptide. It can be seen that $a^{\bullet}$ ions complement even electron *x*-ions in EDD and NETD while *c*′ ions with an additional hydrogen atom complement $z^{\bullet}$ radical ions in niECD. In vibrational

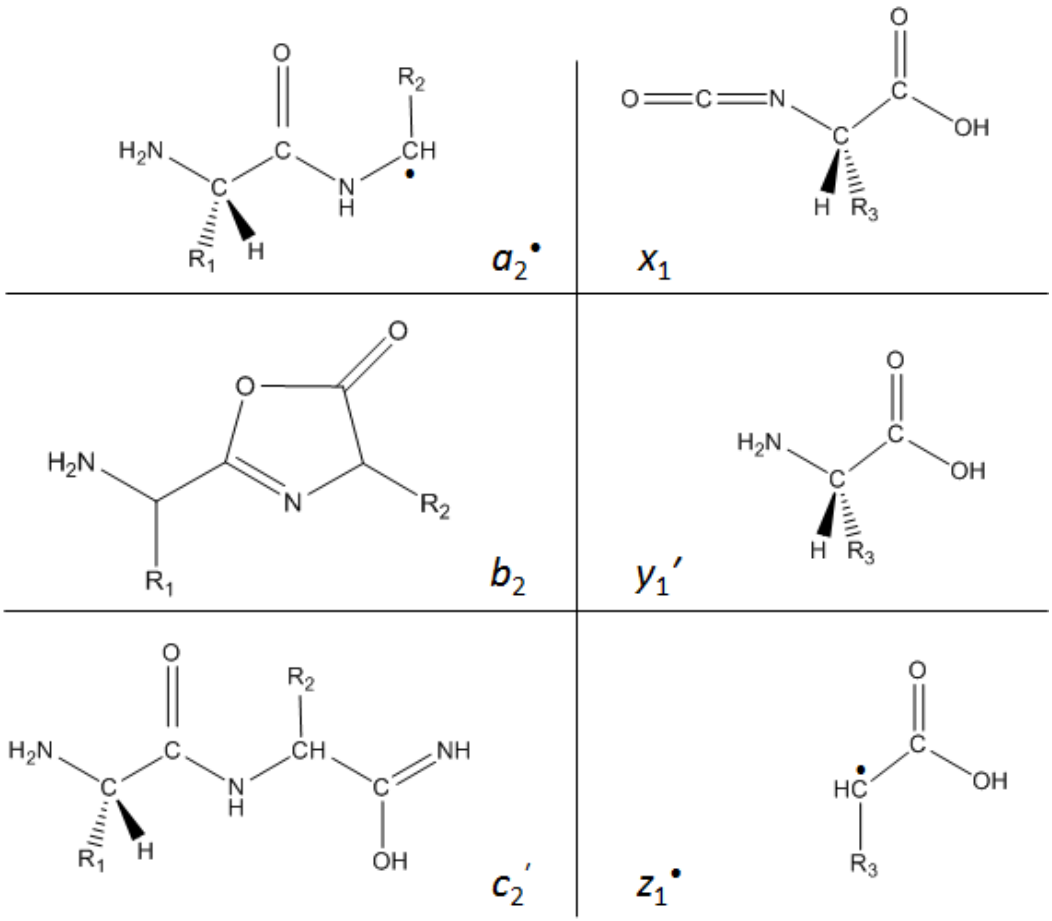

Figure 1.11. Structures of neutral products from MS/MS of a hypothetical tripeptide. Note that *b*-ions are cyclic in CAD, but *b*-ion structure is unknown in ECD.

activation, even-electron *b*-ions complement *y*′ ions, which contain an additional hydrogen atom. To observe an even-electron *a*-ion in ECD, an $a^{\bullet}$ ion must gain a hydrogen atom ($a^{\bullet} + H^{\bullet} = a$). To observe *c*′ and $z^{\bullet}$ ions from a homolytic cleavage in ECD, the $c^{\bullet}$ ion must gain $H^{\bullet}$ to form *c*′ while the $z^{\bullet}$ remains the same.

1.2.7 Positive vs. Negative Ion Mode Mass Spectrometry

Fragmentation techniques in positive ion mode have been used extensively to analyze sulfonated peptides.[68, 185-196] In all but two cases,[188, 193] direct sulfonate localization was not possible without the addition of metal ions to stabilize the sulfonate group. Furthermore as discussed earlier, it is challenging to obtain enough signal abundance in positive ion mode for sulfonated ions when the analyte itself is naturally acidic. Because negative ion mode has been used in far fewer accounts for sulfonation identification and characterization,[161, 170, 190, 193] it may provide another avenue for exploration and discovery in this area.

Complementary techniques to positive ion mode fragmentation methods have existed for decades in the case of vibrational activation methods such as negative ion mode CAD and IRMPD. Only within the past decade have the parallel methods of electron transfer dissociation (ETD) and electron capture dissociation (ECD) been realized. NETD[180] was recently discovered in Professor Donald Hunt's laboratory as the negative ion mode analogue to their previous discovery of positive ion mode ETD whereas[197] EDD was first published by Zubarev and co-workers in 2001 and was suggested to be the negative ion mode equivalent of ECD.[170] However, just recently, a breakthrough in this field discovered in our laboratory shows that there is yet another technique for negative ion mode MS/MS analysis of acidic biomolecules: niECD differs from positive ion mode activation methods in that it does not promote sulfonate loss during or after the activation stage, leading to direct sulfonate localization with sufficient backbone fragmentation to also obtain high sequence coverage. Furthermore, niECD also differs from the other negative ion mode activation techniques because it involves

direct interaction with a positively charged residue within the peptide whereas other ion-electron and ion-ion techniques involve initial interaction with a negatively charged site and subsequent movement of the radical site.

1.2.8 Differentiation of Sulfonation and Phosphorylation using Mass Spectrometry

The masses of phosphorylation and sulfonation as peptide PTMs at a basic pH differ by only 9.5 mDa (79.9663 Da for phosphorylation and 79.9568 Da for sulfonation), creating a challenge for researchers using mass spectrometry as the detection method. It is important to note that this differentiation is not an impossible feat, but it requires a fairly high resolution of ~158,000 at a peptide mass-to-charge ratio of 1500 (see Figure 1.12). As shown by the equations in Figure 1.12, for constant resolution and resolving power over a wide m/z range, this differentiation requires a smaller Δm as a function of increasing m/z, which is difficult to obtain in FT-ICR MS. The most commonly used MS instruments such as IT, triple quadrupoles (QQQ) and Q-TOF instruments consistently achieve a resolution lower than ~ 40,000 in the m/z range from 200–2000. Most of the

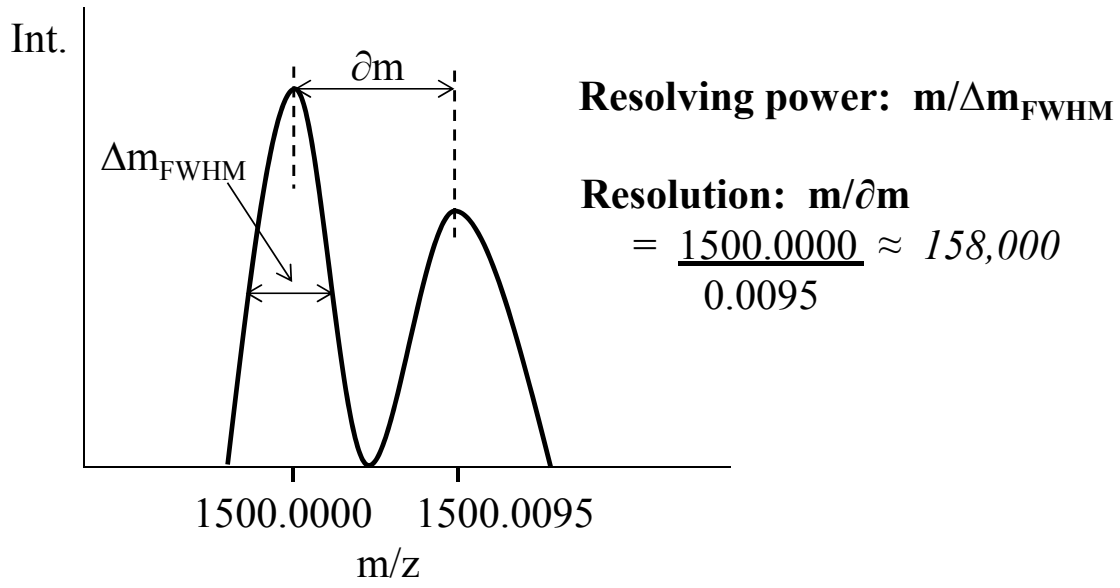

Figure 1.12. Hypothetical mass spectrum (intensity vs. m/z) of two peaks illustrating the difference between resolving power and resolution.[198]

biologically relevant peptides exist well above 400 Da, even at higher charge states such as 3-/+ and 4-/+ while lower charge states such as 1-/+ and 2-/+ can be upwards of 1200–1600 Da for the same peptide. Furthermore, it is also difficult to isolate precursor ions of high charge from their neutral loss. For example, water loss from a 1-/+ ion exists 18 Da away from the peptide ion and is easy to isolate; however, this same water loss from a 4-/+ ion results in a difference of 18/4, or 4.5 Da, which is more difficult.

As discussed earlier, there are several ion activation methods for biomolecule characterization. However, many commercial MS instruments are not yet compatible with several fragmentation methods. For instance, benchtop models of the most commonly used MS instruments (QQQ, Q-TOF, IT) are not equipped to conduct EDD or ECD, and special modifications to these instruments must be made to enable ETD and NETD as well as other laser-induced dissociative techniques.[199] Originally, not all mass spectrometers could be equipped with each electronic activation technique due to the need of a magnetic field for electron confinement. However, recent ion-trap EDD[168] and QqQ ECD[200] suggest that the need of a magnetic field is no longer an issue. As highlighted above, very high mass resolution and mass accuracy are needed to differentiate sulfonation from phosphorylation. The only commercially available mass spectrometers that can meet this demand are Orbitrap™ and FT ICR-MS instruments. Because these instruments also offer high sensitivity and moderate dynamic range,[201-202] Orbitrap™ and FT ICR-MS are the superior MS instruments for this application. I have chosen to use FT ICR-MS throughout this thesis.

Sulfonation is lost during positive-ion mode CAD[186] whereas phosphorylation can be somewhat preserved at low charge states.[203] Nemeth-Cawley, et al. also reported that excess heat from the transfer capillary can result in desulfonation prior to single-stage MS detection.[186] If MS source conditions are tuned carefully to affect a gentler transmission of ions into the high vacuum region of the mass spectrometer, sulfonate loss can be reduced but not completely averted (personal unpublished results).

Differentiation of sulfonation and phosphorylation utilizing various MS-based techniques has been examined extensively (see Seibert and Sakmar[103] and references therein). Several of these techniques rely on the loss of the sulfonate group as a detection method. Jedrzejewski and Lehmann[204] and Rappsilber, et al.[195] have differentiated phosphopeptides from sulfopeptides by comparing the unique m/z losses following skimmer-octopole CAD and by quadrupole CAD, respectively. Sulfopeptides tend to lose only 80 Da, corresponding to the loss of SO_3, while phosphopeptides can lose HPO_3 (80 Da) and/or H_3PO_4 (98 Da) during CAD. More recently, Lehmann published again on these unique losses in CAD, this time adding "beam-type" CAD[†††] and ion-trap CAD on an Orbitrap™.[206] In a departure from the traditional approach illustrated above, Yu, et al. devised an elegant synthetic method for unambiguously determining tyrosine sulfonation sites by labeling all non-sulfonated tyrosines with sulfosuccinimidyl acetate and subjecting the derivatized peptides to CAD.[191] Because CAD induces complete loss of the sulfonate group, all sites that appear as free tyrosines in the MS/MS spectra are actually tyrosine sulfonation sites.[191] At best, these are all subtractive approaches for

[†††] "Beam-type" CAD refers to the type of CAD which employs interacting a fast beam of ions with neutrals to induce fragmentation. This type of fragmentation is typically performed in sector and triple quadrupole MS instruments. Wells and McLuckey, Collision-induced dissociation (CID) of peptides and proteins. In *Methods Enzymol*, 2005; Vol. 402, pp 148-185.

which the overall efficacy is dependent upon the complete loss of a particular group as opposed to its direct detection. In high mass resolution instruments such as Orbitraps™ and FT-ICR mass spectrometers, accurate mass is sufficient to differentiate these isobaric PTMs; however, these particular instruments are not as widely used as lower mass resolution ion trap, QQQ, and Q-TOF instruments that were used in the aforementioned experiments.

1.3 Metal Oxide-Based Enrichment of Poly-Oxyanions

Lewis acid-base interactions involve the acceptance and donation of electrons, respectively, between chemical species. These interactions can occur between coordinatively unsaturated cationic centers of metal oxides and negatively charged poly-oxyanions. The transition metal is usually coordinated to 1–5 oxygens for these types of surfaces. To measure the surface Lewis acidity of metal oxides, researchers have focused much attention on the adsorption characteristics of small molecules such as carbon monoxide and carbon dioxide using infrared spectroscopy.[207-209] Some of these metal oxides include transition metals such as titanium and zirconium as well as non-transition metals such as aluminum, gallium, and calcium to name a few. In this thesis, I focus on titanium dioxide. In the preparation of a titanium dioxide surface, hydrolysis of $TiCl_4$ is carried out at low temperature and pH.[210] Any residual chloride ions that are not separated from the Ti^{4+} metal ions will act as contaminant species on the metal oxide surface, potentially causing a change in surface morphology and functionality. Once hydrolysis is completed with dialysis separation of the counter anion, the surface is dehydrated at high temperature (150–350 ^{o}C) as both excess water and hydroxyls on the metal oxide surface can serve as additional contaminant species. The degree of heat

treatment determines the types of binding sites for coordination of Lewis bases. If treated at a low temperature (150 ^{o}C), the TiO_2 surface will contain adsorbed water while at a higher temperature (350 ^{o}C) there will be hydroxyls that dictate the binding interactions.[207] It has also been suggested that water-adsorbed sites contain a four-coordinate Ti^{4+} while the hydroxyl-adsorbed sites contain a five-coordinate metal center.[209] The number of coordination sites may affect the shape of the metal-ligand complex, which in turn affects the type of interaction that it can form. Furthermore as mentioned above, the specific TiO_2 preparation steps determine the relative amounts of three crystalline forms of TiO_2 (anatase, rutile and amorphous)[207, 209] as well as the amount of contaminant species on the metal oxide surface. These variable conditions can make it extremely difficult to develop reproducible identical surfaces.

As stated earlier, the titanium(IV) cation can exist in a dioxide as a five- or four-coordinate species with hydroxyls or water, respectively, adsorbed on the surface.[209] The unsaturated metal ion has available coordination sites existing from its open-shell electronic configuration. Empty d-orbitals of Ti^{4+} cationic centers with the help of hydroxyl groups and/or water facilitate a reversible Lewis acid-base interaction depending on the pH of the local environment. Specifically, hydroxyl groups residing on the TiO_2 surface following aggressive heat treatment interact with CO and CO_2[207-208] as well as HPO_4^{2-}.[211] Early work by Muljadi, et al. suggested that phosphate interacts very strongly with aluminum hydroxide surfaces and that pH plays a critical role in binding reversibility.[212] More recent studies considering phosphate binding to TiO_2 show similar pH-dependent binding and reversible interactions.[211, 213-214] Connor and McQuillan also reported that phosphates interact most favorably at pH 2.3 and do not interact appreciably

at pH 11.0.[211] In a separate study, the acidities of the TiO_2 surface for anatase and rutile crystalline forms in terms of pK_a were calculated to be 0.5–2.0 and 6.5,[215] respectively, indicating that a surface composed of mostly the anatase crystalline form was used in the previous study.

Infrared spectroscopic studies showed that the binding modes of Lewis base coordination to a metal oxide surface can be determined by the different separations of stretch absorption bands for carboxylates and other interacting species. Most notably, McQuillan determined the binding nature of many types of carboxylic acids[216-217] as well as phosphates.[211] Figure 1.13 displays the chemical interaction for each of the three binding modes: monodentate, chelating bidentate, and bridging bidentate.[216] Monodentate binding, which is seen for disubstituted and some monosubstituted phosphates, involves a single interaction point between the negatively charged oxygen and the positively charged metal ion.[211] Dicarboxylic acids such as phthalic acid have been shown to coordinate to two metal ions via both carboxylates to form a

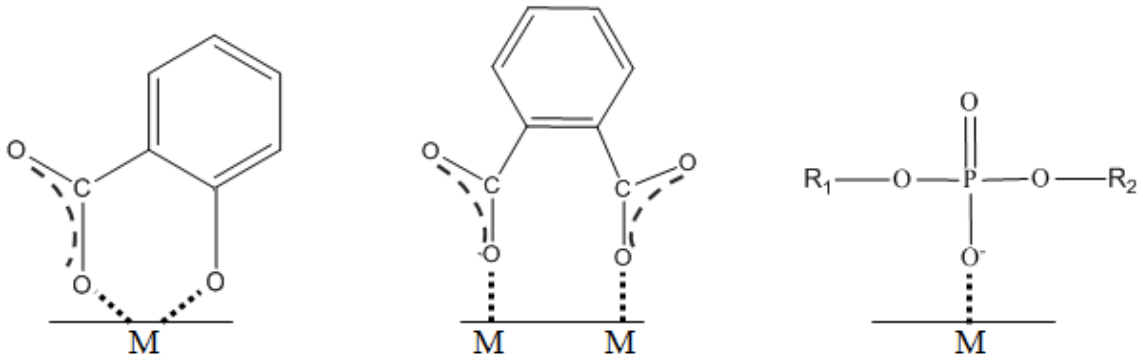

Figure 1.13. Chelating and bridging bidentate as well as monodentate binding modes (left–right, respectively) for poly-oxyanion species interacting with a generic metal oxide surface (M). Left and middle images are recreated from Dobson and McQuillan[217] while the right image was created based on information from Connor and McQuillan.[211]

bridging bidentate strucutre.[217] As for phosphates, there is some ambiguity regarding exactly what binding interaction occurs. Connor and McQuillian clearly state in their 1999 Langmuir article:[211]

> "Analyses of the infrared spectra of the adsorbed phosphate, the adsorption kinetics, and the adsorption isotherm have indicated that phosphate binds strongly as a bidentate surface species, although the infrared spectra have not allowed bridging bidentate and chelate species to be distinguished."

According to this account, phosphates which have two relatively close negatively charged oxygens could interact via either bidentate binding mode (see Figure 1.14). Yet, Larsen, et al. cite this very paper to conclude that phosphate anions coordinate to TiO_2 via a bridging bidentate interaction.[218] As for chelating bidentate interactions, they are the preferred interaction for lactic and glycolic acids, which interact through the carboxyl and the α-OH group.[216]

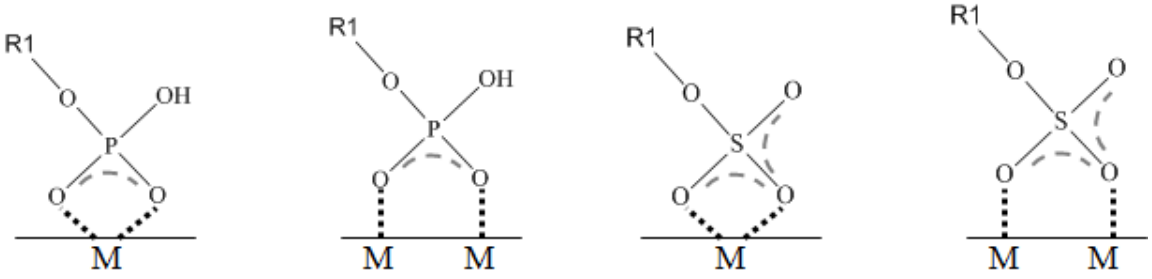

Figure 1.14. Possible metal ion (M) binding modes for phosphorylation and sulfonation on peptides.

Recent attention within the past decade has been focused on applying the experimental work described above to the enrichment of phosphopeptides from biological samples.[177, 213-214, 218-220] Larsen, et al. have shown that TiO_2 microcolumns offer high enrichment selectivity when an aromatic substituted carboxylic acid such as

dihydroxybenzoic acid (DHB) is added to the enrichment solution.[218] They report that DHB competes with non-phosphorylated carboxylate species to reduce non-specific binding. The previously referenced reports from Larsen, et al. were conducted using a MALDI source, which is much more tolerant to DHB than ESI. They comment that "a simple cleaning of the source" will suffice;[213] however, such cleaning may not be a sustainable solution for high-throughput analyses. This particular enrichment procedure may require an additional purification step prior to ESI-based MS analysis, effectively nullifying the protocol's simplicity.

More recently, Andrews and coworkers have presented improvements for phosphopeptide enrichment using TiO_2. Their results indicate that non-specific binding of acidic peptides can be reduced by methyl esterification of carboxylic acids.[214] Furthermore, they show that monophosphorylated and multiply phosphorylated peptides from human cyclin-dependent kinase 2 can be fractionated using a stepwise pH gradient elution from pH 8.5 to 11.5. In previous reports, addition of DHB to the enrichment solution was effective for reducing non-specific binding for mixtures of α- and β-casein[218] but not for more complex mixtures.[221] Instead of using small organic acid additives in the enrichment solution to prevent carboxylate interactions, Andrews and coworkers pursued methyl esterification of carboxylic acids as an alternative. The improved binding selectivity for methyl-esterified phosphopeptides outweighed any issues associated with lack of complete esterification or side reactions.[214] The Håkansson group has also evaluated the use of titanium and zirconium dioxide for the enrichment of phosphopeptides. Kweon and Håkansson reported that highly selective phosphopeptide enrichment can be obtained from microtips coated with 50 μg of zirconium and titanium

dioxide. In this report, the authors showed that singly-phosphorylated peptides were preferentially enriched from ZrO_2 while TiO_2 performed better for enrichment of multiply-phosphorylated peptides.[220] Additionally, phosphopeptide enrichment improved the signal-to-noise ratio of multiply-charged precursor ions for MS analysis, enabling tandem MS analyses such as EDD and ECD for reliable localization of the phosphorylated residues.[177]

Though free sulfonates have been shown to interact with various metal oxide surfaces under acidic conditions,[222-225] there are no published reports indicating that these metal oxides have been used to enrich sulfopeptides. In this thesis, I optimize our original phosphopeptide enrichment procedure for the selective enrichment of sulfopeptides, including determination of the minimum amount of sulfopeptides loaded onto the TiO_2 microtips as well as the binding and elution pH values.

1.4 Current Methods for Enrichment of Sulfonic Acids and Sulfopeptides

At present, there are few methods for analyzing sulfopeptides with mass spectrometry and far fewer employing enrichment prior to MS detection. As discussed previously in Sections 1.2.4 and 1.2.7, the labile sulfonate group is readily lost during vibrational activation but can be differentiated from isobaric phosphorylation due to the characteristic loss of 80 Da from sulfopeptides (compared to the loss of 98 Da for phosphoric acid loss from phosphopeptides during CAD). This neutral loss-based approach is acceptable for cases in which there is sufficient sulfopeptide signal abundance to conduct CAD for structural characterization. However, sulfopeptides measured in biological systems may exist naturally at very low abundance,[78] potentially leading to limited or no MS detection. For this reason, recent efforts have been focused

on enriching peptide sulfonic acids[226] and sulfopeptides[191, 227] prior to MS detection. Chang, et al. oxidized cysteine thiols to form sulfonic acids, which can be enriched using an ionic affinity capture approach.[226] This method employs poly-arginine coated nanodiamonds to bind sulfonic acid moieties at a concentration as low as 0.02%. Though this method boasts excellent enrichment selectivity, the protocol requires preparation as well as functionalization of a highly specialized surface followed by a labor-intensive enrichment procedure. Furthermore, the authors refer to sulfonic acids interchangeably as sulfopeptides, which is an inaccurate assessment. Sulfonic acids do not contain a sulfur-oxygen bond as the point of attachment to the peptide as do sulfonates; thus, these groups can be clearly differentiated by structure. Furthermore, the localization and function of these groups also differ greatly. Sulfonic acids exist as oxidative PTMs that can modulate catalysis and metal binding inside cells.[228] On the other hand, sulfonation of peptides occurs as one of the last PTMs conferred to mostly secreted peptides involved in protein-protein interactions in the extracellular matrix.[1, 7] It is possible that the structural and functional differences of these particular groups may cause different metal-ion binding modes.

To date, there is only one published procedure for the enrichment of sulfopeptides: Amano, et al. suggested that sulfopeptides can be enriched prior to MS detection by using ion-selective enrichment in the presence of a complex protein digest.[227] Specifically, the column-based anion exchanger diethylaminoethyl dextran (DEAE-D) binds sulfonates on peptides at slightly basic pH, and the sulfopeptides are eluted with a stepwise increase in sodium chloride.[227] Despite demonstrating sulfopeptide enrichment, this protocol

requires 1.5–3 M sodium chloride that must be eliminated prior to MS detection, precluding online MS analysis and potentially leading to losses due to sample handling.

For the reasons highlighted above, we believe that titanium dioxide enrichment, which requires neither complex sample preparation nor cleanup prior to MS detection, offers a simple alternative to the aforementioned previously published methods.

1.5 Improving Fragmentation Efficiency in EDD

One troublesome disadvantage that exists for negative ion mode CAD, NETD and EDD is the loss of CO_2 as a major fragmentation event from acidic peptides.[164, 168, 170, 180-181] One possibility would be to introduce a permanent negative charge in place of the negatively charged carboxylate. In designing such a synthesis, one must consider two main requirements: the added moiety should contain a functional group that will react with carboxylates with high selectivity and efficiency as well as a different functional group that will provide a stable negative charge in mildly basic conditions and will not be subject to neutral loss during electronic activation. First, let us consider reactions to cap carboxylic acids. Methyl esterification adds a methyl group to carboxylic acids using methanolic hydrochloric acid[124] or trimethylsilyldiazomethane (a safer alternative to diazomethane)[229] under ambient conditions. Next, let us consider the stable negative charge. Phosphates and sulfonates as well as some alcohols, phenols and sulfides can provide a negative charge at basic pH values from 8–11. However, it is possible that primary sulfides (R-SH) could form disulfide linkages, sequestering their negative charge at basic pH. Phosphates and sulfonates may pose a problem due to a lack of reliable stability in EDD and NETD as discussed above. Phenols from tyrosine as well as alcohols from threonine and serine can be deprotonated at pH 9.6–10 and approximately

pH 13, respectively.[230] Combining these ideas into a single reactant species such as 4-aminonaphthalene sulfonic acid (ANSA) or taurine seemed to be a logical progression based on previously published reports of successful peptide labeling with these reagents.[231-232] Both of these reports cite an improvement in fragmentation efficiency with fragmentation initiated away from the charge in CAD. However, neither of these articles highlights the utility of this approach for reducing neutral loss of CO_2 following electronic activation and fragmentation.

Another possible route for reducing neutral loss of CO_2 in EDD and NETD would be to cap the carboxylic acids as in the previous idea but not provide another source of negative charge. In order to obtain a multiply negatively charged ion after removing a source of negative charge, a proton must be removed from the peptide backbone. Though it seems unlikely, this simple, yet elegant, approach has already been eluded to by Budnik, et al. and references therein.[170] These authors state in this article that EDD is a radical-driven fragmentation process that leads to backbone fragmentation *if* the radical site is located on the backbone. Radical sites in EDD are generated from electron detachment at a site of relatively low electron affinity as discussed earlier. Carboxylic acids, which are thought to be one of the most acidic groups located on peptides, are likely sites for electron detachment due to their low electron affinity as well as the exothermic energy release from losing CO_2.[170] By protecting the carboxylic acids with stable alkyl groups, neither deprotonation nor electron detachment with radical formation can occur at the carboxylic acids. One potential problem with this approach could be decreased ionization efficiency of the peptide of interest, which could be remedied by increasing the accumulation time of the low-abundance ion of interest or deprotonation of a peptide

backbone proton to increase the charge state. This latter option, most likely to occur from an amide, would require a fairly strong base. However, bases with pK_a values of greater than water (~16) would deprotonate water in the spray solvent instead of removing a proton from the peptide backbone. Therefore, hydroxide is the strongest base available if traditional aqueous-organic mixtures are used for the spray solvent. McLuckey, et al. have developed a method for manipulating charge state distributions in negative ion mode MS by introducing a strong base into the drying gas flow during the desolvation stage of ESI.[233] This potentially useful trick may provide an additional means for deprotonation of backbone protons.

Yet another possibility for blocking the carboxylic acids to prevent neutral loss in EDD is to alter the charge carrier. Several recent reports evaluate the use of alkaline earth and divalent transition metal ions as charge carriers in ECD.[196, 234-237] The unique fragmentation behavior of various divalent metal-peptide adducts may lead to a "tunable" system for obtaining complementary fragmentation of these peptides.[236] While there have been considerable advancements with cation adduction, there have been far fewer studies involving anion adduction. Liu and Cole have recently reported that matching the gas-phase basicity (GPB) of the carboxylate with that of the adduct anion helps promote adduction in negative ion mode ESI-MS.[238] Their proposed mechanism for anion interaction involves a halide anion such as chloride adducting to a neutral carboxylic acid, thereby increasing the charge state of the precursor in negative ion mode MS. The authors do not attempt ion-electron reactions to elucidate the gas-phase structure of anion adducted peptides, allowing for further exploration in this area.

1.6 Dissertation Overview

Following the introduction to this thesis, we examine first the enrichment of sulfonated peptides using titanium dioxide (TiO_2) microtips. Optimization of binding and elution pH as well as optimization of minimum binding amount for the most efficient sulfopeptide enrichment is discussed in Chapter 2. We next look at how to directly characterize the post-translational modification site(s) on sulfonated peptides using vibrational, ion-electron, and ion-ion activation methods in negative ion mode (Chapter 3). Representative spectra from each fragmentation method at multiple charge states for various peptides as well as trends in fragmentation behavior are discussed. Finally, we examine how the fragmentation behavior of acidic peptides can be influenced by the addition of a chemical modifier either providing a fixed negative charge or no charge at all (Chapter 4). We have evaluated the potential of each synthetic approach for decreasing neutral loss of CO_2 during EDD and whether we can improve the quality and amount of fragmentation information garnered from fragmentation of these acidic peptides. We have also employed anion adduction of chloride and bromide to several peptides in order to alter the charge carrier and perhaps EDD fragmentation behavior of these peptides. Chapters 2 and 3 are written in manuscript format for journal submission while Chapter 4 is a free standing chapter and will be prepared for publication at a later date.

1.7 References

1. W. B. Huttner, Tyrosine sulfation and the secretory pathway. *Ann. Rev. Physiol.* **1988**, *50*, 363-376.
2. C. Niehrs, R. Beisswanger, W. B. Huttner, Protein tyrosine sulfation, 1993--an update. *Chem. Biol. Interact.* **1994**, *92*, 257-271.
3. C. A. Strott, Sulfonation and molecular action. *Endocr. Rev.* **2002**, *23*, 703-732.

4. R. J. Huxtable, W. M. Lafranconi, *Biochemistry of sulfur*. Plenum Press: New York, **1986**; p xiii, 445 p.
5. P. A. Baeuerle, W. B. Huttner, Tyrosine sulfation of yolk proteins 1, 2, and 3 in Drosophila melanogaster. *J. Biol. Chem.* **1985**, *260*, 6434-6439.
6. C. Niehrs, W. B. Huttner, Purification and characterization of tyrosylprotein sulfotransferase. *EMBO J.* **1990**, *9*, 35-42.
7. K. L. Moore, The biology and enzymology of protein tyrosine O-sulfation. *J. Biol. Chem.* **2003**, *278*, 24243-24246.
8. R. W. H. Lee, W. B. Huttner, (Glu62,Ala30,Tyr8) serves as high-affinity substrate for tyrosylprotein sulfotransferase: A Golgi enzyme. *Proc. Natl. Acad. Sci. U. S. A.* **1985**, *82*, 6143-6147.
9. R. Beisswanger, D. Corbeil, C. Vannier, C. Thiele, U. Dohrmann, R. Kellner, K. Ashman, C. Niehrs, W. B. Huttner, Existence of distinct tyrosylprotein sulfotransferase genes: Molecular characterization of tyrosylprotein sulfotransferase-2. *Proc. Natl. Acad. Sci. U. S. A.* **1988**, *95*, 11134-11139.
10. Y.-B. Ouyang, W. S. Lane, K. L. Moore, Tyrosylprotein sulfotransferase: Purification and molecular cloning of an enzyme that catalyzes tyrosine O-sulfation, a common posttranslational modification of eukaryotic proteins. *Proc. Natl. Acad. Sci. U. S. A.* **1998**, *95*, 2896-2901.
11. Y.-B. Ouyang, K. L. Moore, Molecular cloning and expression of human and mouse tyrosylprotein sulfotransferase-2 and a tyrosylprotein sulfotransferase homologue in *Caenorhabditis elegans*. *J. Biol. Chem.* **1998**, *273*, 24770-24774.
12. D. Corbeil, W. B. Huttner, in *Encyclopedia of Biological Chemistry*, ed. W. Lennarz, M. D. Lane. Elsevier: Amsterdam, **2004**, vol. 4, pp 294-297.
13. M. J. Stone, S. Chuang, X. Hou, M. Shoham, J. Z. Zhu, Tyrosine sulfation: an increasingly recognised post-translational modification of secreted proteins. *Nat. Biotechnol.* **2009**, *25*, 299-317.
14. W. B. Huttner, P. A. Baeuerle, Protein sulfation on tyrosine. *Mod. Cell Biol.* **1988**, *6*, 97-140.
15. A. Hille, T. Braulke, K. von Figura, W. B. Huttner, Occurrence of tyrosine sulfate in proteins - a balance sheet 1. Secretory and lysosomal proteins. *Eur. J. Biochem.* **1990**, *188*, 577-586.
16. C. Kasinathan, P. Ramaprasad, P. Sundaram, Identification and characterization of tyrosylprotein sulfotransferase from human saliva. *Int. J. Biol. Sci.* **2005**, *1*, 141-145.
17. F. R. Bettelheim, Tyrosine-O-sulfate in a peptide from fibrinogen. *J. Am. Chem. Soc.* **1954**, *76*, 2838-2839.
18. H. Gregory, P. M. Hardy, D. S. Jones, G. W. Kenner, R. C. Sheppard, The antral hormone gastrin. Structure of gastrin. *Nature* **1964**, *204*, 931-933.
19. A. Anastasi, G. Bertaccini, V. Erspamer, Pharmacological data on phyllokinin (bradykinyl-isoleucyl-tyrosine O-sulphate) and bradykinyl-isoleucyl-tyrosine. *Br. J. Pharmacol. Chemother.* **1966**, *27*, 479-485.
20. A. Anastasi, V. Erspamer, R. Endean, Isolation and structure of caerulein, an active decapeptide from the skin of *Hyla caerulea*. *Experientia* **1967**, *23*, 699-700.
21. V. Mutt, J. E. Jorpes, Structure of porcine cholecystokinin-pancreozymin 1. Cleavage with thrombin and with trypsin. *Eur. J. Biochem.* **1968**, *6*, 156-162.

22. A. Anastasi, V. Erspamer, R. Endean, Isolation and amino acid sequence of caerulein, the active decapeptide of the skin of *Hyla caerulea*. *Arch. Biochem. Biophys.* **1968**, *125*, 57-68.
23. W. B. Huttner, Sulphation of tyrosine residues-a widespread modification of proteins. *Nature* **1982**, *299*, 273-276.
24. J. S. Edkins, On the chemical mechanism of gastric secretion. *Proceedings of the Royal Society of London, Series B, Containing Papers of a Biological Character* **1905**, *76*, 376.
25. A. C. Ivy, E. Oldberg, A hormone mechanism for gall-bladder contraction and evacuation. *Am. J. Physiol.* **1928**, *86*, 599-613.
26. M. Bodanszky, J. Martinez, G. P. Priestley, J. D. Gardner, V. Mutt, Cholecystokinin (pancreozymin). 4. Synthesis and properties of a biologically active analogue of the C-terminal heptapeptide with epsilon-hydroxynorleucine sulfate replacing tyrosine sulfate. *J. Med. Chem.* **1978**, *21*, 1030-1035.
27. A. H. Johnsen, Phylogeny of the cholecystokinin/gastrin family. *Front. Neuroendocrinol.* **1998**, *19*, 73-99.
28. I. Marseigne, P. Roy, A. Dor, C. Durieux, D. Pelaprat, M. Reibaud, J. C. Blanchardt, B. P. Roques, Full agonists of CCK8 containing a nonhydrolyzable sulfated tyrosine residue. *J. Med. Chem.* **1989**, *32*, 445-449.
29. M. C. Fournie-Zaluski, J. Belleney, B. Lux, C. Durieux, D. Gerard, G. Gacel, B. Maigret, B. P. Roques, Conformational analysis of cholecystokinin CCK26-33 and related fragments by 1H NMR spectroscopy, fluorescence-transfer measurements, and calculations. *Biochemistry* **1986**, *25*, 3778-3787.
30. R. B. Lydiard, Neuropeptides and anxiety: focus on cholecystokinin. *Clin. Chem.* **1994**, *40*, 315-318.
31. P. Cantor, B.N. Andersen, J. F. Rehfeld, Complete tyrosine O-sulfation of gastrin in adult and neonatal cat pancreas. *FEBS Lett.* **1986**, *195*, 272-274.
32. S. J. Brand, B. N. Andersen, J. F. Rehfeld, Complete tyrosine-O-sulphation of gastrin in neonatal rat pancreas. *Nature* **1984**, *309*, 456-458.
33. J. F. Rehfeld, Accurate measurement of cholecystokinin in plasma. *Clin. Chem.* **1998**, *44*, 991-1001.
34. F. Markwardt, Hirudin as an inhibitor of thrombin. *Methods Enzymol.* **1970**, *19*, 924-932.
35. G. M. Clore, D. K. Sukumaran, M. Nilges, J. Zarbock, A. M. Gronenborn, The conformations of hirudin in solution: a study using nuclear magnetic resonance, distance geometry and restrained molecular dynamics. *EMBO J.* **1987**, *6*, 529-537.
36. J. W. Kehoe, C. R. Bertozzi, Tyrosine sulfation: a modulator of extracellular protein-protein interactions. *Chem. Biol.* **2000**, *7*, R57-61.
37. P. Marchese, M. Murata, M. Mazzucato, P. Pradella, L. De Marco, J. Ware, Z. M. Ruggeri, Identification of three tyrosine residues of glycoprotein Iba with distinct roles in von Willebrand factor and a-thrombin binding. *J. Biol. Chem.* **1995**, *270*, 9571-9578.
38. J. Dong, C. Q. Li, J. A. López, Tyrosine sulfation of the glycoprotein Ib-IX complex: identification of sulfated residues and effect on ligand binding. *Biochemistry* **1994**, *33*, 13946-13953.
39. K. J. Clemetson, Primary haemostasis: sticky fingers cement the relationship. *Curr. Biol.* **1999**, *9*, R110-R112.

40. S. R. Stone, J. Hofsteenge, Kinetics of the inhibition of thrombin by hirudin. *Biochemistry* **1986**, *25*, 4622-4628.
41. D. Sako, K. M. Comess, K. M. Barone, R. T. Camphausen, D. A. Cumming, G. D. Shaw, A sulfated peptide segment at the amino terminus of PSGL-1 is critical for P-selectin binding. *Cell* **1995**, *83*, 323-331.
42. T. Pouyani, B. Seed, PSGL-1 recognition of P-selectin is controlled by a tyrosine sulfation consensus at the PSGL-1 amino terminus. *Cell* **1995**, *83*, 333-343.
43. P. P. Wilkins, K. L. Moore, R. P. McEver, R. D. Cummings, Tyrosine sulfation of P-selectin glycoprotein ligand-1 is required for high affinity binding to P-selectin. *J. Biol. Chem.* **1995**, *270*, 22677-22680.
44. D. R. Karp, Post-translational modification of the fourth component of complement. *J. Biol. Chem.* **1983**, *258*, 12745-12748.
45. W. Hsu, G. L. Rosenquist, A. A. Ansari, M. E. Gershwin, Autoimmunity and tyrosine sulfation. *Autoimmun. Rev.* **2005**, *4*, 429-435.
46. J. F. Rehfeld, W. W. van Solinge, The tumor biology of gastrin and cholecystokinin. *Adv. Canc. Res.* **1994**, *63*, 295-347.
47. J. Liu, S. Louie, W. Hsu, K. M. Yu, H. B. Nicholas, Jr., G. L. Rosenquist, Tyrosine sulfation is prevalent in human chemokine receptors important in lung disease. *Am. J. Respir. Cell. Mol. Biol.* **2008**, *38*, 738-743.
48. M. Farzan, G. J. Babcock, N. Vasilieva, P. L. Wright, E. Kiprilov, T. Mirzabekov, H. Choe, The role of post-translational modifications of the CXCR4 amino terminus in stromal-derived factor 1 alpha association and HIV-1 entry. *J. Biol. Chem.* **2002**, *277*, 29484-29489.
49. E. Koltsova, K. Ley, Tyrosine sulfation of leukocyte adhesion molecules and chemokine receptors promotes atherosclerosis. *Arterioscler. Thromb. Vasc. Biol.* **2009**, *29*, 1709-1711.
50. Y. Matsubayashi, Y. Sakagami, Phytosulfokine, sulfated peptides that induce the proliferation of single mesophyll cells of *Asparagus officinalis* L. *Proc. Natl. Acad. Sci. U. S. A.* **1996**, *93*, 7623-7627.
51. H. Yang, Y. Matsubayashi, K. Nakamura, Y. Sakagami, *Oryza sativa* PSK gene encodes a precursor of phytosulfokine-α, a sulfated peptide growth factor found in plants. *Proc. Natl. Acad. Sci. U. S. A.* **1999**, *96*, 13560-13565.
52. S. Wenzl, M. Sumper, Sulfation of a cell surface glycoprotein correlates with the developmental program during embryogenesis of *Volvox carteri*. *Proc. Natl. Acad. Sci. U. S. A.* **1981**, *78*, 3716-3720.
53. S. Wenzl, M. Sumper, Early event of sexual induction in *Volvox*: chemical modification of the extracellular matrix. *Dev. Biol.* **1986**, *115*, 119-128.
54. R. Nichols, S. A. Schneuwly, J. E. Dixon, Identification and characterization of a *Drosophila* homologue to the vertebrate neuropeptide cholecystokinin. *J. Biol. Chem.* **1988**, *263*, 12167-12170.
55. T. M. Kubiak, M. J. Larsen, K. J. Burton, C. A. Bannow, R. A. Martin, M. R. Zantello, D. E. Lowery, Cloning and functional expression of the first *Drosophila melanogaster* sulfakinin receptor DSK-R1. *Biochem. Biophys. Res. Commun.* **2002**, *291*, 313-320.

56. E. Friederich, P. A. Baeuerle, H. Garoff, B. Hovemann, W. B. Huttner, Expression, tyrosine sulfation, and secretion of yolk protein 2 of *Drosophila melanogaster* in mouse fibroblasts. *J. Biol. Chem.* **1988**, *263*, 14930-14938.
57. R. J. Nachman, G. M. Holman, W. F. Haddon, N. Ling, Leucosulfakinin, a sulfated insect neuropeptide with homology to gastrin and cholecystokinin. *Science* **1986**, *234*, 71-73.
58. R. J. Nachman, G. M. Holman, B. J. Cook, W. F. Haddon, N. Ling, Leucosulfakinin-II, a blocked sulfated insect neuropeptide with homology to cholecystokinin and gastrin. *Biochem. Biophys. Res. Commun.* **1986**, *140*, 357-364.
59. T. Janssen, E. Meelkop, M. Lindemans, K. Verstraelen, S. J. Husson, L. Temmerman, R. J. Nachman, L. Schoofs, Discovery of a cholecystokinin-gastrin-like signaling system in nematodes. *Endocrinology* **2008**, *149*, 2826-2839.
60. P. S. Dickinson, J. S. Stevens, S. Rus, H. R. Brennan, C. C. Goiney, C. M. Smith, L. Li, D. W. Towle, A. E. Christie, Identification and cardiotropic actions of sulfakinin peptides in the American lobster *Homarus americanus*. *J. Exp. Biol.* **2007**, *210*.
61. W. H. Lin, K. Larsen, G. L. Hortin, J. A. Roth, Recognition of substrates by tyrosylprotein sulfotransferase. Determination of affinity by acidic amino acids near the target sites. *J. Biol. Chem.* **1992**, *267*, 2876-2879.
62. J. R. Bundgaard, J. Vuust, J. F. Rehfeld, New consensus features for tyrosine O-sulfation determined by mutational analysis. *J. Biol. Chem.* **1997**, *272*, 21700-21705.
63. G. Hortin, R. Folz, J. I. Gordon, A. W. Strauss, Characterization of sites of tyrosine sulfation in proteins and criteria for predicting their occurrence. *Biochem. Biophys. Res. Commun.* **1986**, *141*, 326-333.
64. G. L. Rosenquist, H. B. Nicholas, Jr., Analysis of sequence requirements for protein tyrosine sulfation. *Prot. Sci.* **1993**, *2*, 215-222.
65. S. Wenzl, M. Sumper, Evidence for membrane-mediated control of differentiation during embryogenesis of *Volvox carteri*. *FEBS Lett.* **1979**, *107*, 247-249.
66. M. Sumper, S. Wenzl, Sulphation-desulphation of a membrane component proposed to be involved in control of differentiation in *Volvox carteri*. *FEBS Lett.* **1980**, *114*, 307-312.
67. S.-W. Lee, S.-W. Han, M. Sririyanum, C.-J. Park, Y.-S. Seo, P. C. Ronald, A type I–secreted, sulfated peptide triggers XA21-mediated innate immunity. *Science* **2009**, *326*, 850-853.
68. K. F. Medzihradszky, Z. Darula, E. Perlson, M. Fainzilber, R. J. Chalkley, H. Ball, D. Greenbaum, M. Bogyo, D. R. Tyson, R. A. Bradshaw, A. L. Burlingame, O-sulfonation of serine and threonine: mass spectrometric detection and characterization of a new posttranslational modification in diverse proteins throughout the eukaryotes. *Mol. Cell. Proteomics* **2004**, *3*, 429-440.
69. R. Komori, Y. Amano, M. Ogawa-Ohnishi, Y. Matsubayashi, Identification of tyrosylprotein sulfotransferase in *Arabidopsis*. *Proc. Natl. Acad. Sci. U. S. A.* **2009**, *106*, 15067-15072.
70. A. H. Johnsen, J. F. Rehfeld, Cionin: a disulfotyrosyl hybrid of cholecystokinin and gastrin from the neural ganglion of the protochordate *Ciona intestinalis*. *J. Biol. Chem.* **1990**, *265*, 3054-3058.
71. C. J. Grimmelikhuijzen, F. Sundler, J. F. Rehfeld, Gastrin/CCK-like immunoreactivity in the nervous system of coelenterates. *Histochemistry* **1980**, *69*, 61-68.

72. L. Larsson, J. F. Rehfeld, Evidence for a common evoluntionary origin of gastrin and cholecystokinin. *Nature* **1977**, *269*.
73. G. J. Dockray, Comparative biochemistry and physiology of gut hormones. *Ann. Rev. Physiol.* **1979**, *41*, 83-95.
74. L. R. Johnson, The trophic action of gastrointestinal hormones. *Gastroenterology* **1976**, *70*, 278-288.
75. E. Rozengurt, J. H. Walsh, Gastrin, CCK, signaling, and cancer. *Ann. Rev. Physiol.* **2001**, *63*, 49-76.
76. H. R. Kissileff, F. X. Pi-Sunyer, J. Thornton, G. P. Smith, C-terminal octapeptide of cholecystokinin decreases food intake in man. *Am. J. Clin. Nutr.* **1981**, *34*, 154-160.
77. G. P. Smith, Cholecystokinin and treatment of meal size: proof of principle. *Obesity* **2006**, *14*, 168S-170S.
78. S. A. Young, S. Julka, G. Bartley, J. Gilbert, B. Wendelburg, S.-C. Hung, W. H. K. Anderson, W. Yokoyama, Quantification of the sulfated cholecystokinin CCK-8 in hamster plasma using immunoprecipitation liquid chromatography-mass spectrometry/mass spectrometry. *Anal. Chem.* **2009**, *81*, 9120-9128.
79. H. Yajima, Y. Mori, K. Koyama, T. Takayoshi, M. Setoyama, H. Adachi, T. Kanno, A. Saito, Studies on peptides: LXVIII. Synthesis of the tritriacontapeptide amide corresponding to the entire amino acid sequence of the desulfated form of porcine cholecystokinin-pancreozymin (CCK-PZ). *Chem. Pharm. Bull.* **1976**, *24*, 2794-2802.
80. A. M. Brooks, L. R. Johnson, J. Spencer, M. I. Grossman, Failure of desulfated caerulein to inhibit pentagastrin-stimulated acid secretion. *Amer. J. Physiol.* **1970**, *219*, 794-797.
81. L. R. Johnson, G. F. Stening, M. I. Grossman, Effect of sulfation on the gastrointestinal actions of caerulein. *Gastroenterology* **1970**, *58*, 208-216.
82. P. Torfs, G. Baggerman, T. Meeusen, J. Nieto, R. J. Nachman, J. Calderon, A. De Loof, L. Schoofs, Isolation, identification, and synthesis of a disulfated sulfakinin from the central nervous system of an arthropods the white shrimp *Litopenaeus vannamei*. *Biochem. Biophys. Res. Commun.* **2002**, *299*, 312-320.
83. B. Schjoldager, J. Park, A. H. Johnsen, T. Yamada, J. F. Rehfeld, Cionin, a protochordean hybrid of cholecystokinin and gastrin: biological activity in mammalian systems. *Am. J. Physiol.* **1991**, *260*, G976-G982.
84. B. Schjoldager, J. C. Jorgensen, A. H. Johnsen, Stimulation of rainbow trout gallbladder contraction by cionin, an ancestral member of the CCK/gastrin family. *Gen. Comp. Endocrinol.* **1995**, *98*, 269-278.
85. D. Bagdy, E. Barabas, L. Graf, T. E. Petersen, S. Magnusson, Hirudin. *Methods Enzymol.* **1976**, *45*, 669-678.
86. J.-Y. Chang, The functional domain of hirudin, a thrombin-specific inhibitor. *FEBS Lett.* **1983**, *164*, 307-313.
87. J. Dodt, W. Machleidt, U. Seemuller, R. Maschler, H. Fritz, Isolation and characterization of hirudin isoinhibitors and sequence analysis of hirudin PA. *Biol. Chem. Hoppe-Seyler* **1986**, *367*, 803-811.
88. J. L. Krstenansky, S. J. T. Mao, Antithrombin properties of C-terminus of hirudin using synthetic unsulfated N^{α}-acetyl-hirudin$_{45\text{-}65}$. *FEBS Lett.* **1987**, *211*, 10-16.
89. D. Tripier, Hirudin: a family of iso-proteins. Isolation and sequence determination of new hirudins. *Folia Haematol.* **1988**, *115*, S30-35.

90. J. B. Haycraft, Ueber die einwirkung eines secretes des offlcinellen blutegels auf die gerinnbarkeit des blutes. *Naunyn-Schmiedebergs Arch. Exp. Pathol. Pharmakol.* **1884**, *18*, 209-217.
91. F. Markwardt, Pharmacology of hirudin: one hundred years after the first report of the anticoagulant agent in medicinal leeches. *Biomed. Biochim. Acta* **1985**, *44*, 1007-1013.
92. F. Markwardt, Die isolierung und chemische charakterisierung des hirudins. *Hoppe Seylers Z Physiol. Chem.* **1957**, *308*, 147-156.
93. P. Walsmann, F. Markwardt, Die reaktion zwischen hirudin und thrombin. *Hoppe Seylers Z Physiol. Chem.* **1958**, *312*, 85-98.
94. V. Erspamer, Biogenic amines and active polypeptides of the amphibian skin. *Ann. Rev. Pharmacol.* **1971**, *11*, 327-350.
95. M. Satoh, W. Zieglgansberger, W. Fries, A. Herz, Opiate agonist-antagonist interaction at cortical neurones of naive and tolerant/dependent rats. *Brain Res.* **1974**, *82*, 378-382.
96. H. W. Kosterlitz, J. Hughes, Some thoughts on the significance of enkephalin, the endogenous ligand. *Life Sci.* **1975**, *17*, 91-96.
97. J. Hughes, T. W. Smith, H. W. Kosterlitz, L. A. Fothergill, B. A. Morgan, H. R. Morris, Identification of two related pentapeptides from the brain with potent agonist activity. *Nature* **1975**, *258*, 577-579.
98. S. H. Snyder, Opiate receptor in normal and drug altered brain function. *Nature* **1975**, *257*, 185-189.
99. C. D. Unsworth, J. Hughes, J. S. Morely, O-sulphated leu-enkephalin in brain. *Nature* **1982**, *295*, 519-522.
100. J. D. Belluzzi, L. Stein, Enkephalin may mediate euphoria and drive-reduction reward. *Nature* **1977**, *266*, 556-558.
101. R. Simantov, S. H. Snyder, Morphine-like peptides, leucine enkephalin and methionine enkephalin: interactions with the opiate receptor. *Mol. Pharmacol.* **1976**, *12*, 987-998.
102. M. Amiche, A. Delfour, P. Nicolas, Opoid peptides from frog skin. *EXS* **1998**, *85*, 57-71.
103. C. Seibert, T. P. Sakmar, Toward a framework for sulfoproteomics: synthesis and characterization of sulfotyrosine-containing peptides. *Biopolymers (Pept. Sci.)* **2007**, *90*, 459-477.
104. M. Farzan, C. E. Schnitzler, N. Vasilieva, D. Leung, J. Kuhn, C. Gerard, N. P. Gerard, H. Choe, Sulfated tyrosines contribute to the formation of the C5a docking site of the human C5a anaphylatoxin receptor. *J. Exp. Med.* **2001**, *193*, 1059-1066.
105. C. B. Fieger, M.-C. Huang, J. R. Van Brocklyn, E. J. Goetzl, Type 1 sphingosine 1-phosphate G protein-coupled receptor signaling of lymphocyte functions requires sulfation of its extracellular amino-terminal tyrosines. *FASEB J.* **2005**, *19*, 1926-1928.
106. M. Bonomi, M. Busnelli, L. Persani, G. Vassart, S. Costagliola, Structural differences in the hinge region of the glycoprotein hormone receptors: evidence from the sulfated tyrosine residues. *Mol. Endocrinol.* **2006**, *20*, 3351-3363.
107. B. J. Doranz, J. Rucker, Y. Yi, R. J. Smyth, M. Samson, S. C. Peiper, M. Parmentier, R. G. Collman, R. W. Doms, A dual-tropic primary HIV-1 isolate that uses fusin and the beta-chemokine receptors CKR-5, CKR-3, and CKR-2b as fusion cofactors. *Cell* **1996**, *85*, 1149-1158.

108. H. Choe, M. Farzan, Y. Sun, N. Sullivan, B. Rollins, P. D. Ponath, L. Wu, C. R. Mackay, G. LaRosa, W. Newman, N. Gerard, C. Gerard, J. Sodroski, The [beta]-chemokine receptors CCR3 and CCR5 facilitate infection by primary HIV-1 isolates. *Cell* **1996**, *85*, 1135-1148.
109. M. Farzan, T. Mirzabekov, P. Kolchinsky, R. Wyatt, M. Cayabyab, N. P. Gerard, C. Gerard, J. Sodroski, H. Choe, Tyrosine sulfation of the amino-terminus of CCR5 facilitates HIV-1 entry. *Cell* **1999**, *96*, 667-676.
110. C.-c. Huang, S. N. Lam, P. Acharya, M. Tang, S.-H. Xiang, S. S.-u. Hussan, R. L. Stanfield, J. Robinson, J. Sodroski, I. A. Wilson, R. Wyatt, C. A. Bewley, P. D. Kwong, Structures of the CCR5 N-terminus and of a tyrosine-sulfated antibody with HIV-1 gp120 and CD4. *Science* **2007**, *317*, 1930-1934.
111. C. H. Chen, K. L. Moore, J. A. Leary, The pattern and temporal sequence of sulfation of CCR5 N-terminal peptides by tyrosylprotein sulfotransferase-2: an assessment of the effects of N-terminal residues. *Biochemistry* **2009**, *48*, 5332-5338.
112. A. Zlotnik, J. Morales, J. A. Hedrick, Recent advances in chemokines and chemokine receptors. *Crit. Rev. Immunol.* **1999**, *19*, 1-47.
113. P. D. Kwong, R. Wyatt, J. Robinson, R. W. Sweet, J. Sodroski, W. A. Hendrickson, Structure of an HIV gp120 envelope glycoprotein in complex with the CD4 receptor and a neutralizing human antibody. *Nature* **1998**, *393*, 648-659.
114. K. Godl, A. Hallmann, A. Rappel, M. Sumper, Pherophorins: a family of extracellular matrix glycoproteins from Volvox structurally related to the sex-inducing pheromone. *Planta* **1995**, *196*, 781-787.
115. R. W. Lee, W. B. Huttner, Tyrosine-O-sulfated proteins of PC12 pheochromocytoma cells and their sulfation by a tyrosylprotein sulfotransferase. *J. Biol. Chem.* **1983**, *258*, 11326-11334.
116. W.-C. Chang, T.-Y. Lee, D.-M. Shien, J. B.-K. Hsu, J.-T. Horng, H.-D. Huang, R.-L. Pan, Incorporating support vector machine for identifying protein tyrosine sulfation sites. *J. Comp. Chem.* **2009**, *30*, 2526-2537.
117. F. Monigatti, E. Gasteiger, A. Bairoch, E. Jung, The Sulfinator: predicting tyrosine sulfation sites in protein sequences. *Bioinformatics* **2002**, *18*, 769-770.
118. S. Niu, T. Huang, K. Feng, Y. Cai, Y. Li, Prediction of tyrosine sulfation with mRMR feature selection and analysis. *J. Proteome Res.* **2010**, *9*, 6490-6497.
119. F. Monigatti, B. Hekking, H. Steen, Protein sulfation analysis--a primer. *Biochim. Biophys. Acta* **2006**, *1764*, 1904-1913.
120. W. D. Kumler, J. J. Eiler, The acid strength of mono and diesters of phosphoric acid. The n-alkyl esters from methyl to butyl, the esters of biological importance, and the natural guanidine phosphoric acids. *J. Am. Chem. Soc.* **1943**, *65*, 2355-2361.
121. K. Kitagawa, C. Aida, H. Fujiwara, T. Yagami, S. Futaki, M. Kogire, J. Ida, K. Inoue, Facile solid-phase synthesis of sulfated tyrosine-containing peptides: total synthesis of human big gastrin-II and cholecystokinin (CCK)-39. *J. Org. Chem.* **2001**, *66*, 1-10.
122. P. A. Baeuerle, W. B. Huttner, Tyrosine sulfation is a trans-Golgi-specific protein modification. *J. Cell. Biol.* **1987**, *105*, 2655-2664.
123. W. B. Huttner, Determination and occurrence of tyrosine O-sulfate in proteins. *Methods Enzymol.* **1984**, *107*, 200-223.

124. H. Fraenkel-Conrat, H. S. Olcott, Esterification of proteins with alcohols of low molecular weight. *J. Biol. Chem.* **1945**, *161*, 259-268.
125. A. Hille, P. Rosa, W. B. Huttner, Tyrosine sulfation: a post-translational modification of proteins destined for secretion? *FEBS Lett.* **1984**, *177*, 129-134.
126. S. Young, S. Julka, G. Bartley, J. Gilbert, B. Wendelburg, S.-C. Hung, K. Anderson, W. Yokoyama, in *58th ASMS Conference on Mass Spectrometry and Allied Topics*. American Society for Mass Spectrometry: Salt Lake City, Utah, **2010**.
127. Y. Kanan, A. Hoffhines, A. Rauhauser, A. Murray, M. R. Al-Ubaidi, Protein tyrosine-*O*-sulfation in the retina. *Exp. Eye Res.* **2009**, *89*, 559-567.
128. D. M. Sherry, A. R. Murray, Y. Kanan, K. L. Arbogast, R. A. Hamilton, S. J. Fliesler, M. E. Burns, K. L. Moore, M. R. Al-Ubaidi, Lack of protein-tyrosine sulfation disrupts photoreceptor outer segment morphogenesis, retinal function and retinal anatomy. *Eur. J. Neurosci.* **2010**, *32*, 1461-1472.
129. M. Gharib, M. Marcantonio, S. G. Lehmann, M. Courcelles, S. Meloche, A. Verreault, P. Thibault, Artifactual sulfation of silver-stained proteins: implications for the assignment of phosphorylation and sulfation sites. *Mol. Cell. Proteomics* **2009**, *8*, 506-518.
130. R. E. Bossio, A. G. Marshall, Baseline resolution of isobaric phosphorylated and sulfated peptides and nucleotides by electrospray ionization FT ICR-MS: another step toward mass spectrometry-based proteomics. *Anal. Chem.* **2002**, *74*, 1674-1679.
131. J. R. Bundgaard, J. W. Sen, A. H. Johnsen, J. F. Rehfeld, Analysis of tyrosine-O-sulfation. *Methods Mol. Biol.* **2008**, *446*, 47-66.
132. J. W. Kehoe, Using phage display to select antibodies recognizing post-translational modifications independently of sequence context. *Mol. Cell. Proteomics* **2006**, *5*, 2350-2363.
133. A. J. Hoffhines, Detection and purification of tyrosine-sulfated proteins using a novel anti-sulfotyrosine monoclonal antibody. *J. Biol. Chem.* **2006**, *281*, 37877-37887.
134. J. J. Thomson, *Rays of Positive Electricity and Their Application to Chemical Analysis*. Longmans Green: London, **1913**.
135. A. J. Dempster, A new method of positive ray analysis. *Phys. Rev.* **1918**, *11*, 316-325.
136. J. B. Fenn, M. Mann, C. K. Meng, S. F. Wong, C. M. Whitehouse, Electrospray ionization for mass spectrometry of large biomolecules. *Science* **1989**, *246*, 64-71.
137. S. D.-H. Shi, C. L. Hendrickson, A. G. Marshall, Counting individual sulfur atoms in a protein by ultrahigh-resolution Fourier transform ion cyclotron resonance mass spectrometry: experimental resolution of isotopic fine structure in proteins. *Proc. Natl. Acad. Sci. U. S. A.* **1998**, *95*, 11532-11537.
138. E. N. Nikolaev, I. A. Boldin, R. Jertz, G. Baykut, Initial experimental characterization of a new ultra-high resolution FT-ICR cell with dynamic harmonization. *J. Am. Soc. Mass Spectrom.* **2011**, *22*, 1125-1133.
139. M. Karas, D. Bachmann, F. Hillenkamp, Influence of the wavelength in high-irradiance ultraviolet laser desorption mass spectrometry of organic molecules. *Anal. Chem.* **1985**, *57*, 2935-2939.
140. E. de Hoffmann, V. Stroobant, *Mass Spectrometry Principles and Applications*. 2nd ed.; John Wiley & Sons, Ltd.: Chichester, **2001**.

141. E. O. Lawrence, M. S. Livingston, The production of high speed light ions without the use of high voltages. *Phys. Rev.* **1932**, *40*, 19-35.
142. J. A. Hipple, H. Sommer, H. A. Thomas, A precise method of determining the Faraday by magnetic resonance. *Phys. Rev.* **1949**, *76*, 1877-1818.
143. M. B. Comisarow, A. G. Marshall, Fourier transform ion cyclotron resonance spectroscopy. *Chem. Phys. Lett.* **1974**, *25*, 282-283.
144. I. J. Amster, Fourier transform mass spectrometry. *J. Mass Spectrom.* **1996**, *31*, 1325-1337.
145. S. Guan, A. G. Marshall, Stored waveform inverse Fourier transform (SWIFT) ion excitation in trapped-ion mass spectrometry: theory and applications. *Int. J. Mass Spectrom. Ion Proc.* **1996**, *157-158*, 5-37.
146. J. T. Adamson, K. Hakansson, *Electrospray ionization Fourier transform ion cyclotron resonance mass spectrometry for lectin analysis*. Elsevier: Amsterdam, **2007**.
147. E. B. Ledford, D. L. Rempel, M. L. Gross, Space-charge effects in Fourier transform mass spectrometry - mass calibration. *Anal. Chem.* **1984**, *56*, 2744-2748.
148. P. Kebarle, U. H. Verkerk, Electrospray: from ions in solution to ions in the gas phase, what we know now. *Mass Spectrom Rev* **2009**, *28*, 898-917.
149. W. F. Haddon, F. W. McLafferty, Metastable ion characteristics. VII. Collision-induced metastables. *J. Am. Chem. Soc.* **1968**, *90*, 4745-4746.
150. K. R. Jennings, Collision-induced decompositions of aromatic molecular ions. *Int. J. Mass Spectrom. Ion Phys.* **1968**, *1*, 227-235.
151. D. P. Little, J. P. Speir, M. W. Senko, P. B. M. O'Connor, F. W., Infrared multiphoton dissociation of large multiply charged ions for biomolecule sequencing. *Anal. Chem.* **1994**, *66*, 2809-2815.
152. J. C. Lorquet, Whither the statistical theory of mass spectra? *Mass Spectrom. Rev.* **1994**, *13*, 233-257.
153. K. Biemann, H. A. Scoble, Characterization by tandem mass-spectrometry of structural modifications in proteins. *Science* **1987**, *237*, 992-998.
154. J. H. Bowie, C. S. Brinkworth, S. Dua, Collision-induced fragmentations of the $(M - H)^-$ parent anions of underivatized peptides: an aid to structure determination and some unusual negative ion cleavages. *Mass Spectrom. Rev.* **2002**, *21*, 87-107.
155. N. P. Ewing, C. J. Cassady, Dissociation of multiply charged negative ions for hirudin (54-65), fibrinopeptide B, and insulin A (oxidized). *J. Am. Soc. Mass Spectrom.* **2001**, *12*, 105-116.
156. A. R. Dongre, J. L. Jones, A. Somogyi, V. H. Wysocki, Influence of peptide composition, gas-phase basicity, and chemical modification on fragmentation efficiency: evidence for the mobile proton model. *J. Am. Chem. Soc.* **1996**, *118*, 8365-8374.
157. S. G. Summerfield, S. J. Gaskell, Fragmentation efficiencies of peptide ions following low energy collisional activation. *Int. J. Mass Spectrom. Ion Proc.* **1997**, *165-166*, 509-521.
158. C. S. Brinkworth, S. Dua, A. M. McAnoy, J. H. Bowie, Negative ion fragmentations of deprotonated peptides: Backbone cleavages directed through both Asp and Glu. *Rapid Commun. Mass Spectrom.* **2001**, *15*, 1965-1973.
159. C. S. Brinkworth, S. Dua, J. H. Bowie, Backbone cleavages of $(M-H)^-$ anions of peptides. New backbone cleavages following clyclisation reactions of a C-terminal [CONH]- group with Ser residues and the use of the gamma backbone cleavage initiated

by Gln to differentiate between Lys and Gln residues. *Eur. J. Mass Spectrom.* **2002**, *8*, 53-66.
160. P. Boontheung, C. S. Brinkworth, J. H. Bowie, R. V. Baudinette, Comparison of the positive and negative ion electrospray mass spectra of some small peptides containing pyroglutamate. *Rapid Commun. Mass Spectrom.* **2002**, *16*, 287-292.
161. P. Boontheung, P. F. Alewood, C. S. Brinkworth, J. H. Bowie, P. A. Wabnitz, M. J. Tyler, Negative ion electrospray mass spectra of caerulein peptides: an aid to structural determination. *Rapid Commun. Mass Spectrom.* **2002**, *16*, 281-286.
162. V. Katta, S. K. Chowdhury, B. T. Chait, Use of a single-quadrupole mass spectrometer for collision-induced dissociation studies of multiply charged peptide ions produced by electrospray ionization. *Anal. Chem.* **1991**, *63*, 174-178.
163. J. A. Loo, R. R. O. Loo, K. J. Light, C. G. Edmonds, R. D. Smith, Multiply-charged negative-ions by electrospray ionization of polypeptides and proteins. *Anal. Chem.* **1992**, *64*, 81-88.
164. S. T. Steinborner, J. H. Bowie, The negative ion mass spectra of M-H (-) ions derived from caeridin and dynastin peptides. Internal backbone cleavages directed through Asp and Asn residues. *Rapid Commun. Mass Spectrom.* **1997**, *11*, 253-258.
165. J. A. Loo, C. G. Edmonds, R. D. Smith, Tandem mass spectrometry of very large molecules. 2. Dissociation of multiply charged proline-containing proteins from electrospray ionization. *Anal. Chem.* **1993**, *65*, 425-438.
166. M. W. Senko, J. P. Speir, F. W. McLafferty, Collisional activation of large multiply charged ions using Fourier transform mass spectrometry. *Anal. Chem.* **1994**, *66*, 2801-2808.
167. E. R. Williams, Proton transfer reactivity of large multiply charged ions. *J. Mass Spectrom.* **1996**, *31*, 831-842.
168. F. Kjeldsen, O. A. Silivra, I. A. Ivonin, K. F. Haselmann, M. Gorshkov, R. A. Zubarev, C-alpha-C backbone fragmentation dominates in electron detachment dissociation of gas-phase polypeptide polyanions. *Chem.-Eur. J.* **2005**, *11*, 1803-1812.
169. J. Laskin, Z. Yang, C. Lam, I. K. Chu, Charge-remote fragmentation of odd-electron peptide ions. *Anal. Chem.* **2007**, *79*, 6607-6614.
170. B. A. Budnik, K. F. Haselmann, R. A. Zubarev, Electron detachment dissociation of peptide di-anions: an electron-hole recombination phenomenon. *Chem. Phys. Lett.* **2001**, *342*, 299-302.
171. R. A. Zubarev, Reactions of polypeptide ions with electrons in the gas phase. *Mass Spectrom. Rev.* **2003**, *22*, 57-77.
172. I. Anusiewicz, M. Jasionowski, P. Skurski, J. Simons, Backbone and side-chain cleavages in electron detachment dissociation (EDD). *J. Phys. Chem. A* **2005**, *109*, 11332-11337.
173. S. G. Lias, J. E. Bartmess, J. F. Liebman, J. L. Holmes, R. D. Levin, W. G. Mallard, Gas-phase ion and neutral thermochemistry. *J. Phys. Chem. Ref. Data* **1988**, *17*.
174. S. Campbell, J. L. Beauchamp, M. Rempe, D. L. Lichtenberger, Correlations of lone pair ionization energies with proton affinities of amino acids and related compounds. Site specificity of protonation. *Int. J. Mass Spectrom. Ion Proc.* **1992**, *117*, 83-99.
175. B. A. Budnik, R. A. Zubarev, $MH2^{+\cdot}$ ion production from protonated polypeptides by electron impact: observation and determination of ionization energies and a cross-section. *Chem. Phys. Lett.* **2000**, *316*, 19-23.

176. R. A. Zubarev, M. L. Nielsen, B. A. Budnik, Tandem ionization mass spectrometry of biomolecules. *Eur J Mass Spectrom* **2000**, *6*, 235-240.
177. H. K. Kweon, K. Hakansson, Metal oxide-based enrichment combined with gas-phase ion-electron reactions for improved mass spectrometric characterization of protein phosphorylation. *J. Proteome Res.* **2008**, *7*, 749-755.
178. J. J. Wolff, F. E. Leach III, T. N. Laremore, D. A. Kaplan, M. L. Easterling, R. J. Linhardt, I. J. Amster, Negative electron transfer dissociation of glycosaminoglycans. *Anal. Chem.* **2010**, *82*, 3460-3466.
179. B. Ganisl, T. Valovka, M. Hartl, M. Taucher, K. Bister, K. Breuker, Electron detachment dissociation for top-down mass spectrometry of acidic proteins. *Chem. Eur. J.* **2011**, *17*, 4460-4469.
180. J. J. Coon, J. Shabanowitz, D. F. Hunt, J. E. P. Syka, Electron transfer dissociation of peptide anions. *J. Am. Soc. Mass Spectrom.* **2005**, *16*, 880-882.
181. M. Huzarska, I. Ugalde, D. A. Kaplan, R. Hartmer, M. L. Easterling, N. C. Polfer, Negative electron transfer dissociation of deprotonated phosphopeptide anions: choice of radical cation reagent and competition between electron and proton transfer. *Anal. Chem.* **2010**, *82*, 2873-2878.
182. H. J. Yoo, N. Wang, S. Zhuang, H. Song, K. Håkansson, Negative-ion electron capture dissociation: radical-driven fragmentation of charge-increased gaseous peptide anions. *J. Am. Chem. Soc.* **2011**, *133*, 16790-16793.
183. Y. M. E. Fung, C. M. Adams, R. A. Zubarev, Electron ionization dissociation of singly and multiply charged peptides. *J. Am. Chem. Soc.* **2009**, *131*, 9977-9985.
184. P. Roepstorff, J. Fohlman, Proposal for a common nomenclature for sequence ions in mass spectra for peptides. *Biomed. Mass Spectrom.* **1984**, *11*, 601.
185. J.-L. Wolfender, F. Chu, H. Ball, F. Wolfender, M. Fainzilber, M. A. Baldwin, A. L. Burlingame, Identification of tyrosine sulfation in *Conus pennaceus* conotoxins a-PnIA and a-PnIB: further investigation of labile sulfo- and phosphopeptides by electrospray, matrix-assisted laser desorption/ionization (MALDI) and atmospheric pressure MALDI mass spectrometry. *J. Mass Spectrom.* **1999**, *34*, 447-454.
186. J. F. Nemeth-Cawley, S. Karnik, J. C. Rouse, Analysis of sulfated peptides using positive electrospray ionization tandem mass spectrometry. *J. Mass Spectrom.* **2001**, *36*, 1301-1311.
187. M. Salek, S. Costagliola, W. D. Lehmann, Protein tyrosine-O-sulfation analysis by exhaustive product ion scanning with minimum collision offset in a NanoESI Q-TOF tandem mass spectrometer. *Anal. Chem.* **2004**, *76*, 5136-5142.
188. K. F. Haselmann, B. A. Budnik, J. V. Olsen, M. L. Nielsen, C. A. Reis, H. Clausen, A. H. Johnsen, R. A. Zubarev, Advantages of external accumulation for electron capture dissociation in Fourier transform mass spectrometry. *Anal. Chem.* **2001**, *73*, 2998-3005.
189. K. F. Medzihradszky, S. Guan, D. A. Maltby, A. L. Burlingame, Sulfopeptide fragmentation in electron-capture and electron-transfer dissociation. *J. Am. Soc. Mass Spectrom.* **2007**, *18*, 1617-1624.
190. L. S. Eberlin, Y. Xia, H. Chen, R. G. Cooks, Atmospheric pressure thermal dissociation of phospho- and sulfopeptides. *J. Am. Soc. Mass Spectrom.* **2008**, *19*, 1897-1905.

191. Y. Yu, A. J. Hoffhines, K. L. Moore, J. A. Leary, Determination of the sites of tyrosine O-sulfation in peptides and proteins. *Nat. Methods* **2007**, *4*, 583-588.
192. M. Ueki, M. Yamaguchi, Enhanced detection of sulfo-peptides as onium salts in matrix-assisted laser desorption/ionization time-of-flight mass spectrometry. *Rapid Commun. Mass Spectrom.* **2006**, *20*, 1615-1620.
193. Shannon L. Cook, G. P. Jackson, Metastable atom-activated dissociation mass spectrometry of phosphorylated and sulfonated peptides in negative ion mode. *J. Am. Soc. Mass Spectrom.* **2011**, *22*, 1088-1099.
194. S. W. Taylor, C. Sun, A. Hsieh, N. L. Andon, S. S. Ghosh, A sulfated, phosphorylated 7 kDa secreted peptide characterized by direct analysis of cell culture media. *J. Proteome Res.* **2008**, *7*, 795-802.
195. J. Rappsilber, H. Steen, M. Mann, Labile sulfogroup allows differentiation of sulfotyrosine and phosphotyrosine in peptides. *J. Mass Spectrom.* **2001**, *36*, 832-833.
196. H. Liu, K. Hakansson, Electron capture dissociation of tyrosine O-sulfated peptides complexed with divalent metal cations. *Anal. Chem.* **2006**, *78*, 7570-7576.
197. J. E. P. Syka, J. J. Coon, M. J. Schroeder, J. Shabanowitz, D. F. Hunt, Peptide and protein sequence analysis by electron transfer dissociation mass spectrometry. *Proc. Nat. Acad. Sci. U.S.A.* **2004**, *101*, 9528-9533.
198. A. G. Marshall, C. L. Hendrickson, S. D. H. Shi, Scaling MS plateaus with high-resolution FT-ICR MS. *Anal Chem* **2002**, *74*, 253A-259A.
199. S. A. Smith, C. L. Kalcic, K. A. Safran, P. M. Stemmer, M. Dantus, G. E. Reid, Enhanced characterization of singly protonated phosphopeptide ions by femtosecond laser-induced ionization/dissociation tandem mass spectrometry (fs-LID-MS/MS). *J. Am. Soc. Mass Spectrom.* **2010**, *21*, 2031-2040.
200. V. G. Voinov, M. L. Deinzer, D. F. Barofsky, Radio-frequency-free cell for electron capture dissociation in tandem mass spectrometry. *Anal. Chem.* **2009**, *81*, 1238-1243.
201. A. Makarov, Electrostatic axially harmonic orbital trapping: a high-performance technique of mass analysis. *Anal. Chem.* **2000**, *72*, 1156-1162.
202. A. G. Marshall, C. L. Hendrickson, G. S. Jackson, Fourier transform ion cyclotron resonance mass spectrometry: a primer. *Mass Spectrom. Rev.* **1998**, *17*, 1-35.
203. A. Tholey, J. Reed, W. D. Lehmann, Electrospray tandem mass spectrometric studies of phosphopeptides and phosphopeptide analogues. *J. Mass Spectrom.* **1999**, *34*, 117-123.
204. P. T. Jedrzejewski, W. D. Lehmann, Detection of modified peptides in enzymatic digests by capillary liquid chromatography/electrospray mass spectrometry and a programmable skimmer CID acquisition routine. *Anal. Chem.* **1997**, *69*, 294-301.
205. J. M. Wells, S. A. McLuckey, Collision-induced dissociation (CID) of peptides and proteins. *Methods Enzymol* **2005**, *402*, 148-185.
206. M. Edelson-Averbukh, A. Shevchenko, R. Pipkorn, W. D. Lehmann, Discrimination between peptide O-sulfo- and O-phosphotyrosine residues by negative ion mode electrospray tandem mass spectrometry. *J. Am. Soc. Mass Spectrom.* **2011**, *22*, 2256-2268.
207. D. J. C. Yates, Infrared studies of the surface hydroxyl groups on titanium dioxide and of the chemisorption of carbon monoxide and carbon dioxide. *J. Phys. Chem.* **1961**, *65*, 746-753.

208. V. Bolis, B. Fubini, E. Garpone, C. Morterra, P. Ugliengo, Induced heterogeneity at the surface of group 4 dioxides as revealed by CO adsorption at room temperature. *J. Chem. Soc., Faraday Trans.* **1992**, *88*, 391-398.
209. E. Garrone, V. Bolis, B. Fubini, C. Morterra, Thermodynamic and spectroscopic characterization of ambient temperature heterogeneity among adsorption sites: CO on anatase at ambient temperature. *Langmuir* **1989**, *5*, 892-899.
210. P. A. Connor, K. D. Dobson, A. J. McQuillan, New sol-gel attenuated total reflection infrared spectroscopic method for analysis of adsorption at metal oxide surfaces in aqueous solutions. Chelation of TiO_2, ZrO_2, and Al_2O_3 surfaces by catechol, 8-quinolinol, and acetylacetone. *Langmuir* **1995**, *11*, 4193-4195.
211. P. A. Connor, A. J. McQuillan, Phosphate adsorption onto TiO_2 from aqueous solutions: an in situ internal reflection infrared spectroscopic study. *Langmuir* **1999**, *15*, 2916-2921.
212. D. Muljadi, A. M. Posner, J. P. Quirk, The mechanism of phosphate adsorption by kaolinite, gibbsite and pseudoboehmite. Part I. The isotherms and the effect of pH on the adsorption. *J. Soil Sci.* **1966**, *17*, 212-229.
213. T. E. Thingholm, T. J. Jorgensen, O. N. Jensen, M. R. Larsen, Highly selective enrichment of phosphorylated peptides using titanium dioxide. *Nat. Protoc.* **2006**, *1*, 1929-1935.
214. E. S. Simon, M. Young, A. Chan, Z.-Q. Bao, P. C. Andrews, Improved enrichment strategies for phosphorylated peptides on titanium dioxide using methyl esterification and pH gradient elution. *Anal. Biochem.* **2008**, *377*, 234-242.
215. N. E. Tret'yakov, V. N. Filimonov, An infrared spectroscopic study of the relative proton-donating power of the OH-groups of oxide surfaces. *Kinet. Catal.* **1972**, *13*, 735-737.
216. H. Dobson, A. J. McQuillan, In situ infrared spectroscopic analysis of the adsorption of aliphatic carboxylic acids to TiO_2, ZrO_2, Al_2O_3, Ta_2O_5 from aqueous solutions. *Spectrochim. Acta A* **1999**, *55*, 1395-1405.
217. K. D. Dobson, A. J. McQuillan, In situ infrared spectroscopic analysis of the adsorption of aromatic carboxylic acids to TiO_2, ZrO_2, Al_2O_3, and Ta_2O_5 from aqueous solutions. *Spectrochim. Acta A* **2000**, *56*, 557-565.
218. M. R. Larsen, T. E. Thingholm, O. N. Jensen, P. Roepstorff, T. J. Jorgensen, Highly selective enrichment of phosphorylated peptides from peptide mixtures using titanium dioxide microcolumns. *Mol. Cell. Proteomics* **2005**, *4*, 873-886.
219. S. S. Jensen, M. R. Larsen, Evaluation of the impact of some experimental procedures on different phosphopeptide enrichment techniques. *Rapid Commun. Mass Spectrom.* **2007**, *21*, 3635-3645.
220. H. K. Kweon, K. Hakansson, Selective zirconium dioxide-based enrichment of phosphorylated peptides for mass spectrometric analysis. *Anal. Chem.* **2006**, *78*, 1743-1749.
221. G. Pocsfalvi, M. Cuccurullo, G. Schlosser, S. Scacco, S. Papa, A. Malorni, Phosphorylation of B14.5a subunit from bovine heart complex I identified by titanium dioxide selective enrichment and shotgun proteomics. *Mol. Cell. Proteomics* **2007**, *6*, 231-237.

222. P. Joo, G. Horanyi, Radiotracer study of the specific adsorption of anions on metal oxides in acid media: an experimental approach. *J. Colloid Interf. Sci.* **2000**, *223*, 308-310.
223. G. Horanyi, P. Joo, In situ study of the specific adsorption of HSO_4^-/SO_4^{2-} ions on hematite by radiotracer technique. *J. Colloid Interf. Sci.* **2000**, *227*, 206-211.
224. G. Horanyi, P. Joo, Comparative radiotracer study of the absorption of sulfate and pertechnetate ions on gamma-Al_2O_3. *J. Colloid Interf. Sci.* **2001**, 46-51.
225. G. Horanyi, Investigation of the specific adsorption of sulfate ions on powdered TiO_2. *J. Colloid Interf. Sci.* **2003**, *261*, 580-583.
226. Y.-C. Chang, C.-N. Huang, C.-H. Lin, H.-C. Chang, C.-C. Wu, Mapping protein cysteine sulfonic acid modifications with specific enrichment and mass spectrometry: An integrated approach to explore the cysteine oxidation. *Proteomics* **2010**, *10*, 2961-2971.
227. Y. Amano, H. Shinohara, Y. Sakagami, Y. Matsubayashi, Ion-selective enrichment of tyrosine-sulfated peptides from complex protein digests. *Anal. Biochem.* **2005**, *346*, 124-131.
228. K. G. Reddie, K. S. Carroll, Expanding the functional diversity of proteins through cysteine oxidation. *Curr. Opin. Chem. Biol.* **2008**, *12*, 746-754.
229. E. Kuhnel, D. D. P. Laffan, G. C. Lloyd-Jones, T. Martinez del Campo, I. R. Shepperson, J. L. Slaughter, Mechanism of methyl esterification of carboxylic acids by trimethylsilyldiazomethane. *Angew. Chem. Int. Ed.* **2007**, *46*, 7075-7078.
230. C. R. Cantor, P. R. Schimmel, *Biophysical Chemistry*. W. H. Freeman and Co.: San Francisco, CA, **1980**.
231. I. Lindh, W. J. Griffiths, T. Bergman, J. Sjovall, Charge-remote fragmentation of peptides derivatized with 4-aminonaphthalenesulphonic acid. *Rapid Commun. Mass Spectrom.* **1994**, *8*, 797-803.
232. J. Zhang, W. J. Griffiths, T. Bergman, J. Sjovall, Derivatization of bile acids with taurine for analysis by fast atom bombardment mass spectrometry with collision-induced fragmentation. *J. Lipid Res.* **1993**, *34*, 1895-1900.
233. A. Kharlamova, S. A. McLuckey, Negative electrospray droplet exposure to gaseous bases for the manipulation of protein charge state distributions. *Anal. Chem.* **2011**, *83*, 431-437.
234. R. A. Zubarev, K. F. Haselmann, B. A. Budnik, F. Kjeldsen, F. Jensen, Towards an understanding of the mechanism of electron-capture dissociation: a historical perspective and modern ideas. *Eur. J. Mass Spectrom.* **2002**, *8*, 337-349.
235. H. C. Liu, K. Hakansson, Divalent metal ion-peptide interactions probed by electron capture dissociation of trications. *J. Am. Soc. Mass Spectrom.* **2006**, *17*, 1731-1741.
236. Y. M. E. Fung, H. Liu, T.-W. D. Chan, Electron capture dissociation of peptides metalated with alkaline-earth metal ions. *J. Am. Soc. Mass Spectrom.* **2006**, *17*, 757-771.
237. J. Chamot-Rooke, G. van der Rest, A. Dalleu, S. Bay, J. Lemoine, The combination of electron capture dissociation and fixed charge derivatization increases sequence coverage for O-glycosylated and O-phosphorylated peptides. *J. Am. Soc. Mass Spectrom.* **2007**, *18*, 1405-1413.
238. X. Liu, R. B. Cole, A new model for multiply charged adduct formation between peptides and anions in electrospray mass spectrometry. *J. Am. Soc. Mass Spectrom.* **2011**, *22*, 2125-2136.

CHAPTER II

TITANIUM DIOXIDE ENRICHMENT OF SULFOPEPTIDES

2.1 Introduction

Protein *O*-sulfonation is a widespread post-translational modification (PTM) of tyrosine in vertebrates and invertebrates.[1] However, sulfonation (often incorrectly referred to as sulfation[2-3]) is less common than the isobaric phosphorylation in current literature. A PubMed literature search retrieves nearly 850 journal articles associated with sulfation (plus ~180 journal articles associated with sulfonation) published within the past five years compared with over 10,000 journal articles associated with phosphorylation published within the past two years. Possible reasons for the lack of recent literature covering sulfonation analysis may relate to a lack of understanding of the biological roles of sulfonated species[3] as well as a lack of appropriate analysis methods.

Ivy, et al. reported in 1928 that the presence of a "secretin" they subsequently named cholecystokinin (CCK) stimulates contraction of the gall bladder in cats and dogs.[4] Nearly fifty years later, sulfonated CCK (CCKS) was reported to exhibit neurological function in the mammalian brain.[5] Subsequent discoveries of other sulfopeptides have since confirmed hormonal activity in several organisms.[6-8] In a more

recent report, this sulfonated peptide, which has been shown to also drastically affect mammalian satiation,[9] was quantified in hamster plasma.[10-11] Other reported biological functions of sulfonated peptides and proteins include protein-protein signaling[12] and neuroendocrine function.[13] They also play a critical role in the binding and metabolism of the glycoprotein thyroglobulin by thyroid cells.[14]

Proteins and peptides destined for sulfonation are post-translationally modified in the trans-Golgi network[15] via highly-specific tyrosylprotein sulfotransferases[3, 16] then secreted for extracellular biological activity. Thus, sulfonation is thought to be limited to secretory and membrane proteins and peptides commonly located outside the cell at very low concentrations, making isolation a difficult task. Furthermore, the acid and heat lability of the sulfonate group[17-18] limit the number of feasible analysis and isolation methods.

The use of mass spectrometry (MS) in high-throughput analyses of biologically-derived samples has escalated in the past two decades following the initial implementation of electrospray ionization for sample introduction to mass spectrometry in the early 1990s.[19] The most commonly utilized biomolecular MS ionization approaches are positive-ion mode matrix-assisted laser desorption/ionization (+MALDI) and electrospray ionization mass spectrometry (+ESI-MS). Nemeth-Cawley, et al. have reported that commonly used electrospray conditions for +ESI-MS promote in-source fragmentation of labile sulfonates,[18] possibly precluding detection of intact sulfopeptides. Further, Wolfender, et al. stated that +MALDI-MS is unlikely to reveal the presence of sulfotyrosine.[20] An alternative approach is to analyze sulfopeptides in negative ion mode, in which tyrosine *O*-sulfonate groups are more stable, presumably due to the absence of

a mobile proton.[21] Negative ion mode analysis may be particularly favorable for sulfopeptides because several amino acid residues surrounding the sulfonated tyrosine residue are commonly acidic.[22-25]

One challenge in MS analysis of phosphorylated and sulfonated proteins and peptides is to obtain mass resolution between these isobaric PTMs (Δm = 9 mDa).[26] Many commonly used MS instruments [e.g., triple quadrupole (QQQ), quadrupole time-of-flight (Q-TOF), quadrupole ion trap (QIT)] cannot provide the required mass resolution to distinguish sulfonation and phosphorylation, thus leaving room for misidentifications. In fact, Gharib, et al. recently reported that artificially sulfonated peptides could be routinely misidentified as phosphorylated peptides in low-resolution ESI-MS following protein extraction from silver-stained polyacrylamide gels.[27] High-resolution instruments such as Fourier transform ion cyclotron resonance (FT-ICR) mass spectrometers can offer a mass resolution of ≥400,000 and can thus get around this problem.[26]

There are currently very few isolation methods for sulfonated proteins and peptides.[28-29] Amano, et al. have employed ion-exchange chromatography for sulfopeptide enrichment[28] while, more recently, Chang, et al. have employed ionic affinity capture with poly-arginine coated nanodiamonds for the enrichment of cysteine sulfonic acids.[29] Although these methods offer advantages, they also suffer from inherent drawbacks. The first salt-based method requires sample cleanup prior to detection by mass spectrometry, which can result in sample loss. The second method is quite complex and requires synthesis of the binding materials. While these methods expand our toolbox

for sulfonate analysis, there is room for improvement in the enrichment and detection of sulfonated proteins and peptides.

Recent reports have shown that metal oxides may act as Lewis acids to interact with phosphorylated peptides.[30-33] This interaction can be manipulated through pH modification of the binding (low pH) and elution (high pH) conditions.[31, 34] Reports published by McQuillan and co-workers in the late 1990s to early 2000s illustrate the capabilities of metal oxides to interact with poly-oxyanions, such as phosphorylated groups[34] and carboxylic acid groups[35-36] but contained no data regarding the possible interaction of sulfonate moieties with metal oxides. During the same time, others showed that the chemically similar sulfate group (in its non-substituted free form) can interact with a variety of metal-oxide surfaces, including goethite,[37] hematite,[38-40] alumina,[41] as well as titanium dioxide.[42] Here, we present a TiO_2-based enrichment method that is similar to our previously published method for phosphopeptide enrichment[31] but is fully optimized for sulfopeptide enrichment.

2.2 Materials and methods

2.2.1 Sample Preparation

Bovine serum albumin and equine apomyoglobin (BSA and ApoMb; Sigma, St. Louis, MO) were each prepared in 25 mM ammonium bicarbonate, pH 8.0 (Fisher Scientific, Fair Lawn, NJ). Proteins were reduced with 10 mM dithiothreitol (Sigma) for 1 h at 37 ^{o}C then alkylated with 2.5 mM iodoacetamide (Sigma) in the dark at room temperature for 1 h. Following reduction and alkylation (for BSA only), proteins were

digested with trypsin at a 1:100 enzyme/protein ratio at 37 ^{o}C for 18 h. The digestion was stopped with 2 μL of 50% formic acid (Acros Organics, Fair Lawn, NJ) and stored at -80 ^{o}C until further use.

2.2.2 Enrichment Procedure

The enrichment protocol used here was modified from a previously published protocol for phosphopeptide enrichment.[31] Titanium dioxide microtips (50 μg) were purchased or provided as a gift from Glygen (Columbia, MD). The enrichment samples consisted of one or more sulfopeptides [sulfonated cholecystokinin fragment 26-33 (CCKS, DyMGWMDF-NH_2; Advanced ChemTech, Louisville, KY), sulfonated hirudin fragment 55-65 (HIR, DFEEIPEEyLQ; Advanced ChemTech) and sulfonated caerulein (CRL, pEQDyTGWMDF-NH_2; Bachem, Torrance, CA)] mixed with either an ApoMb or a BSA tryptic digest at various molar ratios. For the proof of concept and enrichment optimization experiments (Figures 1 and 2, respectively), either an ApoMb or BSA digest was mixed with CCKS at a molar ratio of 1:1. Following optimization, all sulfopeptides were introduced at molar ratios of protein digest to sulfopeptide ranging from 1:1 to 8:1. To bind sulfopeptides, 10 μL of 3.3% v/v formic acid at pH 2.0-3.5 mixed with the dried sample of interest was aspirated and dispensed 20 times followed by two 10 μL washes with HPLC-grade water (Fisher) using 10 aspirate-dispense cycles to remove any non-specifically interacting species. In the final step, 10 μL of 0.25% v/v ammonium hydroxide (Sigma) at pH 10.0 was aspirated and dispensed 10 times to elute the sulfopeptides. After enrichment, peptide solutions were neutralized then dried in a vacuum concentrator (Eppendorf, Hamberg, Germany). Samples were reconstituted for ESI-FT-ICR MS analysis in either positive-ion mode (1:1 H_2O:ACN, 0.1% FA) or

negative-ion mode (1:2:1 ACN:H_2O:IPA, 0.25% v/v piperidine or 1:1 H_2O:IPA, 1% v/v TEA).

2.2.3 Mass Spectrometry

Mass measurements were performed on a 7-T hybrid quadrupole (Q)-FT-ICR mass spectrometer (Apex-Q, Bruker Daltonics, Billerica, MA) equipped with an Apollo II electrospray ionization source. The ESI flow rate was set at 70 μL/h and N_2 nebulizing gas was operated at 2.0 bar. Ions were accumulated in the first hexapole for 0.05 s then transferred through the quadrupole in broadband (rf-only) mode to the second hexapole, where ions were accumulated for 0.5-1 s. Ions were then transferred through the high-voltage ion optics and dynamically trapped in the ICR cell. The accumulation process was looped three times prior to excitation and detection as an image current in the ICR cell. Frequencies corresponding to m/z 200 to 2000 were displayed using the Bruker XMASS software (v. 7.0.6) with 256k data points summed over 10-16 scans.

2.2.4 Data Analysis

Open-source MIDAS software (v. 3.21)[43] was used for fast Fourier transformation and peak picking. Calculated m/z ratios for proteins and peptides were acquired from MS Product in Protein Prospector (http://prospector.ucsf.edu/prospector/mshome.htm) and the PeptideMass tool in Expasy (http://www.expasy.ch/tools/peptide-mass.html). Internal calibration was performed using a two-term frequency-to-mass calibration[44] in Microsoft Excel. These calculated values were compiled into an in-house generated macro and searched against experimental m/z ratios for peak identification and accurate mass matching. Peaks of less than or equal to 15 ppm error and greater than 2% relative abundance were accepted for percent relative abundance calculations. Peak abundances

were normalized to charge by summing all peaks associated with a particular protein or sulfopeptide of a particular charge state then dividing by that charge state. The percent relative abundance of the summed peaks associated with a protein or a sulfopeptide was calculated by dividing the normalized abundance of the summed peaks by the total normalized abundance for all identified peaks in the spectrum. Calculated error for repeat control and enrichment data sets was less than 10% in all cases.

2.3 Results

2.3.1 Proof-of-Concept Experiment: Positive-Ion Mode Analysis of Titanium Dioxide-Enriched Sulfopeptides

Titanium dioxide enrichment protocols have been used extensively by our group and others for the enrichment of phosphopeptides.[30-33, 45] The proposed mechanism behind phosphopeptide interaction with titanium dioxide and other metal oxide materials suggests that these materials should also interact with other poly-oxyanion species.[46] Thus, we evaluated our phosphopeptide enrichment protocol for enrichment of sulfonated peptides from digestion mixtures.

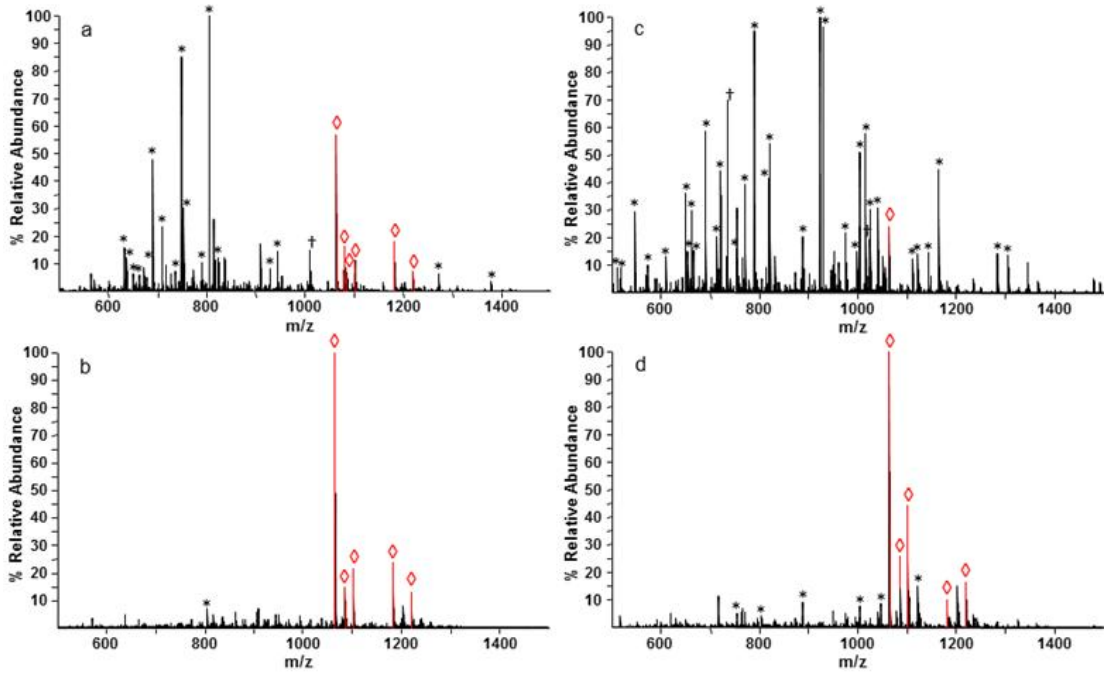

Figure 2.1a – d. Positive-ion mode ESI-MS spectra of an ApoMb (1a, 1b) or BSA (1c, 1d) protein digest mixed with sulfonated cholecystokinin fragment 26-33 (CCKS) at a 1:1 molar ratio before (a, c) and after (b, d) titanium dioxide (TiO_2) enrichment. ApoMb and BSA peaks are labeled with asterisks (*) and trypsin autolysis peaks with a dagger (†) while CCK/S peaks are labeled in red with a diamond (◊).

As shown in Figure 2.1a, a mixture of an ApoMb digest and CCKS at an equimolar ratio in positive ion mode ESI produces signal corresponding mostly to ApoMb peptides. Prior to enrichment, 26±3% of the total identifiable ion signal belongs to cholecystokinin, either in its desulfonated or sulfonated form (CCK/S). After TiO_2 enrichment (Figure 2.1b), the most abundant peaks are protonated or salt-adducted CCK following loss of the labile sulfonate group during in-source fragmentation, which has been observed and documented in the literature.[18] The total relative abundance of CCK/S improves to 94±2% for an approximate 3.5-fold increase in sulfopeptide signal following enrichment. Additionally, there is only one remaining ApoMb peak, corresponding to the doubly protonated peptide VEADIAGHGQEVLIR, present after TiO_2 enrichment. This

particular peptide is highly acidic with four carboxylic acid moieties. It has been previously shown that peptides with multiple carboxylic acids can also remain in phosphopeptide enrichment by titanium and zirconium dioxide.[31] The observed high selectivity against non-sulfonated peptide ions suggests that TiO_2 enrichment can be optimized as a highly selective method for the enrichment of sulfopeptides.

When altering the sample matrix, enrichment still occurred to a high degree. In Figure 2.1c, a single CCK/S peak representing 2±1% of the total relative identifiable ion abundance is barely noticeable in a complex spectrum containing over 30 BSA peptide peaks. Following TiO_2 enrichment (Figure 2.1d), CCK/S peaks dominate the spectrum and represent 74±2% of the total relative abundance with few BSA peaks observed. At an equimolar ratio to a protein tryptic digest, CCKS could be enriched ~4–25-fold from a mixture containing an ApoMb or a BSA digest, respectively. Additionally, in the non-enriched spectra (Figures 2.1a, 2.1c), there are considerably more relatively abundant peaks ($\geq$ 15%) that could not be identified in comparison to the enriched spectra that have no unidentifiable peaks at the same relative abundance.

2.3.2 Optimization of loading amount and binding conditions for 50 µg titanium dioxide microtips

For titanium dioxide enrichment to work properly, there is a minimum loading amount for the particular size of microtip used (here 50 µg) as well as optimum pH values for both binding and elution of sulfopeptides. As previously reported,[31] the minimum loading amount for the most efficient phosphopeptide enrichment was 50–100 pmol, though as low as 25 pmol of material could be enriched with 50 µg TiO_2 or ZrO_2 microtips. In Figure 2.2a–d, the enrichment efficiency for different loading amounts of a

CCKS:ApoMb mixture from 50 to 300 pmol was examined. Table 2.1 highlights the percent relative abundance of ApoMb and CCK/S calculated for spectra in Figure 2.2. The highest percentage of relative sulfopeptide abundance after enrichment resulted from loading 200 pmol each of CCKS and ApoMb peptides onto the 50 µg microtips.

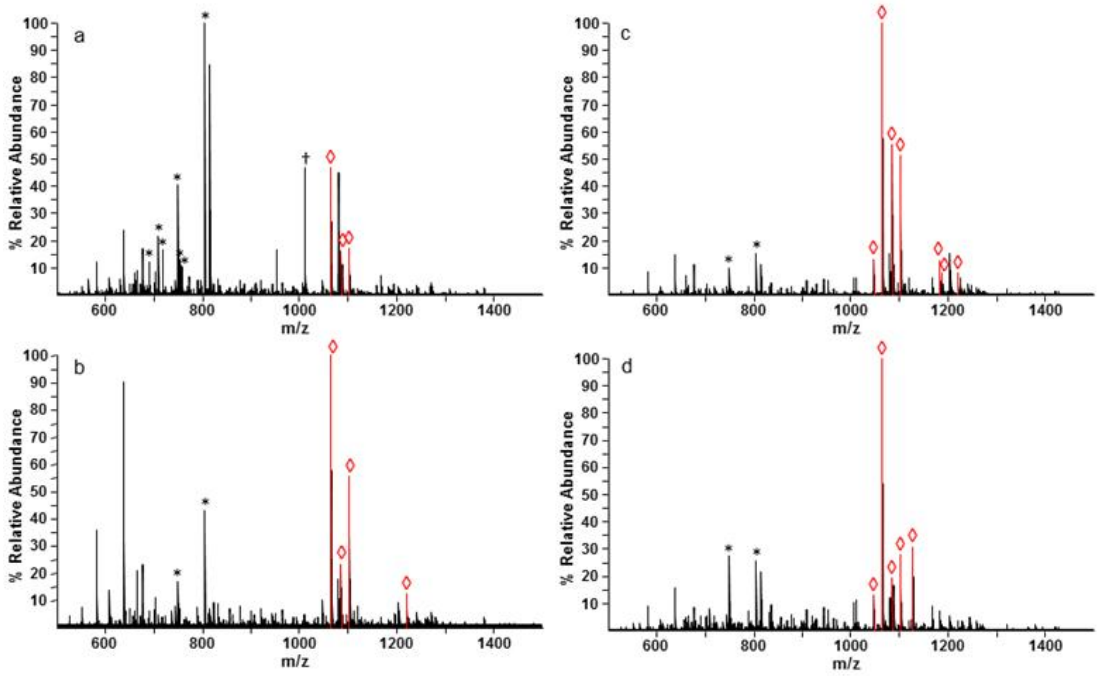

Figure 2.2a – d. Positive-ion mode ESI-MS spectra of an ApoMb digest mixed with CCKS at a 1:1 molar ratio and TiO_2-enriched at 50pmol (a), 100pmol (b), 200pmol (c), and 300pmol (d) of each protein digest/sulfonated peptide mixture loaded onto the TiO_2 tips. ApoMb peaks are labeled with asterisks (*) and trypsin autolysis peaks with a dagger (†) while CCK/S peaks are labeled in red with a diamond (◊).

	50 pmol	100 pmol	200 pmol	300 pmol
CCK/S	37%	74%	88%	69%

Table 2.1. Calculated percent relative abundance for equimolar ratios of CCKS and ApoMb following TiO_2 enrichment at a binding pH of 2.5 and an elution pH of 10.0. The estimated error for these measurements is 2%.

It is important to note that, in each spectrum, the relative abundance of ApoMb and unknown peaks is much higher for amounts that are below 200 pmol. It is possible that this lower selectivity is due to non-selective binding by carboxylate groups. Larsen et al. have proposed bridging and chelating bidentate binding modes for phosphate and carboxylate species, respectively, with the TiO_2 surface present in microcolumns from GL Sciences.[32] These authors cite reports from McQuillan, et al. who used TiO_2 sol-gel films exhibiting a structure that is "predominantly amorphous with a small anatase content."[34] The latter report suggests that carbonate and phosphate bind to the same surface sites. Our observed selectivity of sulfopeptide binding to the TiO_2 surface suggests either that sulfonate groups bind more strongly than carboxylates to the same sites, or that sulfonate and carboxylate exhibit different binding modes, similar to phosphate/carboxylate. In either case, having or exceeding a minimum binding amount for sulfonate enrichment is crucial to maintaining highly selective binding. Li, et al. have suggested that determining an optimal ratio of TiO_2 enrichment material to phosphorylated peptides is critical for improving enrichment selectivity.[47]

Alternatively, it is possible to reduce the amount of titanium dioxide present in the microtips or reduce the number of carboxylic acids in the enrichment mixture. First, reducing the physical amount of TiO_2 in the microtips provides a smaller surface area of interaction, thus requiring less minimum starting material. We attempted enrichment of varying amounts from 1–50 pmol sulfopeptide at 1:1–1:10 ratio of sulfopeptide to BSA digest with smaller microtips containing ~25 μg titanium dioxide material, but poor reproducibility and limited enrichment selectivity hampered progress (data not shown). Perhaps a superior method for miniaturization of the microtips would be to pursue an

online LC-based enrichment approach to provide both enhanced sensitivity and selectivity while also potentially reducing losses from sample handling.[48-50] Secondly, reducing the number of carboxylic acids present may prevent non-specific interactions. Methyl esterification of carboxylic acids, in combination with pH gradient elution, has been reported to improve phosphopeptide binding to titanium dioxide particles.[45] These authors report using methanolic HCl for methyl esterification; however, there are a number of ways to esterify carboxylic acids but several of these methods require the use of acid (or produce it as a reaction by-product). This method works for phosphopeptides because they tolerate acid well; however, sulfopeptides are acid labile and produce a range of sulfonated and desulfonated products following methyl esterification (data not shown). Furthermore, this particular procedure does not yield complete esterification on all sites, leading to a mixture of reaction products which can complicate mass spectral interpretation.[51] One synthetic approach that does not require the use or formation of acid instead employs trimethylsilyldiazomethane in anhydrous THF, benzene, toluene and methanol.[52-53] This approach was attempted but not pursued here due to generated sample complexity; however, this approach appears to be the most viable alternative to acid-producing methyl esterification procedures.

Another possible way to improve selectivity would be to manipulate the binding sites. These proposed binding sites include bridging bidentate and chelating bidentate sites on the titanium dioxide surface.[32] A few ways to manipulate these sites would be to alter the number of each type of binding site or block the chelating binding site that interacts with carboxylic acids[36] with a substituted aromatic carboxylic acid such as 2,5-dihydroxybenzoic acid (DHB).[32] However, first, it would be difficult to manipulate the

number of a certain type of binding site, considering that such manipulation requires prior knowledge of the surface heterogeneity. Furthermore, the crystalline composition of titanium dioxide, which may contain various combinations of amorphous, anatase, and rutile structures, found in commercial products is proprietary information. It is important to know the surface chemistry of the binding material for the following reasons: 1) TiO_2 anatase and rutile hydroxyl groups have very different surface pK_a values (0.5-2.0 vs. 6.5, respectively) and, thus, different binding capabilities,[54-55] 2) the number of different surface coordination sites that influence the binding capability likely depend upon the titanium dioxide preparation method,[56-57] and 3) the presence of metal ions and other contaminant species can affect the Lewis acid properties of the Ti^{4+} center.[58] Secondly, although the use of substituted carboxylic acids was shown to dramatically improve the selectivity of titanium dioxide for binding phosphopeptides,[32-33] these authors report that DHB can cause contamination of the electrospray ionization source, thus rendering this procedure less ideal for direct infusion ESI but great for more salt-tolerant MS analyses such as MALDI-MS. If sample throughput is not an issue, LC purification prior to ESI-MS analysis should be conducted to eliminate excess DHB. We applied DHB to our samples prior to enrichment but this strategy suffered from ion suppression and source contamination (data not shown) and this procedure was therefore not further pursued.

Selectivity of sulfopeptide enrichment also depends upon the binding pH value. In our previously published phosphopeptide enrichment method, the ideal binding pH values were found to be pH 2–3.[31] Because sulfotyrosine has a slightly lower pK_a value than phosphotyrosine,[59-61] it is expected that the optimal binding pH would be lower for sulfopeptide binding. For optimal elution, the pH value must be high enough to disrupt

the interactions of sulfonate poly-oxyanions with the TiO_2 surface due to sulfonate neutralization and/or change of the TiO_2 surface to a Lewis base. This ideal pH value was determined to be pH 10.8–11.5 for phosphopeptide elution.[31]

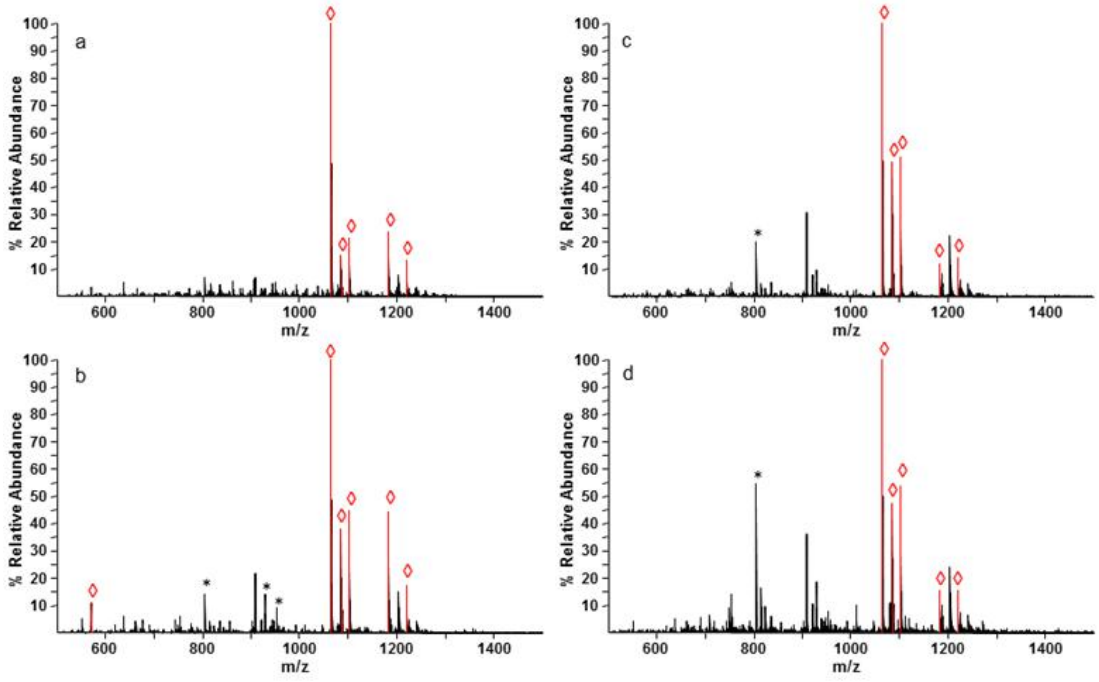

Figure 2.3a – d. Positive-ion mode ESI-MS spectra of an ApoMb digest mixed with CCKS at a 1:1 molar ratio and TiO_2-enriched using binding pH 2.0 (a), 2.5 (b), 3.0 (c), 3.5 (d) and eluting pH 10.0. ApoMb peaks are labeled with asterisks (*) and trypsin autolysis peaks with a dagger (†) while CCK/S peaks are labeled in red with a diamond (◊).

	pH 2.0/10.0	pH 2.5/10.0	pH 3.0/10.0	pH 3.5/10.0
CCK/S	94±2%	89±2%	80±8%	72±2%

Table 2.2. Calculated percent relative abundance with error for an equimolar ratio of CCKS and ApoMb (200 pmol each) following TiO_2 enrichment at binding pH 2.0 and elution pH 10.0.

Figure 2.3a–d and Table 2.2 illustrate the effect of increasing the binding pH from pH 2.0 to 3.5 (a–d, respectively) while the elution pH was held constant at pH 10.0. If the binding pH is much lower than pH 2.0, there is a risk of eliminating the sulfonate

ester via acid hydrolysis.[17] As the binding pH increases, we observed that non-selective binding of ApoMb peptides also increased, which likely causes suppression of the CCK/S signal. We believe that increasing the pH facilitates more carboxylate binding because the binding pH is approaching the average pK_a of protein carboxylates. It was determined that pH values of 2.0 and 10.0 were ideal for binding and elution, respectively, of sulfopeptides. These values support our initial hypothesis that a lower binding pH is more suitable for selective sulfopeptide enrichment compared to phosphopeptide enrichment.

2.3.3 Negative-Ion Mode Analysis of Titanium Dioxide-Enriched Sulfopeptides

It has been suggested that, for many sulfopeptides, several acidic amino acid residues are required near the potential sulfonation site to facilitate this post-translational modification, as discussed in detail elsewhere.[22-24] As a result, sulfopeptides should ionize much better in negative-ion mode than in positive-ion mode MS. Consequently, for negative-ion mode analysis, it was possible to lower the initial amounts of sulfopeptides prior to TiO_2 enrichment in comparison to similar samples analyzed in positive-ion mode (Figures 2.1a, 2.1c).

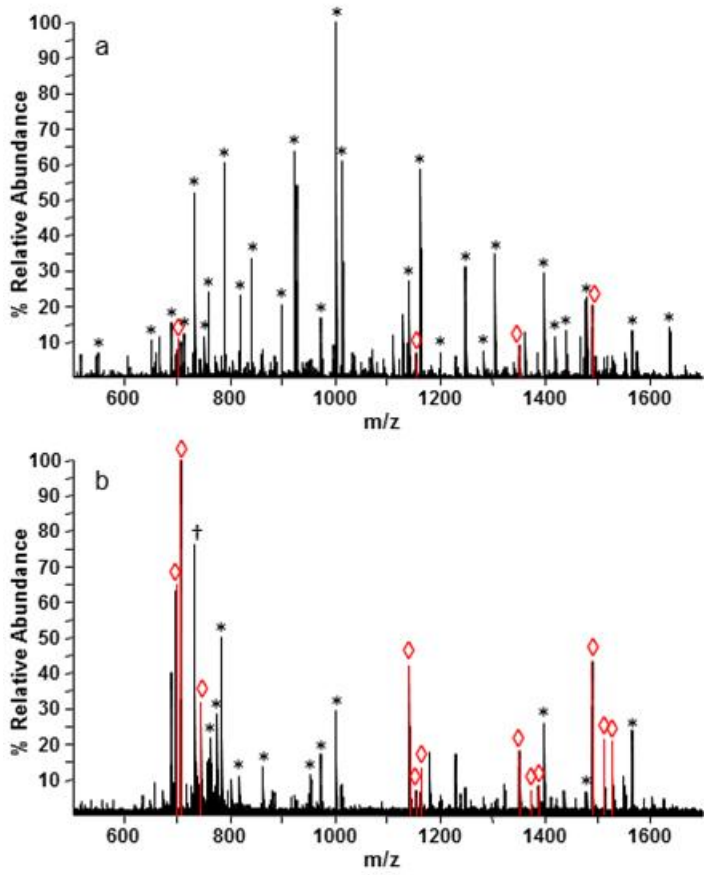

Figure 2.4a-b. Negative-ion mode ESI-MS spectra before (a) and after (b) TiO_2 enrichment of a BSA digest mixed with three sulfopeptides CCKS, CRL, and HIR at a molar ratio of 8:4:4:1, respectively. BSA peaks are labeled with asterisks (*) and trypsin autolysis peaks with a dagger (†) while sulfopeptide peaks are labeled in red with a diamond (◊).

Figure 2.4a–b shows the negative-ion mode ESI-MS spectra of a BSA digest mixed with the sulfopeptides CCKS, CRL, and HIR at a molar ratio of 8:4:4:1 before (a) and after (b) TiO_2 enrichment. Similar to the positive ion mode data (Figures 2.1-2.3), we consider the combination of sulfonated and desulfonated sulfopeptide peaks to represent the overall sulfonated signal. In negative-ion mode ESI-MS, we observe a much larger fraction of sulfonate-retaining peaks compared to desulfonated peaks. The performed enrichment improved the overall relative abundance of sulfonated peaks from

8% to 56% following negative ion ESI-MS. Although there is a 7-fold improvement in overall sulfopeptide signal, there are quite a few abundant BSA peaks as well as a trypsin autolysis peak accounting for much of the identifiable signal in the enriched spectrum. It is important to note that nearly all of the BSA peaks that appear in the enriched spectrum correspond to peptides with three or more acidic groups, including the C-termini of each peptide ion (e.g., $[DAFLGSFLYEYSR - H]^-$, $[DLGEEHFK - H]^-$, $[TVMENFVAFVDK - H]^-$). It is possible that peptides with multiple acidic residues are more likely to interact via their carboxylic acid moieties if there are available interaction sites. However, it is unlikely that the primary interacting species for all peptides would be the carboxylate group because there is noticeable improvement in the enrichment of three different sulfopeptides in the presence of a complex protein digest with a very low rate of co-purification of non-sulfopeptides.

2.3.4 Differentiation of Phosphopeptides and Sulfopeptides after Titanium Dioxide Enrichment

In a more complex biological mixture, both phosphopeptides and sulfopeptides may exist at relatively low intra- and extracellular concentrations, respectively. Differentiation of these isobaric PTMs is essential to unraveling the biological significance of individual modifications on proteins and peptides. It is widely accepted that the structural and biological functionalities of phosphopeptides indeed change from a normal physiological state to a malignant cancerous state, and such changes may occur for sulfopeptides as well.[62-63] In order to differentiate these PTMs by mass, a high-resolution, high mass-accuracy instrument such as an Orbitrap™ or an FT-ICR mass spectrometer is needed. Because such high-end instruments are not always available,

other methods can be used to differentiate sulfopeptides from phosphopeptides. Alkaline phosphatase can be used to cleave phosphate moieties[64] before enrichment if no information from phosphorylated species is desired. However, if both phosphorylated and sulfonated peptides are desired, they can be enriched together and subsequently differentiated based on the high tendency of sulfopeptides to lose 80 Da (SO_3) via in-source fragmentation during +ESI-MS. Unfortunately, these two species cannot be optimally enriched simultaneously due to the differences in binding and elution pH. It may also be possible to use ion pairing experiments to effectively differentiate these isobaric species.[65]

2.4 Conclusion

Here we present a selective method for the enrichment of sulfopeptides using titanium dioxide microtips. Percent relative abundance of sulfopeptide signal was improved by ~4-25-fold in positive-ion mode analyses when using different sulfopeptides and tryptic peptides to form a mixture. In negative-ion mode, sulfopeptides were enriched up to 7-fold with some retention of acidic matrix peptides. It is important to note that the effectiveness of this protocol depends upon determining and maintaining the optimal binding and elution pH values as well as the minimum required amount of starting material to load onto the microtips. Some co-purification of non-sulfonated species may be caused by interactions of peptide carboxylate groups if there are several acidic residues within a particular peptide. Our current protocol is a simple, stand-alone technique for enriching sulfopeptides from mixtures.

2.5 References

1. W. B. Huttner, Sulphation of tyrosine residues-a widespread modification of proteins. *Nature* **1982**, *299*, 273-276.
2. R. J. Huxtable, W. M. Lafranconi, *Biochemistry of sulfur*. Plenum Press: New York, **1986**; p xiii, 445 p.
3. C. A. Strott, Sulfonation and molecular action. *Endocr. Rev.* **2002**, *23*, 703-732.
4. A. C. Ivy, E. Oldberg, A hormone mechanism for gall-bladder contraction and evacuation. *Am. J. Physiol.* **1928**, *86*, 599-613.
5. J. J. Vanderhaeghen, J. C. Signeau, W. Gepts, New peptide in the vertebrate CNS reacting with antigastrin antibodies. *Nature* **1975**, *257*, 604-605.
6. R. A. Gregory, H. J. Tracy, The constitution and properties of two gastrins extracted from hog antral mucosa. *Gut* **1964**, *5*, 103-114.
7. A. Anastasi, V. Erspamer, R. Endean, Isolation and amino acid sequence of caerulein, the active decapeptide of the skin of *Hyla caerulea*. *Arch. Biochem. Biophys.* **1968**, *125*, 57-68.
8. C. D. Unsworth, J. Hughes, J. S. Morely, O-sulphated leu-enkephalin in brain. *Nature* **1982**, *295*, 519-522.
9. H. R. Kissileff, F. X. Pi-Sunyer, J. Thornton, G. P. Smith, C-terminal octapeptide of cholecystokinin decreases food intake in man. *Am J Clin Nutr* **1981**, *34*, 154-160.
10. S. Young, S. Julka, G. Bartley, J. Gilbert, B. Wendelburg, S.-C. Hung, K. Anderson, W. Yokoyama, in *58th ASMS Conference on Mass Spectrometry and Allied Topics*. American Society for Mass Spectrometry: Salt Lake City, Utah, **2010**.
11. S. A. Young, S. Julka, G. Bartley, J. Gilbert, B. Wendelburg, S.-C. Hung, W. H. K. Anderson, W. Yokoyama, Quantification of the sulfated cholecystokinin CCK-8 in hamster plasma using immunoprecipitation liquid chromatography-mass spectrometry/mass spectrometry. *Anal. Chem.* **2009**, *81*, 9120-9128.
12. C. Niehrs, R. Beisswanger, W. B. Huttner, Protein tyrosine sulfation, 1993--an update. *Chem. Biol. Interact.* **1994**, *92*, 257-271.
13. A. H. Johnsen, Phylogeny of the cholecystokinin/gastrin family. *Front. Neuroendocrinol.* **1998**, *19*, 73-99.
14. M. Marino, D. Andrews, R. T. McCluskey, Binding of rat thyroglobulin to heparan sulfate proteoglycans. *Thyroid* **2000**, *10*, 551-559.
15. P. A. Baeuerle, W. B. Huttner, Tyrosine sulfation is a trans-Golgi-specific protein modification. *J. Cell. Biol.* **1987**, *105*, 2655-2664.
16. C. Niehrs, M. Kraft, R. W. Lee, W. B. Huttner, Analysis of the substrate specificity of tyrosylprotein sulfotransferase using synthetic peptides. *J. Biol. Chem.* **1990**, *265*, 8525-8532.
17. F. R. Bettelheim, Tyrosine-O-sulfate in a peptide from fibrinogen. *J. Am. Chem. Soc.* **1954**, *76*, 2838-2839.
18. J. F. Nemeth-Cawley, S. Karnik, J. C. Rouse, Analysis of sulfated peptides using positive electrospray ionization tandem mass spectrometry. *J. Mass Spectrom.* **2001**, *36*, 1301-1311.
19. J. B. Fenn, M. Mann, C. K. Meng, S. F. Wong, C. M. Whitehouse, Electrospray ionization for mass spectrometry of large biomolecules. *Science* **1989**, *246*, 64-71.

20. J.-L. Wolfender, F. Chu, H. Ball, F. Wolfender, M. Fainzilber, M. A. Baldwin, A. L. Burlingame, Identification of tyrosine sulfation in *Conus pennaceus* conotoxins a-PnIA and a-PnIB: further investigation of labile sulfo- and phosphopeptides by electrospray, matrix-assisted laser desorption/ionization (MALDI) and atmospheric pressure MALDI mass spectrometry. *J. Mass Spectrom.* **1999**, *34*, 447-454.
21. T. Yagami, K. Kitagawa, C. Aida, H. Fujiwara, S. Futaki, Stabilization of a tyrosine O-sulfate residue by a cationic functional group: formation of a conjugate acid-base pair. *J. Pept. Res.* **2000**, *56*, 239-249.
22. G. Hortin, R. Folz, J. I. Gordon, A. W. Strauss, Characterization of sites of tyrosine sulfation in proteins and criteria for predicting their occurrence. *Biochem. Biophys. Res. Commun.* **1986**, *141*, 326-333.
23. W. H. Lin, K. Larsen, G. L. Hortin, J. A. Roth, Recognition of substrates by tyrosylprotein sulfotransferase. Determination of affinity by acidic amino acids near the target sites. *J. Biol. Chem.* **1992**, *267*, 2876-2879.
24. G. L. Rosenquist, H. B. Nicholas, Jr., Analysis of sequence requirements for protein tyrosine sulfation. *Prot. Sci.* **1993**, *2*, 215-222.
25. J. R. Bundgaard, J. Vuust, J. F. Rehfeld, New consensus features for tyrosine O-sulfation determined by mutational analysis. *J. Biol. Chem.* **1997**, *272*, 21700-21705.
26. R. E. Bossio, A. G. Marshall, Baseline resolution of isobaric phosphorylated and sulfated peptides and nucleotides by electrospray ionization FT ICR-MS: another step toward mass spectrometry-based proteomics. *Anal. Chem.* **2002**, *74*, 1674-1679.
27. M. Gharib, M. Marcantonio, S. G. Lehmann, M. Courcelles, S. Meloche, A. Verreault, P. Thibault, Artifactual sulfation of silver-stained proteins: implications for the assignment of phosphorylation and sulfation sites. *Mol. Cell. Proteomics* **2009**, *8*, 506-518.
28. Y. Amano, H. Shinohara, Y. Sakagami, Y. Matsubayashi, Ion-selective enrichment of tyrosine-sulfated peptides from complex protein digests. *Anal. Biochem.* **2005**, *346*, 124-131.
29. Y.-C. Chang, C.-N. Huang, C.-H. Lin, H.-C. Chang, C.-C. Wu, Mapping protein cysteine sulfonic acid modifications with specific enrichment and mass spectrometry: An integrated approach to explore the cysteine oxidation. *Proteomics* **2010**, *10*, 2961-2971.
30. H. K. Kweon, K. Hakansson, Metal oxide-based enrichment combined with gas-phase ion-electron reactions for improved mass spectrometric characterization of protein phosphorylation. *J. Proteome Res.* **2008**, *7*, 749-755.
31. H. K. Kweon, K. Hakansson, Selective zirconium dioxide-based enrichment of phosphorylated peptides for mass spectrometric analysis. *Anal. Chem.* **2006**, *78*, 1743-1749.
32. M. R. Larsen, T. E. Thingholm, O. N. Jensen, P. Roepstorff, T. J. Jorgensen, Highly selective enrichment of phosphorylated peptides from peptide mixtures using titanium dioxide microcolumns. *Mol. Cell. Proteomics* **2005**, *4*, 873-886.
33. T. E. Thingholm, T. J. Jorgensen, O. N. Jensen, M. R. Larsen, Highly selective enrichment of phosphorylated peptides using titanium dioxide. *Nat. Protoc.* **2006**, *1*, 1929-1935.

34. P. A. Connor, A. J. McQuillan, Phosphate adsorption onto TiO_2 from aqueous solutions: an in situ internal reflection infrared spectroscopic study. *Langmuir* **1999**, *15*, 2916-2921.
35. H. Dobson, A. J. McQuillan, In situ infrared spectroscopic analysis of the adsorption of aliphatic carboxylic acids to TiO_2, ZrO_2, Al_2O_3, Ta_2O_5 from aqueous solutions. *Spectrochim. Acta A* **1999**, *55*, 1395-1405.
36. K. D. Dobson, A. J. McQuillan, In situ infrared spectroscopic analysis of the adsorption of aromatic carboxylic acids to TiO_2, ZrO_2, Al_2O_3, and Ta_2O_5 from aqueous solutions. *Spectrochim. Acta A* **2000**, *56*, 557-565.
37. M. A. Ali, D. A. Dzombak, Competitive Sorption of Simple Organic Acids and Sulfate on Goethite. *Environ. Sci. Technol.* **1996**, *30*, 1061-1071.
38. G. Horanyi, P. Joo, In situ study of the specific adsorption of HSO_4^-/SO_4^{2-} ions on hematite by radiotracer technique. *J. Colloid Interf. Sci.* **2000**, *227*, 206-211.
39. P. Joo, G. Horanyi, Radiotracer study of the specific adsorption of anions on metal oxides in acid media: an experimental approach. *J. Colloid Interf. Sci.* **2000**, *223*, 308-310.
40. S. Hug, In situ Fourier transform infrared measurements of sulfate adsorption on hematite in aqueous solutions. *J. Colloid Interf. Sci.* **1997**, *188*, 415-422.
41. G. Horanyi, P. Joo, Comparative radiotracer study of the absorption of sulfate and pertechnetate ions on gamma-Al_2O_3. *J. Colloid Interf. Sci.* **2001**, 46-51.
42. G. Horanyi, Investigation of the specific adsorption of sulfate ions on powdered TiO_2. *J. Colloid Interf. Sci.* **2003**, *261*, 580-583.
43. M. W. Senko, J. D. Canterbury, S. Guan, A. G. Marshall, A high-performance modular data system for Fourier transform ion cyclotron resonance mass spectrometry. *Rapid Commun. Mass Spectrom.* **1996**, *10*, 1839-1844.
44. E. B. Ledford, D. L. Rempel, M. L. Gross, Space-charge effects in Fourier transform mass spectrometry - mass calibration. *Anal. Chem.* **1984**, *56*, 2744-2748.
45. E. S. Simon, M. Young, A. Chan, Z.-Q. Bao, P. C. Andrews, Improved enrichment strategies for phosphorylated peptides on titanium dioxide using methyl esterification and pH gradient elution. *Anal. Biochem.* **2008**, *377*, 234-242.
46. K. A. Kraus, H. O. Philips, T. A. Carlson, J. S. Johnson, in *Second International Conference on Peaceful Uses of Atomic Energy*. Geneva, Switzerland, **1958**, p 3.
47. Q. Li, Z. Ning, J. Tang, N. Song, R. Zeng, Effect of peptide-to-TiO_2 beads ratio on phosphopeptide enrichment selectivity. *J. Proteome Res.* **2009**, *8*, 5375-5381.
48. M. W. H. Pinkse, P. M. Uitto, M. J. Hilhorst, B. Ooms, A. J. R. Heck, Selective isolation at the femtomole level of phosphopeptides from proteolytic digests using 2D-nano LC-ESI-MS/MS and titanium oxide precolumns. *Anal. Chem.* **2004**, *76*, 3935-3943.
49. D. C. Hoth, J. G. Rivera, L. A. Colon, Metal oxide monolithic columns. *J. Chromatogr. A* **2005**, *1079*, 392-396.
50. G. T. Cantin, T. R. Shock, S. K. Park, H. D. Madhani, J. R. Yates III, Optimizing TiO_2-based phosphopeptide enrichment for automated multidimensional liquid chromatography coupled to tandem mass spectrometry. *Anal. Chem.* **2007**, *79*, 4666-4673.
51. S. S. Jensen, M. R. Larsen, Evaluation of the impact of some experimental procedures on different phosphopeptide enrichment techniques. *Rapid Commun. Mass Spectrom.* **2007**, *21*, 3635-3645.

52. M. D. Crenshaw, D. B. Cummings, Preparation, derivatization with trimethylsilyldiazomethane, and GC/MS analysis of a "pool" of alkyl methylphosphonic acids for use as qualitative standards in support of counterterrorism and the chemical weapons convention. *Phosphorus, Sulfur Silicon Relat. Elem.* **2004**, *179*, 1009-1018.
53. A. Presser, A. Hufner, Trimethylsilyldiazomethane – a mild and efficient reagent for the methylation of carboxylic acids and alcohols in natural products. *Monatsh. Chem.* **2004**, *135*, 1015-1022.
54. N. E. Tret'yakov, V. N. Filimonov, An infrared spectroscopic study of the relative proton-donating power of the OH-groups of oxide surfaces. *Kinet. Catal.* **1972**, *13*, 735-737.
55. J. Nawrocki, M. P. Rigney, A. McCormick, P. W. Carr, Chemistry of zirconia and its uses in chromatography. *J. Chromatogr. A* **1993**, *657*, 229-282.
56. D. J. C. Yates, Infrared studies of the surface hydroxyl groups on titanium dioxide and of the chemisorption of carbon monoxide and carbon dioxide. *J. Phys. Chem.* **1961**, *65*, 746-753.
57. E. Garrone, V. Bolis, B. Fubini, C. Morterra, Thermodynamic and spectroscopic characterization of ambient temperature heterogeneity among adsorption sites: CO on anatase at ambient temperature. *Langmuir* **1989**, *5*, 892-899.
58. V. Bolis, B. Fubini, E. Garpone, C. Morterra, P. Ugliengo, Induced heterogeneity at the surface of group 4 dioxides as revealed by CO adsorption at room temperature. *J. Chem. Soc., Faraday Trans.* **1992**, *88*, 391-398.
59. J. G. Jones, K. S. Dodgson, Biosynthesis of L-tyrosine O-sulphate from the methyl and ethyl esters of L-tyrosine. *Biochem. J.* **1965**, *94*, 331-336.
60. R. Hoffmann, I. Reichert, W. O. Wachs, M. Zeppezauer, H. R. Kalbitzer, 1H and 31P NMR spectroscopy of phosphorylated model peptides. *Int. J. Pept. Prot. Res.* **1994**, *44*, 193-198.
61. G. S. Baldwin, M. F. Bailey, B. P. Shehan, I. Sims, R. S. Norton, Tyrosine modification enhances metal-ion binding. *Biochem. J.* **2008**, *416*, 77-84.
62. J. F. Rehfeld, W. W. van Solinge, The tumor biology of gastrin and cholecystokinin. *Adv. Canc. Res.* **1994**, *63*, 295-347.
63. E. Rozengurt, J. H. Walsh, Gastrin, CCK, signaling, and cancer. *Ann. Rev. Physiol.* **2001**, *63*, 49-76.
64. Y. Yu, A. J. Hoffhines, K. L. Moore, J. A. Leary, Determination of the sites of tyrosine O-sulfation in peptides and proteins. *Nat. Methods* **2007**, *4*, 583-588.
65. Y. Zhang, E. P. Go, H. Jiang, H. Desaire, A novel mass spectrometric method to distinguish isobaric monosaccharides that are phosphorylated or sulfated using ion-pairing reagents. *J. Am. Soc. Mass Spectrom.* **2005**, *16*, 1827-1839.

CHAPTER III

CHARACTERIZATION OF *O*-SULFOPEPTIDES BY NEGATIVE ION MODE TANDEM MASS SPECTROMETRY: SUPERIOR PERFORMANCE OF NEGATIVE-ION ELECTRON CAPTURE DISSOCIATION

3.1 Introduction

Acidic post-translational modifications (PTMs) such as phosphorylation and sulfonation on proteins and peptides are important for many biological processes, including signal processing[1] and protein-protein interactions,[2] respectively, as well as growth regulation in cancer for both PTMs.[3-6] Localization of these acidic PTMs is critically important for determining their biological function but is challenging with direct gas-phase activation in positive ion mode tandem mass spectrometry (MS/MS). Positive-ion mode collision-activated dissociation (CAD), which is the most commonly used MS/MS activation technique, cleaves the weakest bonds, which correspond to the labile acidic PTMs, preventing their direct localization.[7-9] PTM identification can also be challenging for sulfonation (SO_3) and phosphorylation (HPO_3) as they both result in a neutral loss of 80 Da (Δm = 9 mDa).[10] Furthermore, recent work suggests that the locations of phosphate groups can scramble during the CAD activation process if neutral phosphate loss and/or rearrangement events produce abundant product ion species.[11-13]

To circumvent the loss of structural information regarding *O*-sulfonated sites, Yu, et al.[14] have shown that selective and stoichiometric acetylation of non-sulfonated tyrosines in sulfopeptides followed by positive-ion mode CAD MS/MS allows site determination of tyrosine sulfonation. Because the sulfonate groups are lost during collisional activation, in contrast to the stable acetyl groups, detected free tyrosines are assumed to have been sulfonated. Similar to the aforementioned method, most efforts to improve the analysis of sulfonate occurrence in peptides by positive ion CAD MS/MS are focused on its neutral loss, as opposed to its direct identification.[9, 15-17]

Ion-electron[18-22] and ion-ion[23-24] activation reactions have been employed for direct acidic PTM localization in positive ion mode MS/MS analysis. While sulfonate retention is generally not observed for protonated sulfopeptides in positive-ion mode electron-capture dissociation (ECD) or electron transfer dissociation (ETD), metal-ion adduction was shown to successfully retain the sulfonate groups and thus allow unambiguous localization of sulfotyrosine residues with both these techniques. [24-25] The caveats to incorporating metal-ion adduction for enhanced sulfosite localization include possible ion suppression and distribution of ion signal amongst multiple ionic forms and charge states. Sulfonate retention in ECD[22] and ETD[26] of protonated sulfopeptides have been noted, however, in both those cases arginine-containing peptides were studied (one and three arginines, respectively[22, 26]) representing special cases with sequestered protons. Another drawback of ECD/ETD is that both techniques require multiply positively charged ions, which can be challenging to generate for naturally acidic sulfopeptides.[27-29] Sulfonate retention is also observed during metastable atom-activated dissociation (MAD) of singly-protonated peptide ions,[30] providing excellent sequence coverage from *a*, *b*, *c*, *w*,

x, *y,* and *z*-ions with many sulfonate-retaining fragments for sulfonated cholecystokinin and leucine-enkephalin. However, uninformative neutral loss of H_2O, CO_2, and SO_3 are often the most abundant fragmentation events.

Due to their inherent acidic nature, peptides containing phosphate and sulfonate groups show improved ionization in negative-ion mode,[31-32] suggesting that negative ion mode analysis would be more favorable. Negative-ion mode CAD of phospho- and sulfopeptides produces similar neutral PTM losses as in positive-ion mode.[8, 32-33] Furthermore, negative-ion mode peptide CAD typically produces more complex MS/MS spectra arising from multiple fragmentation events as well as side chain losses in comparison to positive-ion mode CAD.[34-35] Budnik, et al.[36] have shown that electron detachment dissociation (EDD) of the sulfopeptide caerulein produced even- and odd-electron *a*, *c*, and *z* ions with significant neutral loss but with 100% sequence coverage as well as localization of the sulfonate group in a Fourier-transform ion cyclotron resonance (FT ICR) instrument while Kjeldsen, et al.[37] reported that sulfonate and phosphate localization are also possible with EDD in a quadrupole ion trap (QIT). These authors also report that EDD efficiency is rather low—on the order of 2-15% in a QIT and 5-20% in FT ICR-MS. In negative-ion mode MAD, extensive series of product ions with sulfonate retention and some neutral loss were observed.[30] The reported MAD experiments utilized peptide concentrations of 20–40 μM, which may preclude analysis of low-abundance, biologically-derived peptides. Furthermore, there is currently no commercial instrument available to conduct MAD. Atmospheric pressure thermal dissociation (APTD)[38] may offer another alternative approach to sulfonate site determination. APTD of sulfopeptide anions produced some *c*- and *y*-ions but mostly

resulted in SO_3 neutral loss as well as neutral fragments that require an additional step of reionization. Only a single, sulfonate-containing ion was observed after APTD and no sulfonate-containing ions were detected following reionization.

Negative electron transfer dissociation (NETD) enables multiply-charged anionic species to transfer an electron to an acceptor reagent, leading to activation and fragmentation resulting in EDD-like product ions with and without retention of phosphate groups.[39] This technique, however, tends to exhibit extensive neutral losses including some phosphoric acid losses that could possibly be reduced with careful choice of the radical cation reagent.[40] NETD has been used to successfully fragment sulfonated glycosaminoglycans;[41] however, NETD has not previously been employed for sulfopeptide MS/MS characterization. Negative-ion mode ECD (niECD) involves electron capture by gaseous peptide zwitterions with an overall negative charge, leading to activation and ECD-like fragmentation with complete retention of phosphate and sulfonate groups.[42] NETD and niECD look promising for advancing phosphopeptide, sulfopeptide, and other acidic biomolecule fragmentation. In this work, we have expanded niECD to additional sulfopeptides and compared its performance to negative-ion mode CAD, EDD, and NETD with the goal to determine the superior method for sulfopeptide MS/MS characterization.

3.2 Materials and methods

3.2.1 Peptide Standards

Sulfonated cholecystokinin fragment 26-33 (DyMGWMDF-NH_2, CCKS; Advanced ChemTech, Louisville, KY), hirudin fragment 54-65 (DFEEIPEEyLQ, HIR;

Advanced ChemTech), Leu-enkephalin (yGGFL, Leu-Enk; Protea Biosciences, Morgantown, WV), sulfonated human gastrin-17 II (pEGPWLEEEEEAyGWMDF-NH_2, GST; Sigma, St. Louis, MO), caerulein (pEQDyTGWMDF-NH_2, CRL; Bachem, Torrance, CA) and cionin (NyyGWMDF-NH_2, CN; Bachem), where lower case 'y' in all peptides corresponds to a sulfo-tyrosine residue, were used without further purification. HPLC-grade isopropanol (IPA) was purchased from Fisher (Fair Lawn, NJ), LC/MS-grade water was purchased from J.T. Baker (Phillipsburg, NJ), ES tuning mix was purchased from Agilent (Santa Clara, CA) and triethylamine (TEA) was purchased from Sigma.

3.2.2 Mass Spectrometry

Sulfopeptides were directly infused via an electrospray ionization (ESI) source (Apollo II, Bruker Daltonics, Billerica, MA) at 0.5–5 μM concentration in 1:1 IPA:H_2O, 1% TEA. All negative ion mode CAD, EDD, and niECD experiments were performed on a 7T quadrupole (Q)-FT ICR-MS instrument equipped with a hollow dispenser cathode to generate electrons (Apex-Q, Bruker Daltonics). NETD experiments were performed on a more recent 7T Q-FT ICR-MS instrument equipped with an Apollo II ESI source as well as a chemical ionization source with a fluoranthene reagent (SolariX, Bruker Daltonics).

The ESI flow rate was set at 70 μL/h, and N_2 nebulizing gas was operated at 2.0 bar. Ions were accumulated in the first hexapole for 0.05 s then selectively filtered by the quadrupole according to m/z. Mass-selected ions were transferred to the second hexapole, where ions were accumulated for 0.5-1 s, varied per peptide ion to obtain optimum signal

abundance (~1-5 x 10^7 in arbitrary units) for MS/MS. Ions travelling through the high-voltage ion optics were dynamically trapped in the ICR cell. The cell accumulation process was looped three times prior to MS/MS, excitation and detection as an image current in the ICR cell. Time-domain data were Fourier transformed, and the resulting frequencies corresponding to m/z 200 to 2000 were displayed using Bruker XMASS software (v. 7.0.6) with 256k data points summed over 32 scans with the exception of hirudin, which was summed over 64 scans. Open-source MIDAS software (v. 3.21)[43] was used for data analysis. External calibration was performed using a two-term frequency-to-mass calibration[44] in Microsoft Excel. Calculated m/z ratios for peptides and their product ions were obtained from MS Product in Protein Prospector (http://prospector.ucsf.edu/prospector/mshome.htm) and the PeptideMass tool in Expasy (http://www.expasy.ch/tools/peptide-mass.html). These calculated values were compiled into a home-built macro and searched against experimental m/z ratios for peak identification and accurate mass matching. Mass assignments of less than or equal to 15 ppm error are reported here.

3.2.3 CAD, EDD and niECD Experiments

For all CAD experiments, the DC offset on the second hexapole was used as a collision voltage and was modified from 10-30 V to yield maximum product ion abundance for each sulfopeptide. The maximum laboratory frame of reference energy for all CAD experiments is well below that of high-energy CAD (~1 keV).[45] For all EDD experiments, multiply-charged anionic sulfopeptides were irradiated with ~18-20 eV electrons for up to 3 s while the lens electrode was held 0.2-1 V higher than the cathode

bias voltage. The lens voltage regulates the number of electrons passing through the ICR cell.[46] For all niECD experiments, singly and/or doubly-charged anionic sulfopeptides were irradiated with 4.5–6 eV electrons for up to 5 s while the lens electrode was held 0.5-1.5 V lower than the cathode bias voltage to produce the maximum abundance charge-increased radical anion. The electron energy and irradiation time in both EDD and niECD were varied as per peptide and charge state to yield maximum product ion abundance.

3.2.4 NETD Experiments

The ESI flow rate was set to 100–120 μL/h, and the nebulizer gas was operated at 1.3 L/min. Ions were accumulated in the first octopole for 20 ms then mass-selectively filtered as per peptide mass and charge state by the quadrupole. Mass-selected ions were transferred to the hexapole collision cell and accumulated for 2-5 s. Prior to side-kick trapping of product ions in the ICR cell (-7 V side-kick voltage with 2 V side-kick offset), analyte ions and radical cationic fluoranthene reagent (m/z 202) were accumulated in the collision cell. Both analyte and fluoranthene reagent accumulation times were varied per peptide ion and charge state to obtain the highest signal abundance prior to NETD (~$1x10^8$ in arbitrary units, which is comparable to $1x10^7$ signal abundance on the Apex-Q instrument). Following electron-transfer events in the collision cell, product ions were transferred to the ICR cell via a transfer hexapole, excited, and detected as an image current. Time-domain data were Fourier transformed, and the resulting frequencies corresponding to m/z 200 to 3000 were displayed using the Bruker SolariXcontrol software (v. 1.5) with 512k data points summed over 32 scans. External calibration was

performed daily on the SolariX with ES tuning mix and this calibration was applied to each data acquisition event. DataAnalysis software (v. 4.0) was used for peak picking. Calculated m/z ratios for peptides and their product ions were acquired and searched against experimental m/z ratios with an error tolerance of 15 ppm similar to the Apex-Q data.

3.2.5 Fragmentation Efficiency Calculations

Fragmentation efficiencies for ion-ion and ion-electron reactions were calculated by taking a ratio of the summed charge-normalized product ion signal to the summed charge-normalized product ion signal, charge-increased/reduced signal, and structurally non-informative neutral loss signal from the precursor ion according to previous literature.[47] CAD fragmentation efficiencies were not calculated because precursor ion signal in CAD can be depleted very easily, leading to nearly 100% fragmentation efficiency. Instead, percent sequence coverage, percent sulfonate retention as well as the percent of known vs. unknown peaks in the product ion spectra were calculated. Error calculations were carried out for representative data from each fragmentation technique and applied to the rest of the data from that particular technique. For CAD, EDD, and NETD, three independent fragmentations of doubly-deprotonated hirudin were averaged and standard deviations were calculated. For niECD, three independent datasets from fragmentation of singly-deprotonated hirudin were used for averaging and error calculations.

3.3 Results

3.3.1 Negative-Ion CAD of Sulfopeptides

In CAD, ions collide with neutral gas molecules, creating an activated energetic ion, which then dissipates excess energy through unimolecular dissociation, e.g., at peptide backbone amide bonds to produce *b* and *y′* ions.[7] In negative ion mode CAD, it is also common to observe *a*, *c*, *x*- and *z*-ions[48] as well as neutral losses of H_2O, SO_3, HPO_3, H_3PO_4, and amino acid side chains.[34, 49-50]

Figures 3.1a-c show CAD of singly-, doubly- and triply-deprotonated hirudin, respectively.[*] In all three spectra, neutral loss of H_2O, NH_3, and SO_3 are the major fragmentation pathways followed by backbone fragmentation to yield mostly *y′* ions, which contain the acidic C-terminus. This neutral loss tendency during vibrational activation has been reported elsewhere for non-sulfonated hirudin.[48] Previous work has also shown that backbone bond cleavages in negative-ion CAD are preferred at or near the site of charge.[34, 48, 51] Thus, we expected that the observed *y′* ions should be most prominent N or C-terminal to acidic amino acid residues (D/E) or to the sulfotyrosine. With respect to the hirudin sequence, negative-ion CAD cleavages near D/E are more prominent than other backbone bond cleavages as shown in Figures 3.1a–c. Because there are seven likely sites for deprotonation (one aspartic acid, four glutamic acids, sulfotyrosine, and the C-terminus) within the hirudin sequence, there should be a distribution of species with different charge locations at all charge states studied, leading

[*] Because the exact site(s) of deprotonation for all peptides analyzed are not known, we have assigned the first site of deprotonation to the sulfonate group due to its lower pK_a value while subsequent deprotonation sites are believed to be carboxylic acids. It is highly possible that there are a range of possible conformers with different charge-carrying sites, especially at higher charge states. The specific site(s) of deprotonation were not explored in this work.

to a diverse set of product ions. However, at the lower charge states, the sulfonate group must compete for deprotonation with several carboxylic acids. If the sulfotyrosine residue is protonated, proton-initiated sulfonate cleavage[52] may be a dominant fragmentation pathway, which may result in a lower occurrence of backbone cleavage at lower charge states. Indeed, Zaia and Costello[53] have demonstrated the following correlation between sulfonate retention on glycosaminoglycan backbone fragments and precursor ion charge state: at higher charge states, there is a higher probability of deprotonation at the sulfonate groups, thus, yielding charge-localized fragmentation without loss of the sulfonate groups. Additionally, more highly charged precursor ions produce stress on the glycosidic sugar backbone.

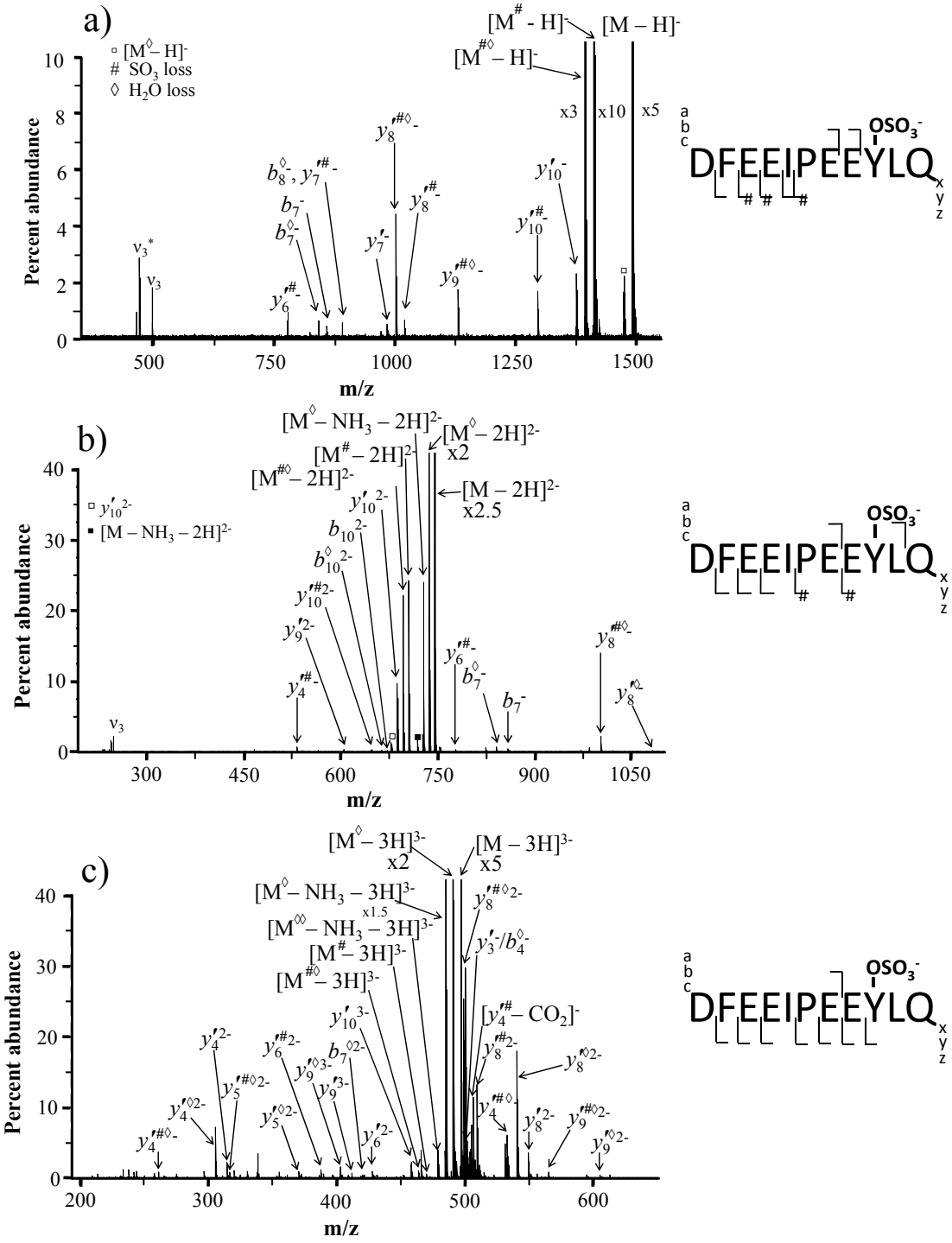

Figure 3.1a – c. Negative ion mode CAD of singly- (a), doubly- (b) and triply-deprotonated (c) sulfonated hirudin fragment 55-65. Sulfonate loss (#), water loss (◊), and electronic noise (*) are indicated on the spectra.

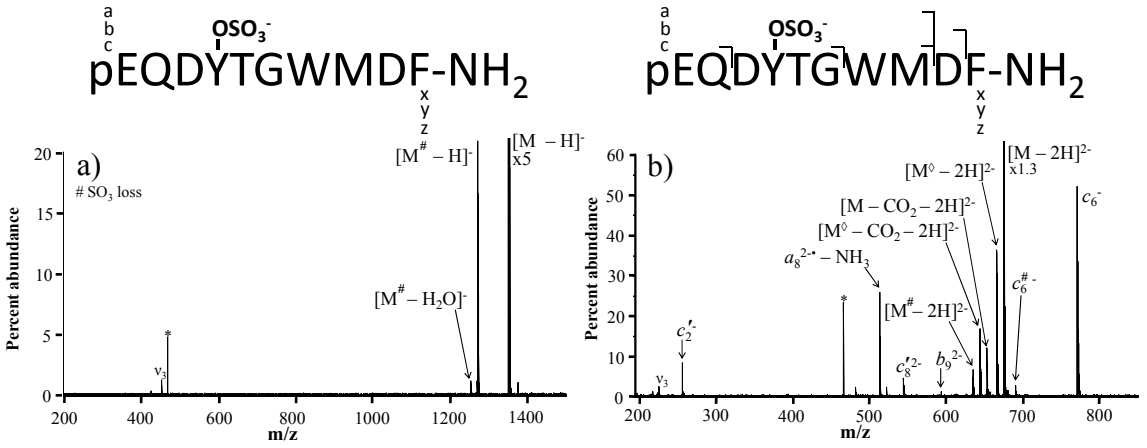

Figure 3.2a–b. Negative ion mode CAD of singly- (a) and doubly-deprotonated (b) sulfonated caerulein. Sulfonate loss is indicated by # while electronic noise is indicated by *.

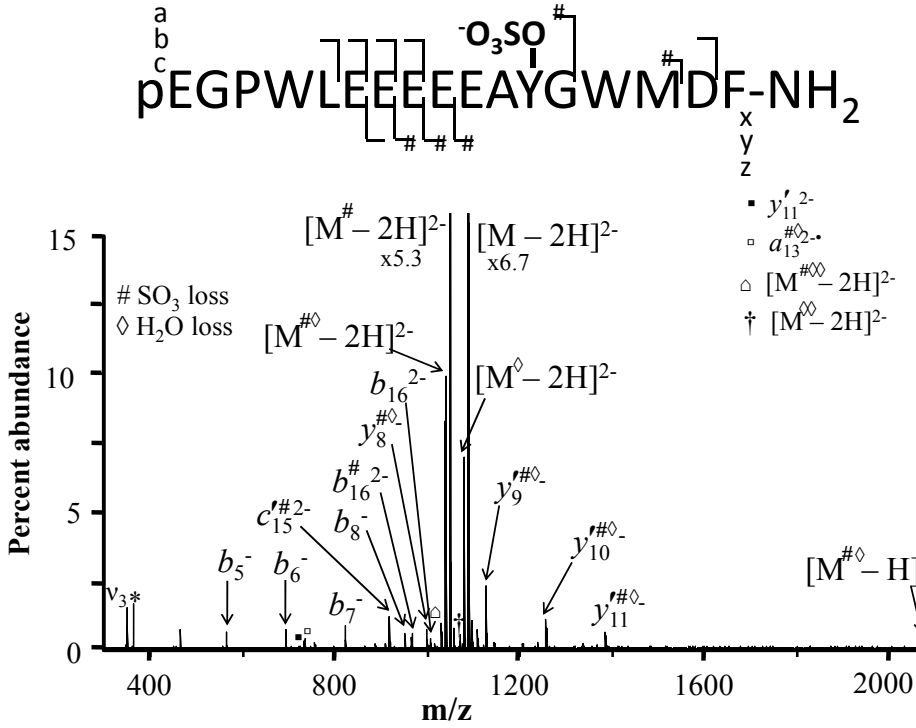

Figure 3.3. Negative ion mode CAD of doubly-deprotonated sulfonated human gastrin II. Sulfonate loss and water loss are indicated by # and ◊, respectively, while electronic noise is indicated by *.

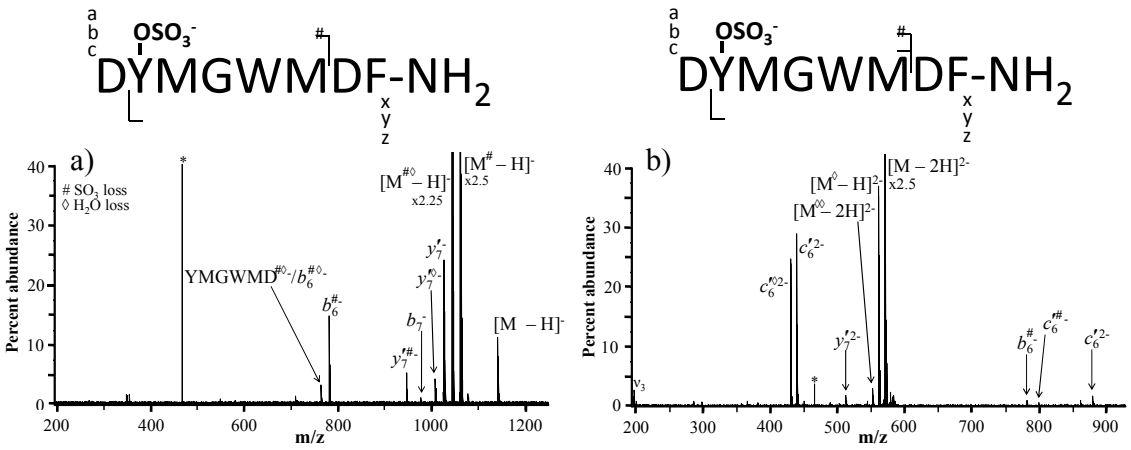

Figure 3.4a – b. Negative ion mode CAD of singly- (a) and doubly-deprotonated (b) sulfonated cholecystokinin (CCKS). Sulfonate loss and water loss are indicated by # and ◊, respectively, while electronic noise is indicated by *.

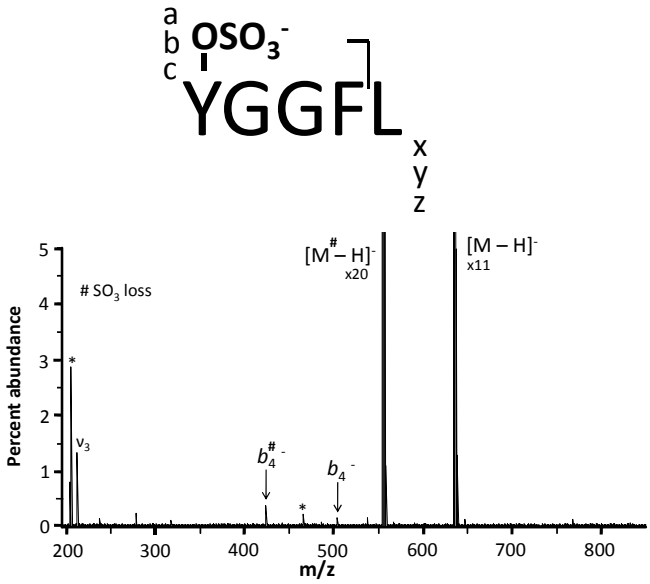

Figure 3.5. Negative ion mode CAD of singly-deprotonated sulfonated leucine-enkephalin. Sulfonate loss is indicated by # while electronic noise is indicated by *.

For hirudin, CAD in the 3- charge state produced higher sulfonate retention compared to the lower charge states. Figures 3.2-3.5 show negative ion mode CAD of caerulein (CRL), gastrin II (GST), cholecystokinin (CCKS), and leucine enkephalin (Leu-Enk), respectively. A side-by-side comparison of CAD of singly- and doubly-

deprotonated CRL (Figure 3.2) shows that backbone fragmentation as well as sulfonate retention is favored at the higher charge state. In fact, CAD of singly-deprotonated CRL produced dominant SO_3 loss and some combined (SO_3 + H_2O) loss from the precursor ion while CAD of doubly-deprotonated CRL produced ~4x lower abundance of SO_3 loss from the precursor ion and five backbone product ions (whereas no backbone fragments were observed in CAD of the 1- precursor ion). Also, CAD of gastrin II in the 3- and 4- charge states exhibited increased sulfonate retention compared with CAD of the doubly-deprotonated precursor ion (Figure 3.3 and Table 3.1). Thus, higher charge states may play a critical role in unambiguous identification and localization of acidic post-translational modifications when using vibrational activation techniques such as CAD. CAD of singly- and doubly-deprotonated CCKS (Figure 3.4) produced only 2-3 backbone fragments each originating from either the C- or N-terminus, but no sulfonate localization was possible. Similar low degree of structural information was also obtained for CAD of singly-deprotonated Leu-Enk (Figure 3.5), which produced a single b_4 ion overshadowed by dominant SO_3 loss from the precursor ion.

3.3.2 EDD of Sulfopeptides

In EDD multiply-deprotonated peptides are irradiated with high-energy electrons ($\geq$ 10 eV) to detach an electron, leaving a charge-reduced radical anion which typically fragments at C_α–C backbone bonds to produce $a^\bullet$ and x ions with retention of acidic PTMs.[36-37] However, neutral losses of H_2O, CO_2, NH_3, and some amino acid side chains are frequently observed as major fragmentation pathways.[36]

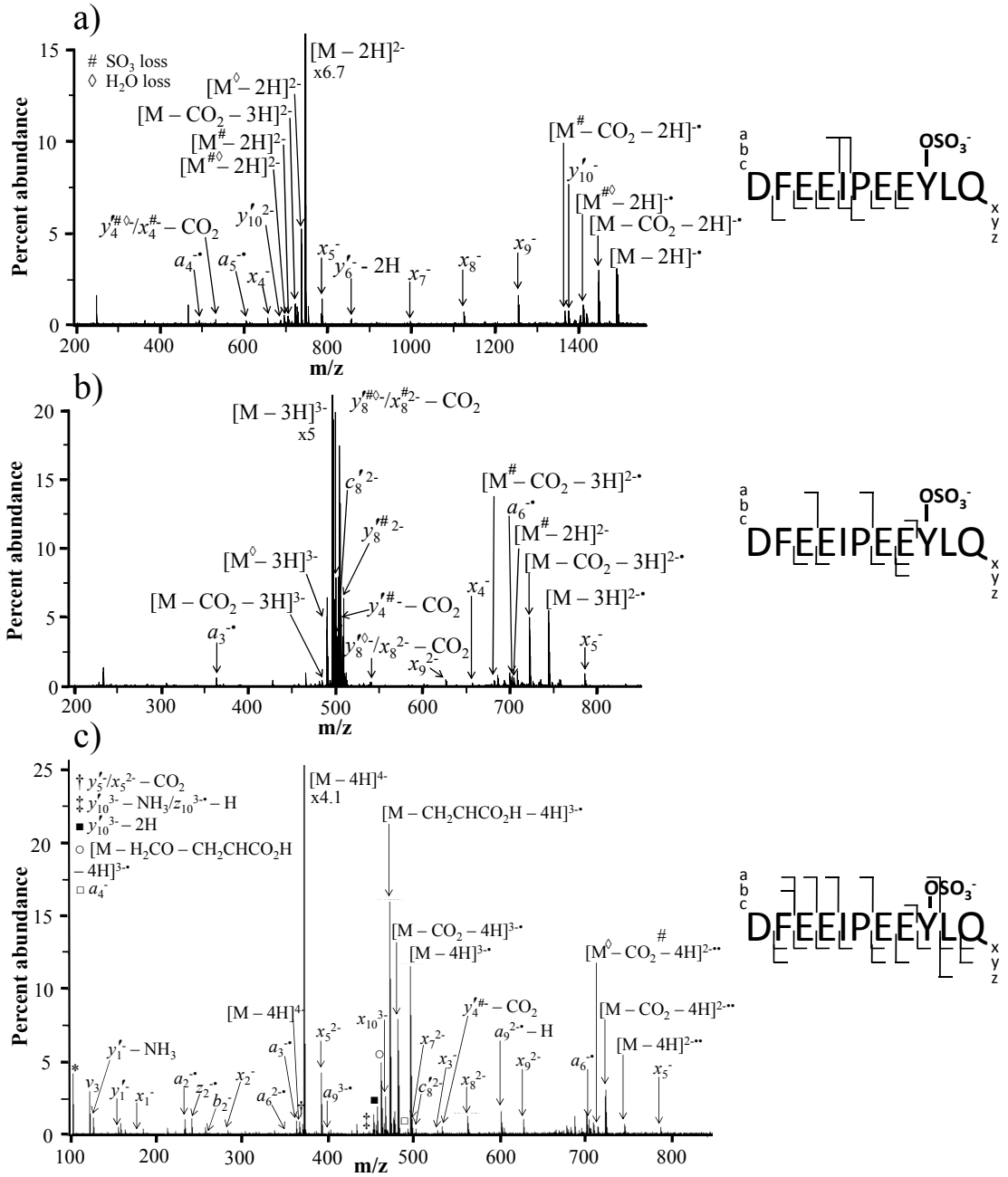

Figure 3.6a – c. EDD of doubly- (a), triply- (b) and quadruply-deprotonated (c) sulfonated hirudin. Sulfonate loss is indicated by # and water loss is indicated by ◊.

EDD of doubly-, triply-, and quadruply-deprotonated hirudin (Figures 3.6a-c; respectively) produced up to eight *x* ions with sulfonate retention improving as a function

of charge state, as well as up to five *a*• ions compared to eight *b*/*y*-ions observed in CAD. For the lower charge states, the extent of this complementary information is reduced by significant neutral losses of CO_2 and H_2O. Despite abundant loss of H_2CO and CH_3CHCO_2H in EDD of the 4- charge state, extensive structural information was realized. The number of sulfonate-containing product ions from EDD of the 4- precursor ion far exceeded that seen in the 2- and 3- charge state (20 cleavages compared to 7-9 cleavages, respectively.

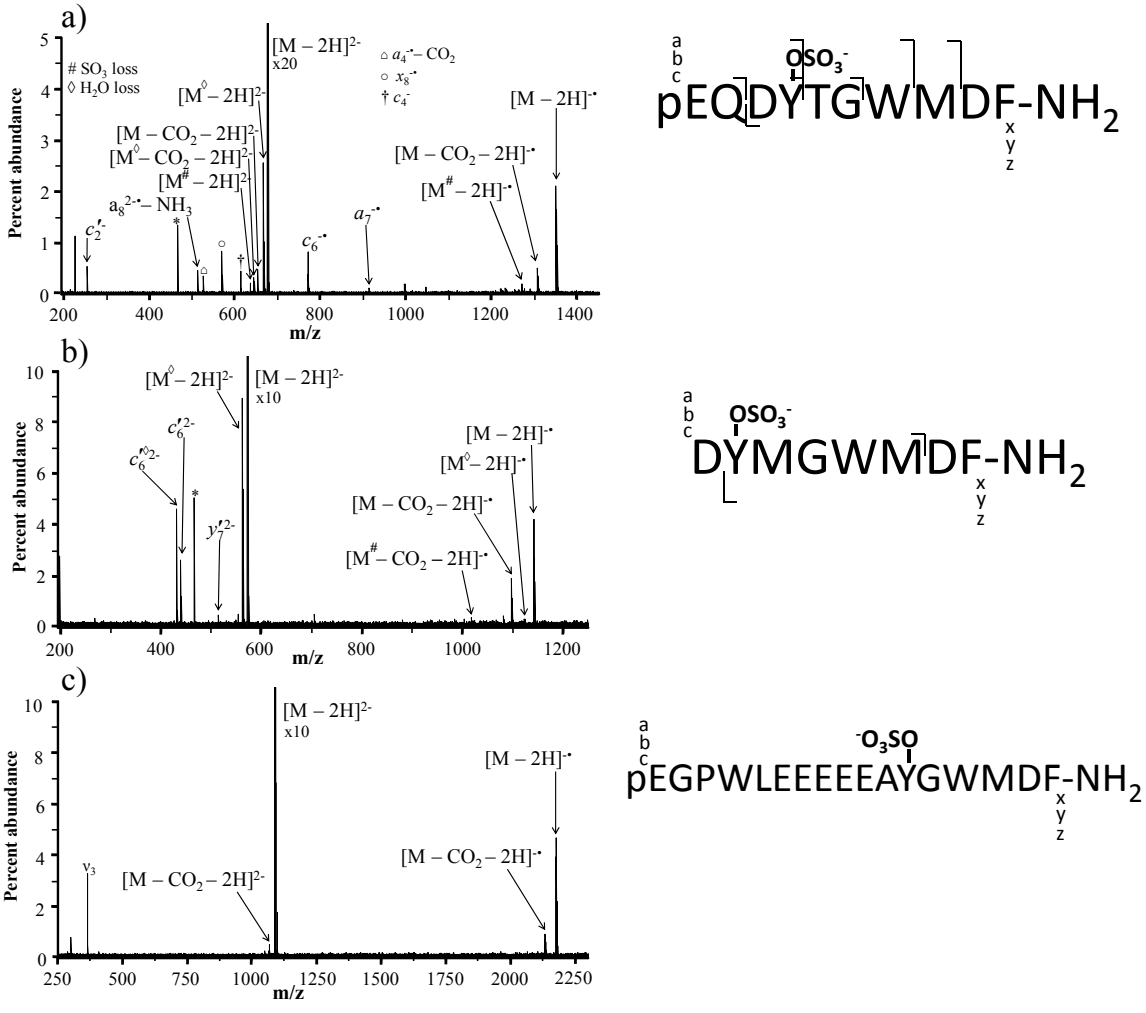

Figure 3.7a–c. EDD of doubly-deprotonated CRL (a), CCKS (b), and GST (c). Sulfonate loss and water loss are indicated by # and ◊, respectively, while electronic noise is indicated by *.

EDD of doubly-deprotonated precursor ions differs widely as per sulfopeptide. EDD of CRL (Figure 3.7a) produced six sulfonate-retaining backbone product ions and suffered little neutral loss from the charge-reduced precursor ion species. In comparison to CAD of this doubly-deprotonated ion (Figure 3.2b), there was only slightly improved sequence coverage (56% for EDD vs. 44% for CAD) with similar sulfonate retention; however, EDD was able to localize the sulfonate group via the complementary product ions $c_4'^-$ and $x_8'^-$. Unlike EDD of CRL, EDD of doubly-deprotonated CCKS (Figure 3.7b) produced mainly neutral loss peaks from both the doubly-deprotonated precursor ion and the charge-reduced radical species with only two sulfonate-retaining product ions ($c_6'^-$, $y_7'^-$) observed. In EDD of doubly-deprotonated gastrin II (Figure 3.7c), electron detachment and CO_2 loss were the only observable events. It is possible that a compact tertiary structure prevents the latter peptide from successfully dissociating in lower charge states. Though EDD of higher charge state peptides was not extensively evaluated here, reports from Taucher, et. al[54] and Yang, et. al[55] for nucleic acids suggest that EDD of higher charge states leads to improved fragmentation efficiency and sequence coverage. It is also interesting to note that the vast majority of the observed product ions in EDD of the aforementioned sulfopeptides correspond to cleavages adjacent to acidic residues, either sulfotyrosine or acidic amino acids (D/E), as previously reported in the literature.[37]

3.3.3 NETD of Sulfopeptides

In NETD, multiply-deprotonated anionic precursor ions transfer an electron to an acceptor reagent, resulting in ion activation and further EDD-like fragmentation. For doubly- (Figure 3.8a) and triply-deprotonated hirudin (data not shown), NETD appears to be more effective for fragmenting the lower charge state, possibly due to poor isolation of

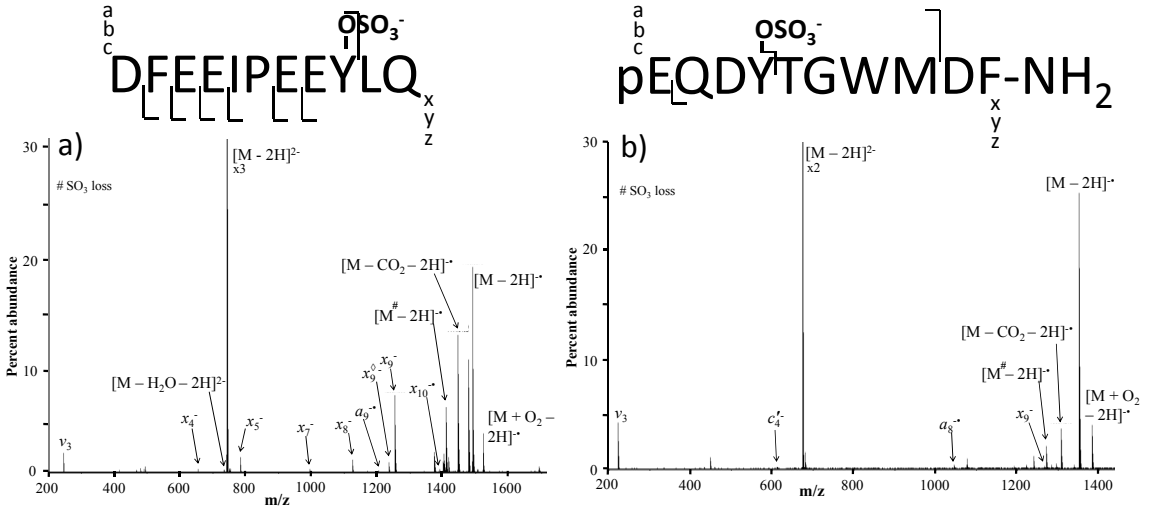

Figure 3.8a-b. NETD of doubly-deprotonated sulfonated hirudin (a) and caerulein (b). Sulfonate loss is indicated by #.

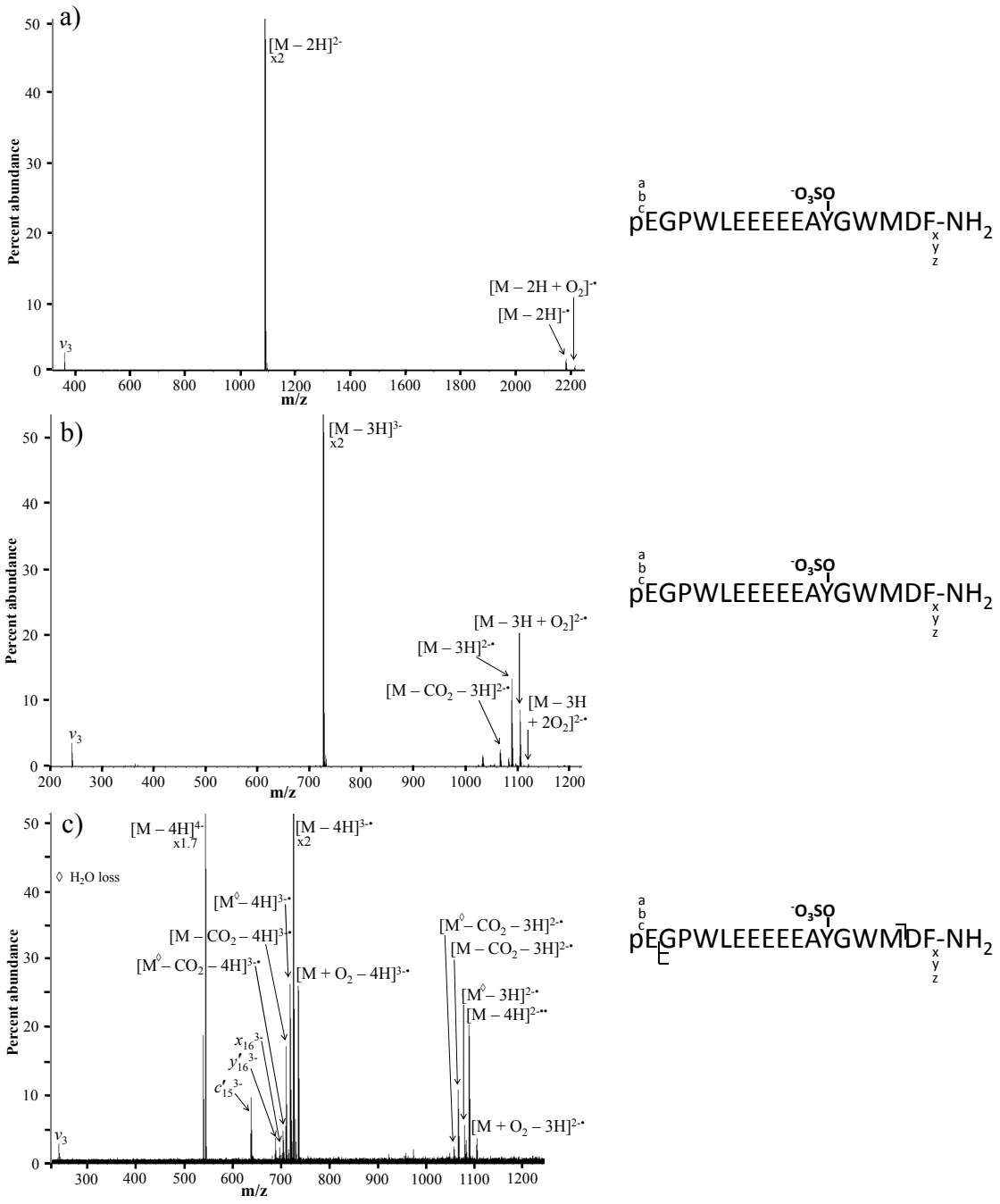

Figure 3.9a–c. NETD of doubly- (a), triply- (b) and quadruply-deprotonated (c) sulfonated human gastrin II. No sulfonate loss was observed in any of these three spectra. Water loss is indicated by ◊.

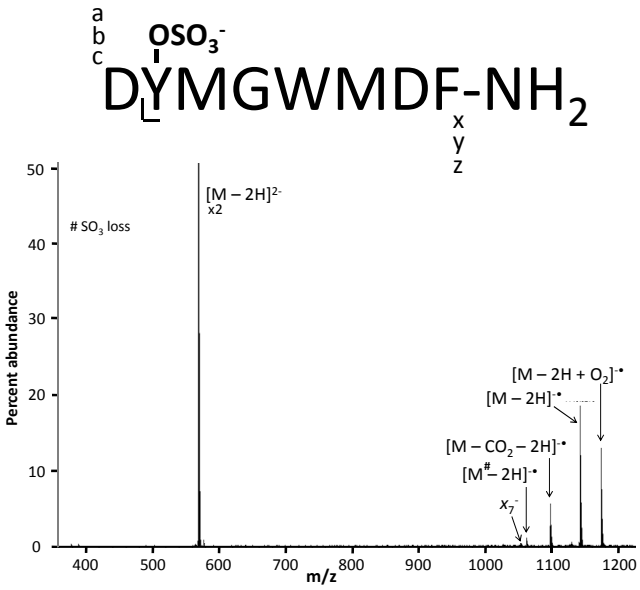

Figure 3.10. NETD of doubly-deprotonated sulfonated cholecystokinin (CCKS). Sulfonate loss is indicated by #.

the triply-deprotonated precursor ion. An extensive series of sulfonate-retaining *x* ions is observed for the 2- precursor, despite the presence of highly-abundant neutral loss peaks from the precursor ion. Oxygen adduct(s) to the charge-reduced precursor ion were observed for this sulfopeptide and other investigated sulfonated ions as has been reported recently in ETD.[56-57] NETD of other doubly-charged precursors did not produce similar analytically useful fragmentation behavior. In fact, NETD of caerulein (Figure 3.8b), gastrin II (Figure 3.9a–c), and cholecystokinin (Figure 3.10) produced very few or no fragments other than neutral loss peaks. Upon fragmentation of higher charge states (in cases for which sufficient precursor ion signal abundance was achievable, e.g. gastrin II (Figure 3.9c)), there was only three backbone fragmentation events. The observed peaks correspond to single- or double-residue loss from the N- and/or C-terminus. This lack of fragmentation in the center of gastrin II suggests that, despite having multiple charges,

intramolecular coulombic repulsion may not be sufficient for this ion to overcome secondary structural constraints. Several previous reports have shown that thermal activation of the precursor ions prior to ion-electron[58] or ion-ion activation[59,60-62] or thermal activation of the charge-reduced species after ion activation[63] may significantly improve fragmentation efficiency. For sulfopeptides, however, vibrational activation is challenging due to the extreme gas-phase lability of the sulfonate group.

3.3.4 niECD of Sulfopeptides

In niECD, singly- and/or multiply-deprotonated precursor ions are irradiated with relatively low-energy (4.5-6 eV) electrons, allowing for electron capture to occur. The charge-increased species that are produced upon electron capture dissociates to generate c' and $z^{\bullet}$ product ions, some of which contain higher charge than the original precursor ion. This type of fragmentation is beneficial for several reasons: 1) because signal is proportional to charge in ICR instrumentation, achieving higher charge states from low-charge-state precursors improves ion signal; and 2) improved fragmentation efficiency is often observed when dissociating higher charge states due to an increased likelihood of having one or more charges on each of the fragments produced from a single backbone fragmentation event. We have proposed that a gaseous zwitterion may be necessary for electron capture to occur by a negative ion,[42] i.e., precursor ions would need two deprotonation sites and an additional proton for an overall singly-deprotonated state or three deprotonation sites and an additional proton for an overall doubly-deprotonated state. Sequence analysis of many known sulfopeptides suggests that ≤ 3 acidic amino acid residues (excluding an often observed D/E flanking the sulfotyrosine residue) as well

as one basic amino acid residue are frequently observed within the ± 5-residue window from the site of tyrosine sulfonation although this trend has not been universally verified.[27, 29, 64-65] Furthermore, Bundgaard, et al. have proposed that the presence of a basic residue two positions away to the N-terminal side of the potential tyrosine sulfonation site enhances the degree of sulfonation.[66] Thus, an overall negative zwitterion appears quite favorable for sulfopeptides in general.

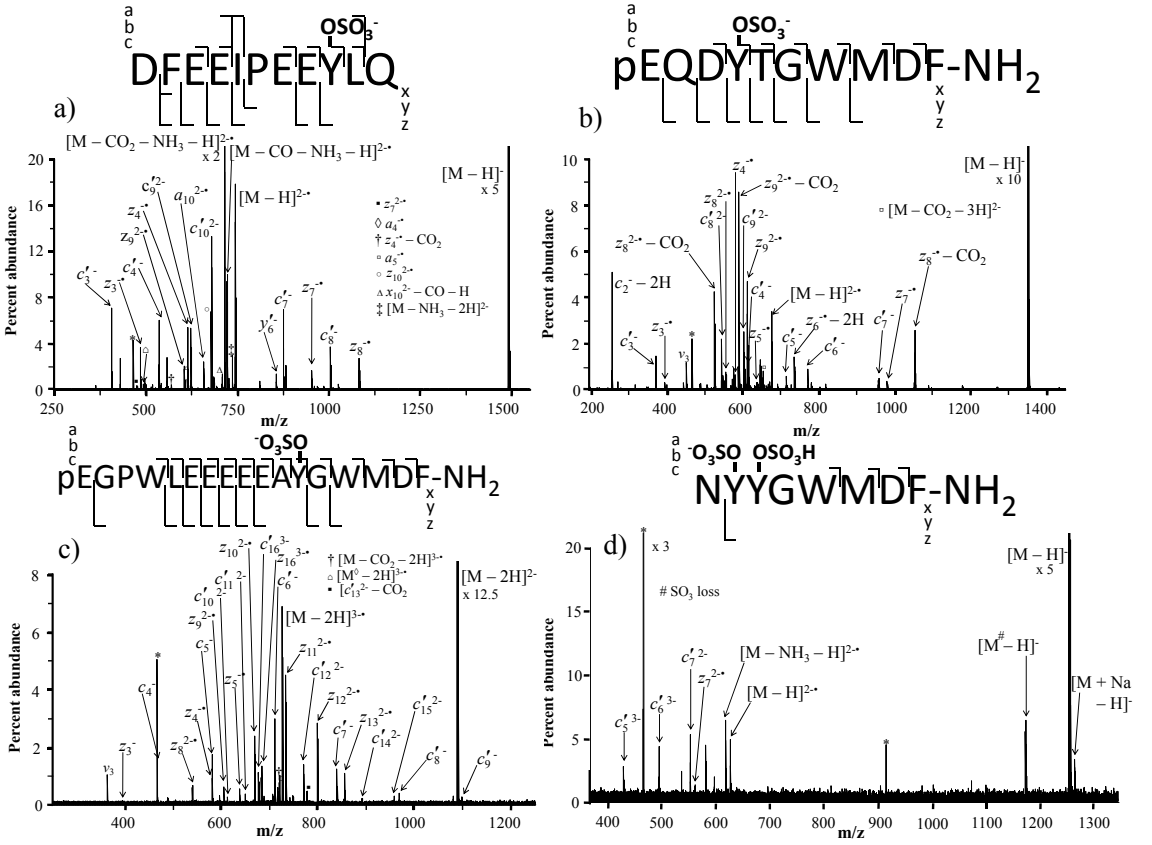

Figure 3.11a–d. niECD of singly-deprotonated sulfonated hirudin (a), doubly-deprotonated sulfonated gastrin II (b), singly-deprotonated sulfonated human caerulein (c) and singly-deprotonated sulfonated cionin (d). Sulfonate loss observed in (d) is indicated by #. Electronic noise is indicated by *.

Figure 3.11a–d shows niECD of four different sulfopeptides, all of which were analyzed above with the previously discussed techniques with the exception of cionin. In

each spectrum there are several abundant c' and/or $z^{\bullet}$ ions which were not observed in negative-ion CAD, EDD nor NETD, demonstrating the complementarity of niECD to the methods discussed above. It is important to note that neutral loss of H_2O is not observed in niECD while loss of CO_2 and NH_3 are minor fragmentation events. Furthermore, there is nearly complete sulfonate retention in niECD, which was also observed for NETD but not for negative-ion CAD nor EDD. The only instance of sulfonate loss was observed in niECD of singly-deprotonated cionin (Figure 3.11d). We believe that sulfonate loss is more likely for this precursor ion because cionin contains two side-by-side sulfonate residues, of which it may be unlikely to deprotonate both residues. Leaving one of the sulfonate residues protonated may result in proton-driven loss of SO_3[52] as discussed above.

3.3.5 Comparison of the Sulfopeptide Fragmentation Efficiencies for Anion MS/MS Techniques

Table 3.1 summarizes the calculated averages and standard deviations for fragmentation efficiency (in percent) in EDD, NETD, and niECD as well as the percent sequence coverage and percent of known vs. unknown peaks in each spectrum for all techniques. It is important to note that fragmentation efficiency was not calculated for CAD because vibrational activation can be easily tuned to give nearly perfect fragmentation efficiency. In CAD, sulfonate retention is either poor or non-existent for all singly-deprotonated ions analyzed here but increases as a function of charge state. In EDD and NETD, fragmentation efficiency suffers due to the high amount of neutral loss compared to backbone product ion abundance. However, these techniques yield nearly

complete sulfonate retention with a few exceptions (cionin 2- and hirudin 3- in EDD, see Table 3.1). In niECD, all calculated values for fragmentation efficiency, sequence coverage, sulfonate retention, and the relative amount of known peaks in the spectra were greater than 80% with the exception of two precursor ions (cionin 1- and hirudin 1-). For example, CAD of singly-deprotonated caerulein and cionin exhibit poor or non-existent

Peptide, z	Fragmentation Method*			
	CAD (+/- error)	EDD (+/- error)	NETD (+/- error)	niECD (+/- error)
Gastrin, 2-	--, 44, 11, 98	0, 0, 100, 77	0, 0, 100, 100	81, 88, 100, 89
3-	--, 50, 85, 96	1, 6, 90, 77	1, 6, 100, 88	N/A
4-	--, 13, 100, 100	11, 44, 98, 90	8, 18, 100, 95	N/A
Hirudin, 1-	--, 70, 4, 100	N/A	N/A	49(7), 80(14), 100(0), 91(5)
2-	--, 67(21), 75(6), 99(1)	29(5), 80(17), 86(1), 87(5)	22(2), 57(15), 89(0.2), 83(4)	N/A
3-	--, 70, 75, 80	58, 50, 56, 61	9, 20, 99, 70	N/A
Caerulein, 1-	--, 0, 0, 97	N/A	N/A	91, 100, 100, 85
2-	--, 44, 95, 97	25, 44, 97, 85	1, 22, 94, 87	N/A
Cholecystokinin, 1-	--, 43, 11, 99	N/A	N/A	90, 86, 100, 89
2-	--, 29, 98, 90	21, 29, 98, 99	2, 14, 96, 97	N/A
Cionin, 1-	--, 0, 0, 100	N/A	N/A	33, 57, 64, 84
2-	--, 29, 0, 93	3, 14, 38, 79	--	N/A

*All values are given as percentages and are listed in this order: percent fragmentation efficiency, percent sequence coverage, percent sulfonate retention, and percent of identifiable peaks in each spectrum.

Table 3.1. Calculated fragmentation efficiencies of EDD, NETD, and niECD as well as percent sequence coverage, sulfonate retention and percent of known vs. unknown product ion signal in spectra for all four techniques.

percent sequence coverage and sulfonate retention. niECD of these same precursor ions shows a dramatic improvement in these numbers despite a lower percentage of identifiable peaks in the spectra. Furthermore, CAD, EDD, and NETD of doubly-deprotonated gastrin II either have moderate sequence coverage with poor sulfonate retention (for CAD) or have no backbone cleavages yet complete sulfonate retention (for EDD and NETD). However, niECD of this precursor ion exhibits high percent fragmentation efficiency, sequence coverage, and sulfonate retention. Clearly, niECD

produces the highest overall performance for sulfonate retention at low charge states and provides both a high level of fragmentation efficiency and sequence coverage relative to the other techniques for all charge states analyzed.

3.4 Conclusion

In this work, a variety of negative ion mode MS/MS activation techniques have been evaluated for the fragmentation of sulfopeptides. While the majority of positive ion mode fragmentation techniques lead to facile SO_3 loss, all negative ion mode techniques evaluated here exhibit some degree of sulfonate retention, allowing for direct localization of this acidic PTM in many cases. In general, negative ion mode CAD, EDD, NETD, and niECD of sulfopeptides examined here are favorable because sulfopeptides are naturally acidic and thus providing several potential sites for deprotonation. CAD provides limited sulfonate retention for singly-deprotonated ions; however, sulfonate retention improves as a function of increasing charge state. EDD of doubly-deprotonated precursor ions shows improved sulfonate retention compared to negative-ion CAD, but EDD backbone fragmentation efficiency suffers greatly from neutral loss. Complete sulfonate retention is observed in NETD, but neutral loss is also a major fragmentation pathway, potentially precluding peptide sequence characterization. By contrast, with the exception of hirudin, niECD provides complete sulfonate retention and extensive sequence coverage with less than 5% structurally-noninformative neutral loss.

3.5 References

1. P. Cohen, The regulation of protein function by multisite phosphorylation – a 25 year update. *Trends Biochem. Sci.* **2000**, *25*, 596-601.
2. J. W. Kehoe, C. R. Bertozzi, Tyrosine sulfation: a modulator of extracellular protein-protein interactions. *Chem. Biol.* **2000**, *7*, R57-61.

3. J. F. Rehfeld, W. W. van Solinge, The tumor biology of gastrin and cholecystokinin. *Adv. Canc. Res.* **1994**, *63*, 295-347.
4. E. Rozengurt, J. H. Walsh, Gastrin, CCK, signaling, and cancer. *Ann. Rev. Physiol.* **2001**, *63*, 49-76.
5. G. L. Matters, C. McGovern, J. F. Harms, K. Markovic, K. Anson, C. Jayakumar, M. Martenis, C. Awad, J. P. Smith, Role of endogenous cholecystokinin on growth of human pancreatic cancer. *Int. J. Oncol.* **2011**, *38*, 593-601.
6. J. Zhang, P. L. Yang, N. S. Gray, Targeting cancer with small molecule kinase inhibitors. *Nat. Rev. Cancer* **2009**, *9*, 28-39.
7. K. Biemann, H. A. Scoble, Characterization by tandem mass-spectrometry of structural modifications in proteins. *Science* **1987**, *237*, 992-998.
8. A. Tholey, J. Reed, W. D. Lehmann, Electrospray tandem mass spectrometric studies of phosphopeptides and phosphopeptide analogues. *J. Mass Spectrom.* **1999**, *34*, 117-123.
9. K. F. Medzihradszky, Z. Darula, E. Perlson, M. Fainzilber, R. J. Chalkley, H. Ball, D. Greenbaum, M. Bogyo, D. R. Tyson, R. A. Bradshaw, A. L. Burlingame, O-sulfonation of serine and threonine: mass spectrometric detection and characterization of a new posttranslational modification in diverse proteins throughout the eukaryotes. *Mol. Cell. Proteomics* **2004**, *3*, 429-440.
10. R. E. Bossio, A. G. Marshall, Baseline resolution of isobaric phosphorylated and sulfated peptides and nucleotides by electrospray ionization FT ICR-MS: another step toward mass spectrometry-based proteomics. *Anal. Chem.* **2002**, *74*, 1674-1679.
11. A. M. Palumbo, G. E. Reid, Evaluation of Gas-Phase Rearrangement and Competing Fragmentation Reactions on Protein Phosphorylation Site Assignment Using Collision Induced Dissociation-MS/MS and MS3. *Anal. Chem.* **2008**, *80*, 9735-9747.
12. N. Mischerikow , A. F. M. Altelaar, D. Navarro, S. Mohammed, A. J. R. Heck, Comparative assessment of site assignments in CID and ETD spectra of phosphopeptides discloses limited relocation of phosphate groups. *Mol. Cell. Proteomics* **2010**, *9*, 2140-2148.
13. M. Aguiar, W. Haas, S. A. Beausoleil, J. Rush, S. P. Gygi, Gas-Phase Rearrangements Do Not Affect Site Localization Reliability in Phosphoproteomics Data Sets. *J. Proteome Res.* **2010**, *9*, 3103-3107.
14. Y. Yu, A. J. Hoffhines, K. L. Moore, J. A. Leary, Determination of the sites of tyrosine O-sulfation in peptides and proteins. *Nat. Methods* **2007**, *4*, 583-588.
15. J. Rappsilber, H. Steen, M. Mann, Labile sulfogroup allows differentiation of sulfotyrosine and phosphotyrosine in peptides. *J. Mass Spectrom.* **2001**, *36*, 832-833.
16. J. F. Nemeth-Cawley, S. Karnik, J. C. Rouse, Analysis of sulfated peptides using positive electrospray ionization tandem mass spectrometry. *J. Mass Spectrom.* **2001**, *36*, 1301-1311.
17. S. W. Taylor, C. Sun, A. Hsieh, N. L. Andon, S. S. Ghosh, A sulfated, phosphorylated 7 kDa secreted peptide characterized by direct analysis of cell culture media. *J. Proteome Res.* **2008**, *7*, 795-802.
18. R. A. Zubarev, Reactions of polypeptide ions with electrons in the gas phase. *Mass Spectrometry Reviews* **2003**, *22*, 57-77.

19. S. D. H. Shi, M. E. Hemling, S. A. Carr, D. M. Horn, I. Lindh, F. W. McLafferty, Phosphopeptide/phosphoprotein mapping by electron capture dissociation mass spectrometry. *Anal. Chem.* **2001**, *73*, 19-22.
20. A. Stensballe, O. N. Jensen, J. V. Olsen, K. F. Haselmann, R. A. Zubarev, Electron capture dissociation of singly and multiply phosphorylated peptides. *Rapid Commun. Mass Spectrom.* **2000**, *14*, 1793-1800.
21. N. L. Kelleher, R. A. Zubarev, K. Bush, B. Furie, B. C. Furie, F. W. McLafferty, C. T. Walsh, Localization of labile posttranslational modifications by electron capture dissociation: the case of gamma-carboxyglutamic acid. *Anal. Chem.* **1999**, *71*, 4250-4253.
22. K. F. Haselmann, B. A. Budnik, J. V. Olsen, M. L. Nielsen, C. A. Reis, H. Clausen, A. H. Johnsen, R. A. Zubarev, Advantages of external accumulation for electron capture dissociation in Fourier transform mass spectrometry. *Anal. Chem.* **2001**, *73*, 2998-3005.
23. J. E. P. Syka, J. J. Coon, M. J. Schroeder, J. Shabanowitz, D. F. Hunt, Peptide and protein sequence analysis by electron transfer dissociation mass spectrometry. *Proc. Nat. Acad. Sci. U.S.A.* **2004**, *101*, 9528-9533.
24. K. F. Medzihradszky, S. Guan, D. A. Maltby, A. L. Burlingame, Sulfopeptide fragmentation in electron-capture and electron-transfer dissociation. *J. Am. Soc. Mass Spectrom.* **2007**, *18*, 1617-1624.
25. H. Liu, K. Hakansson, Electron capture dissociation of tyrosine O-sulfated peptides complexed with divalent metal cations. *Anal. Chem.* **2006**, *78*, 7570-7576.
26. L. M. Mikesh, B. Ueberheide, A. Chi, J. J. Coon, J. E. P. Syka, J. Shabanowitz, D. F. Hunt, The Utility of ETD Mass Spectrometry in Proteomic Analysis. *Biochim. Biophys. Acta* **2006**, *1764*, 1811-1822.
27. G. Hortin, R. Folz, J. I. Gordon, A. W. Strauss, Characterization of sites of tyrosine sulfation in proteins and criteria for predicting their occurrence. *Biochem. Biophys. Res. Commun.* **1986**, *141*, 326-333.
28. W. B. Huttner, Tyrosine sulfation and the secretory pathway. *Ann. Rev. Physiol.* **1988**, *50*, 363-376.
29. W. H. Lin, K. Larsen, G. L. Hortin, J. A. Roth, Recognition of substrates by tyrosylprotein sulfotransferase. Determination of affinity by acidic amino acids near the target sites. *J. Biol. Chem.* **1992**, *267*, 2876-2879.
30. Shannon L. Cook, G. P. Jackson, Metastable atom-activated dissociation mass spectrometry of phosphorylated and sulfonated peptides in negative ion mode. *J. Am. Soc. Mass Spectrom.* **2011**, *22*, 1088-1099.
31. R. D. Smith, J. A. Loo, C. G. Edmonds, C. J. Barinaga, H. R. Udseth, New developments in biochemical mass-spectrometry - electrospray ionization. *Anal. Chem.* **1990**, *62*, 882-899.
32. J. A. Loo, R. R. O. Loo, K. J. Light, C. G. Edmonds, R. D. Smith, Multiply-charged negative-ions by electrospray ionization of polypeptides and proteins. *Anal. Chem.* **1992**, *64*, 81-88.
33. A. P. Hunter, D. E. Games, Chromatographic and mass-spectrometric methods for the identification of phosphorylation sites in phosphoproteins. *Rapid Commun. Mass Spectrom.* **1994**, *8*, 559-570.

34. S. T. Steinborner, J. H. Bowie, The negative ion mass spectra of M-H (-) ions derived from caeridin and dynastin peptides. Internal backbone cleavages directed through Asp and Asn residues. *Rapid Commun. Mass Spectrom.* **1997**, *11*, 253-258.
35. P. Boontheung, C. S. Brinkworth, J. H. Bowie, R. V. Baudinette, Comparison of the positive and negative ion electrospray mass spectra of some small peptides containing pyroglutamate. *Rapid Commun. Mass Spectrom.* **2002**, *16*, 287-292.
36. B. A. Budnik, K. F. Haselmann, R. A. Zubarev, Electron detachment dissociation of peptide di-anions: an electron-hole recombination phenomenon. *Chem. Phys. Lett.* **2001**, *342*, 299-302.
37. F. Kjeldsen, O. A. Silivra, I. A. Ivonin, K. F. Haselmann, M. Gorshkov, R. A. Zubarev, C-alpha-C backbone fragmentation dominates in electron detachment dissociation of gas-phase polypeptide polyanions. *Chem.-Eur. J.* **2005**, *11*, 1803-1812.
38. L. S. Eberlin, Y. Xia, H. Chen, R. G. Cooks, Atmospheric pressure thermal dissociation of phospho- and sulfopeptides. *J. Am. Soc. Mass Spectrom.* **2008**, *19*, 1897-1905.
39. J. J. Coon, J. Shabanowitz, D. F. Hunt, J. E. P. Syka, Electron transfer dissociation of peptide anions. *J. Am. Soc. Mass Spectrom.* **2005**, *16*, 880-882.
40. M. Huzarska, I. Ugalde, D. A. Kaplan, R. Hartmer, M. L. Easterling, N. C. Polfer, Negative electron transfer dissociation of deprotonated phosphopeptide anions: choice of radical cation reagent and competition between electron and proton transfer. *Anal. Chem.* **2010**, *82*, 2873-2878.
41. J. J. Wolff, F. E. Leach III, T. N. Laremore, D. A. Kaplan, M. L. Easterling, R. J. Linhardt, I. J. Amster, Negative electron transfer dissociation of glycosaminoglycans. *Anal. Chem.* **2010**, *82*, 3460-3466.
42. H. J. Yoo, N. Wang, S. Zhuang, H. Song, K. Håkansson, Negative-ion electron capture dissociation: radical-driven fragmentation of charge-increased gaseous peptide anions. *J. Am. Chem. Soc.* **2011**, *133*, 16790-16793.
43. M. W. Senko, J. D. Canterbury, S. Guan, A. G. Marshall, A high-performance modular data system for Fourier transform ion cyclotron resonance mass spectrometry. *Rapid Commun. Mass Spectrom.* **1996**, *10*, 1839-1844.
44. E. B. Ledford, D. L. Rempel, M. L. Gross, Space-charge effects in Fourier transform mass spectrometry - mass calibration. *Anal. Chem.* **1984**, *56*, 2744-2748.
45. J. M. Wells, S. A. McLuckey, Collision-induced dissociation (CID) of peptides and proteins. *Methods Enzymol* **2005**, *402*, 148-185.
46. J. Yang, K. Hakansson, Characterization and optimization of electron detachment dissociation Fourier transform ion cyclotron resonance mass spectrometry. *Int J Mass Spectrom* **2008**, *276*, 144-148.
47. S. J. Pitteri, P. A. Chrisman, S. A. McLuckey, Electron-Transfer Ion/Ion Reactions of Doubly Protonated Peptides: Effect of Elevated Bath Gas Temperature. *Anal. Chem.* **2005**, *77*, 5662-5669.
48. N. P. Ewing, C. J. Cassady, Dissociation of multiply charged negative ions for hirudin (54-65), fibrinopeptide B, and insulin A (oxidized). *J. Am. Soc. Mass Spectrom.* **2001**, *12*, 105-116.

49. J. H. Bowie, C. S. Brinkworth, S. Dua, Collision-induced fragmentations of the $(M - H)^-$ parent anions of underivatized peptides: an aid to structure determination and some unusual negative ion cleavages. *Mass Spectrom. Rev.* **2002**, *21*, 87-107.
50. D. Bilusich, J. H. Bowie, Fragmentations of (M-H)- anions of underivatized peptides. Part 2: characteristic cleavages of Ser and Cys and of disulfides and other post-translational modifications, together with some unusual internal processes. *Mass Spectrom. Rev.* **2009**, *28*, 20-34.
51. R. J. Waugh, J. H. Bowie, A review of the collision-induced dissociations of deprotonated dipeptides and tripeptides. An aid to structure determination. *Rapid Commun. Mass Spectrom.* **1994**, *8*, 169-173.
52. T. Yagami, K. Kitagawa, C. Aida, H. Fujiwara, S. Futaki, Stabilization of a tyrosine O-sulfate residue by a cationic functional group: formation of a conjugate acid-base pair. *J. Pept. Res.* **2000**, *56*, 239-249.
53. J. Zaia, C. E. Costello, Tandem Mass Spectrometry of Sulfated Heparin-Like Glycosaminoglycan Oligosaccharides. *Anal. Chem.* **2003**, *75*, 2445-2455.
54. M. Taucher, K. Breuker, Top-Down Mass Spectrometry for Sequencing of Larger (up to 61 nt) RNA by CAD and EDD. *J. Am. Soc. Mass Spectrom.* **2010**, *21*, 918-929.
55. J. Yang, K. Hakansson, Characterization of oligodeoxynucleotide fragmentation pathways in infrared multiphoton dissociation and electron detachment dissociation by Fourier transform ion cyclotron double resonance. *Eur. J. Mass Spectrom.* **2009**, *15*, 293-304.
56. Yu Xia, Paul A. Chrisman, Sharon J. Pitteri, David E. Erickson, S. A. McLuckey, Ion/Molecule Reactions of Cation Radicals Formed from Protonated Polypeptides via Gas-Phase Ion/Ion Electron Transfer. *J. Am. Chem. Soc.* **2006**, *128*, 11792-11798.
57. S. A. McLuckey, T. Y. Huang, Ion/ion reactions: new chemistry for analytical MS. *Anal. Chem.* **2009**, *81*, 8669-8676.
58. D. M. Horn, Y. Ge, F. W. McLafferty, Activated ion electron capture dissociation for mass spectral sequencing of larger (42 kDa) proteins. *Anal. Chem.* **2000**, *72*, 4778-4784.
59. D. L. Swaney, G. C. McAlister, M. Wirtala, J. C. Schwartz, J. E. P. Syka, J. J. Coon, Supplemental activation method for high-efficiency electron-transfer dissociation of doubly protonated peptide precursors. *Anal. Chem.* **2007**, *79*, 477-485.
60. R. A. Zubarev, N. A. Kruger, E. K. Fridriksson, Mark A. Lewis, D. M. Horn, B. K. Carpenter, F. W. McLafferty, Electron Capture Dissociation of Gaseous Multiply-Charged Proteins Is Favored at Disulfide Bonds and Other Sites of High Hydrogen Atom Affinity. *J. Am. Chem. Soc.* **1999**, *121*, 2857-2862.
61. F. W. McLafferty, D. M. Horn, K. Breuker, Y. Ge, M. A. Lewis, B. Cerda, R. A. Zubarev, B. K. Carpenter, Electron Capture Dissociation of Gaseous Multiply Charged Ions by Fourier-Transform Ion Cyclotron Resonance. *Journal of the American Society for Mass Spectrometry* **2001**, *12*, 245-249.
62. V. A. Mikhailov, H. J. Cooper, Activated Ion Electron Capture Dissociation (AI ECD) of Proteins: Synchronization of Infrared and Electron Irradiation with Ion Magnetron Motion. *J. Am. Soc. Mass Spectrom.* **2009**, *20*, 763-771.
63. K. Hakansson, M. J. Chalmers, J. P. Quinn, M. A. McFarland, C. L. Hendrickson, A. G. Marshall, Combined Electron Capture and Infrared Multiphoton Dissociation for

Multistage MS/MS in a Fourier Transform Ion Cyclotron Resonance Mass Spectrometer. *Anal. Chem.* **2003**, *75*, 3256-3262.
64. W. B. Huttner, P. A. Baeuerle, Protein sulfation on tyrosine. *Mod. Cell Biol.* **1988**, *6*, 97-140.
65. G. L. Rosenquist, H. B. Nicholas, Jr., Analysis of sequence requirements for protein tyrosine sulfation. *Prot. Sci.* **1993**, *2*, 215-222.
66. J. R. Bundgaard, J. Vuust, J. F. Rehfeld, New consensus features for tyrosine O-sulfation determined by mutational analysis. *J. Biol. Chem.* **1997**, *272*, 21700-21705.

CHAPTER IV

IMPROVING BACKBONE FRAGMENTATION EFFICIENCY IN ELECTRON DETACHMENT DISSOCIATION OF ACIDIC PEPTIDE IONS

4.1 Introduction

Electron detachment dissociation (EDD) was first realized for polypeptides by Zubarev and colleagues in 2001 as an alternative electron-based fragmentation technique to positive ion mode electron capture dissociation (ECD) for analysis of acidic analytes in negative ion mode.[1] Briefly, multiply charged anions are irradiated on the millisecond to second time scale with high-energy electrons in excess of 10 eV to allow detachment of an electron from the multiply deprotonated analyte. The excess energy likely also causes electronic excitation and leads to subsequent radical-driven fragmentation of the ion. Zubarev originally described EDD as "intramolecular ECD" because the initially proposed mechanism suggested that electron capture occurs following electron detachment.[2] In this mechanism, the positively-charged radical "hole" resulting from electron detachment combines with an intramolecular electron.[1] The recombination energy from this exothermic process is $\simeq$5 eV,[3] making electronic excitation of the ion possible (where the minimum energy for this process is $\simeq$ 5–7 eV[4]). The initial EDD publication[1] reported several types of product ions ($a^{\bullet}$, c, $c^{\bullet}$, $z^{\bullet}$) with most favorable

cleavage at N-C_α bonds but later work involving EDD in a quadrupole ion trap revised the product ion preference to place $a^\bullet$ and *x*-ion formation as the most favorable, followed by other product ions. Radical $a^\bullet$ ions and even-electron *x* ions are formed more readily than radical $x^\bullet$ ions and even-electron *a* ions due to an energy barrier of 74.2 kJ/mol,[5] where 100 kJ/mol$\simeq$1 eV. (Please refer to Introduction, Figure 1.9 for the EDD mechanism.)

Håkansson, Amster, Zubarev and others have reported EDD characterization of acidic analytes such as oligonucleotides,[6-7] sulfonated oligosaccharides,[8-9] sulfopeptides,[1] and phosphopeptides.[5, 10] Despite the formation of structurally informative $a^\bullet/x$ ions from acidic peptides as well as glycosidic and cross-ring fragments from acidic sugars, EDD also results in water loss from charge-reduced sugars and extensive neutral loss of carbon dioxide from aspartic and glutamic acid side chains as well as peptide C-termini, which may preclude formation of structurally informative product ions. This "Achilles' heel" is believed to be a dominant characteristic of EDD due to the fact that deprotonation of a peptide, for instance, occurs favorably at a carboxylic acid ($pK_a^{R\text{-}COOH} \leq 4.5$) while electron detachment occurs at a site of relatively low electron affinity[1] ($EA_{R\text{-}COO^-}\simeq$3.4-3.6 eV for acetate[11] and benzoate[12]). It is also possible to deprotonate and subsequently detach an electron from a backbone peptide amide;[5] however, this site is less acidic than carboxylic acids. Thus, because fragmentation commonly occurs near the site of electron detachment,[5, 13] it follows that carbon dioxide loss in EDD is energetically favorable compared to fragmentation of the peptide backbone. We hypothesize that chemical derivatization of carboxylic acids or use of alternative anion charge carriers may lead to reduction and/or elimination of CO_2 loss in peptide EDD and, consequently, improved

peptide backbone fragmentation efficiency and subsequent structural characterization of acidic peptides that typically fragment poorly in EDD (due to extensive CO_2 loss).

The nature of the charge carrier has been shown to play a key role in ECD fragmentation behavior. Zubarev and coworkers compared ECD of doubly-protonated and zinc-adducted angiotensin II dications and found that c/z-ion formation decreased upon metal adduction.[14] Williams and coworkers further investigated the effect of metal adduction on ECD behavior, reporting that electron capture at alkali metal adducts neutralized the cation, resulting in metalated *c*/*z*-ions.[15] Liu and Håkansson[16] examined ECD of a divalent metal-adducted peptide and found that relative abundances of *c*/*z* product ions changed significantly depending on the metal type and that *c*/*z*-ion formation was shut down for soft metals such as nickel and cobalt. The same authors reported in a separate study that sulfonation can be preserved by adducting divalent metal cations to tyrosine-*O*-sulfopeptides.[17] Chamot-Rooke and coworkers have reported that ECD of *O*-glycosylated and *O*-phosphorylated peptides derivatized at the N-terminus with a fixed charge phosphonium group exhibited drastically improved sequence coverage and PTM site localization compared to the same but underivatized peptides.[18] Recently, Chan and coworkers showed that ECD of Mn^{2+} and Zn^{2+}-adducted peptides produced metalated and non-metalated *c*/*z*-ions, ECD of Fe^{2+}, Co^{2+}, and Ni^{2+}-adducted peptides produced metalated *a*/*y*-ions, and ECD of Cu^{2+}-adducted peptides produced *a*/*x*-ions.[19] The unique fragmentation behavior of various divalent metal adducts may lead to a "tunable" system for obtaining complementary fragmentation.[20] These authors have also utilized alkaline earth metals to evaluate the change in ECD behavior of synthetic peptides, observing a series of *c* and/or *z*-ions containing the adducted metal ion.[20] *Ab initio* calculations of

Mg^{2+}-adducted N-methyl Gly-Gly as a model system suggested that Mg^{2+}, when coordinated to carbonyl oxygens, enhances the acidity of the amide proton by pulling electron density toward the carbonyl oxygen, which has also been reported elsewhere.[21-22] This enhanced acidity promotes a relatively low energy hydrogen atom transfer from the amide to the N-terminus (ΔH_{rxn} = +5 kJ/mol, $E_{transition}$ = +15 kJ/mol).[20] In this case, charge separation is more easily facilitated than that observed for protonated model systems, leading to a zwitterion in the presence of a highly basic site. Zwitterionic structures may promote different fragmentation behavior, possibly due to the presence of more precursor ion conformers, leading to a wider variety of neutralization events at the mobile proton or other protonated sites upon electron capture.[19] Other work has shown that the specific gas-phase structure(s) are critical to ECD fragmentation behavior.[23-24]

Contrary to metal adduction to peptides, anion adduction to proteins and peptides has recently been performed in both positive-[25-26] and negative-ion mode electrospray ionization mass spectrometry (ESI-MS).[27] Specifically, in negative-ion mode, Liu and Cole report that matching the gas-phase basicity of adduct anions to carboxylates can increase the charge state up to 3- for chloride-adducted fibrinopeptide B and ACTH 22-39.[27] The specific points of interaction for anion adduction were proposed as either hydrogens of carboxylic acids or protonated amino/imino groups. The carboxylic acid sites are favored due to closer matching of the adduct-carboxylic acid gas-phase basicities which can stabilize the interaction. These authors also reported that the propensity of adduct loss with or without the hydrogen in ESI-MS depends upon the relative gas-phase basicities of the adduction site and the adduct anion. Specifically, an anion of lower gas-

phase basicity adducted to a site of higher gas-phase basicity will most likely depart with the hydrogen atom, leaving the deprotonated carboxylate.

In addition to ESI-MS analysis of anion-adducted peptides, EDD of chloride-adducted oligosaccharides has been reported.[28] These authors found that EDD of chloride-adducted oligosaccharides provided complementary structural information including more cross-ring and glycosidic cleavages compared to EDD of deprotonated precursor ions. Furthermore, some chloride-adducted product ions were observed in EDD of singly chloride-adducted, singly-deprotonated maltoheptose but not in EDD of the branched sugar DSLNT.

Here, we examine the EDD behavior of non-acidic peptides (i.e., peptides lacking carboxylic acids). Further, for acidic peptides, we employ carboxylic acid derivatization with 4-aminonaphthalene sulfonic acid (ANSA)[29] and anion adduction to seek a solution for reducing carbon dioxide loss in EDD. Finally, N-terminal acetylation was explored as a means to alter peptide gas-phase structure and thus possibly the EDD fragmentation behavior.

4.2 Materials and methods

4.2.1 Peptide Standards

Neuromedin B (GNLWATGHFM-NH_2; Sigma, St. Louis, MO), neuromedin C (GNHWAVGHLM-NH_2; Sigma), disulfide-bonded vasopressin (CYFQNCPRG-NH_2; Sigma), desulfonated caerulein (pEQDYTGWMDF-NH_2; Bachem, Torrance, CA), angiotensin I (DRVYIHPFHL; Sigma), sulfonated and desulfonated cholecystokinin fragment 26-33 (DyMGWMDF-NH_2, CCKS and CCK, respectively; Advanced

ChemTech, Louisville, KY), neurokinin B (DMHDFFVGLM-NH_2, Sigma), [Gly-OH]-leutinizing hormone releasing hormone (pEHWSYGLRPG, LHRH; Sigma), [Met-OH]-substance P (RPKPQQFFGLM; Sigma), bradykinin fragment 2-9 (PPGFSPFR; Sigma), sulfonated hirudin fragment 54-65 (DFEEIPEEyLQ; Advanced ChemTech) and sulfonated cionin (NyyGWMDF-NH_2; Bachem) were used without further purification unless otherwise noted. LC/MS-grade water and methanol were purchased from J.T. Baker (Phillipsburg, NJ), ES tuning mix was purchased from Agilent (Santa Clara, CA), and triethyl amine, dithiothreitol, 1-ethyl-3-(3-dimethylaminopropyl)carbodiimide (EDC), ANSA, glacial acetic acid, pyridine and hydrochloric acid were purchased from Sigma.

4.2.2 Preparation of Non-Acidic Peptides

Neuromedin B and C were diluted to a concentration of 2 μM in 50:50 MeOH:H_2O with 1% TEA prior to MS analysis in negative ion mode. Vasopressin was reduced with 10 mM dithiothreitol (DTT) in 50:50 methanol:water (MeOH:H_2O) for 1 hr at 55 ^oC. No cleanup was carried out prior to analysis in order to prevent conversion back to the disulfide-bonded form.

4.2.3 Preparation of ANSA-Derivatized Desulfonated Caerulein

Derivatization of carboxylic acids with ANSA was carried out based on a previously published protocol from Lindh, et al.[29] Briefly, 100 nmol of CRL-SO_3 was dried in a vacuum centrifuge and reconstituted in 50 μL of coupling buffer (8% pyridine in ~1% HCl, pH 5.0), 50 μL 1M EDC and 400 μL 250 mM ANSA. The reaction proceeded for 2 hr at 25 ^oC and was stopped with 50 μL glacial acetic acid. The derivatized peptide was purified by liquid chromatography separation on an Agilent Zorbax C_8 column (4.6 x 150 mm) at 1 mL/min flow rate with a linear gradient of 2-

100% acetonitrile in 0.1% formic acid over 20 min and monitored at 214 nm. Sample fractions (1.5 mL) were dried in a vacuum centrifuge then reconstituted in 50:50 MeOH:H_2O with 1% TEA prior to negative ion mode MS analysis.

4.2.4 Preparation of Anion-Adducted Acidic Peptides

LHRH, Met-OH substance P and angiotensin I were mixed with either ammonium bromide or ammonium chloride at a 64:3.2 μM ratio based on a previously published protocol.[27]

4.2.5 Mass Spectrometry

All samples were directly infused in negative ion mode in 50:50 MeOH:H_2O without TEA using an ESI source (Apollo II, Bruker Daltonics, Billerica, MA) unless otherwise noted. All experiments were performed on a 7T Q-FT ICR-MS instrument equipped with a hollow cathode dispenser to generate electrons (solariX-Q, Bruker Daltonics). The ESI flow rate was set to 70 or 140 μL/hr for anion adduction experiments and the nebulizing gas was flowing at 1.3 L/min. The voltage applied to the capillary, the end plate offset and the first skimmer were carefully optimized for each analyte to prevent loss of the adduct. Ions were accumulated in the first hexapole for 10 ms then mass-selectively filtered as per peptide and charge state by the quadrupole. Mass-selected ions were transferred to the second hexapole and accumulated for 0.3 - 27.5 s. Ions were dynamically trapped in the ICR cell then irradiated for 1–2.5 s with 18.5-20.5 eV electrons generated from a hollow dispenser cathode with a + 0.2-1 V bias voltage held on the lens electrode with respect to the cathode bias voltage. Resulting product ions were detected as an image current following resonant excitation. Time-domain data were Fourier transformed, and the resulting frequencies corresponding to

m/z 300 to 2500 were displayed using the Bruker solariXcontrol software (v. 1.5) with 512k data points summed over 32 scans.

4.2.6 Data Analysis

External calibration was performed daily on the solariX using ES tuning mix and this calibration was applied to each data acquisition event. DataAnalysis software (v. 4.0) was used for peak picking. Calculated m/z ratios for peptides and their product ions were obtained from MS Product in Protein Prospector (http://prospector.ucsf.edu/prospector/mshome.htm) and the PeptideMass tool in Expasy (http://www.expasy.ch/tools/peptide-mass.html). These calculated values were compiled into an in-house built macro and searched against experimental m/z ratios for peak identification and accurate mass matching. Mass assignments with an error tolerance ≤15 ppm are reported here.

4.3 Results

4.3.1 EDD of Non-Acidic Peptides

Figure 4.1 shows EDD spectra of the doubly-deprotonated peptides neuromedin B, neuromedin C, and reduced vasopressin (a–c, respectively) all of which do not contain any carboxylic acids. EDD of neuromedin B and C resulted in extensive fragmentation, exhibiting *a*, *b*, *c* and *x*, *y*, *z*-ions with little neutral loss. C-terminal *x* and $z^{\bullet}$ ions dominate the spectra with fewer N-terminal ions, corresponding to 89% sequence coverage for both neuromedin peptides. The only bond that was not cleaved in both cases was the histidine-leucine bond. Several $z^{\bullet}$ - 2H and $z^{\bullet}$ - H ions were observed in both neuromedin B and C EDD spectra. Such ions have been previously reported for

ECD[30] but not EDD. Our group has also reported EDD fragments with the same charge state as the precursor ion, which is observed here for two *z*-ions. We also observed neutral loss of a leucine side chain ($CH(CH_3)_2$, 43.0548), which has been reported in ECD,[31] from the doubly-deprotonated precursor ions as well as the charge-reduced species for neuromedin B only.

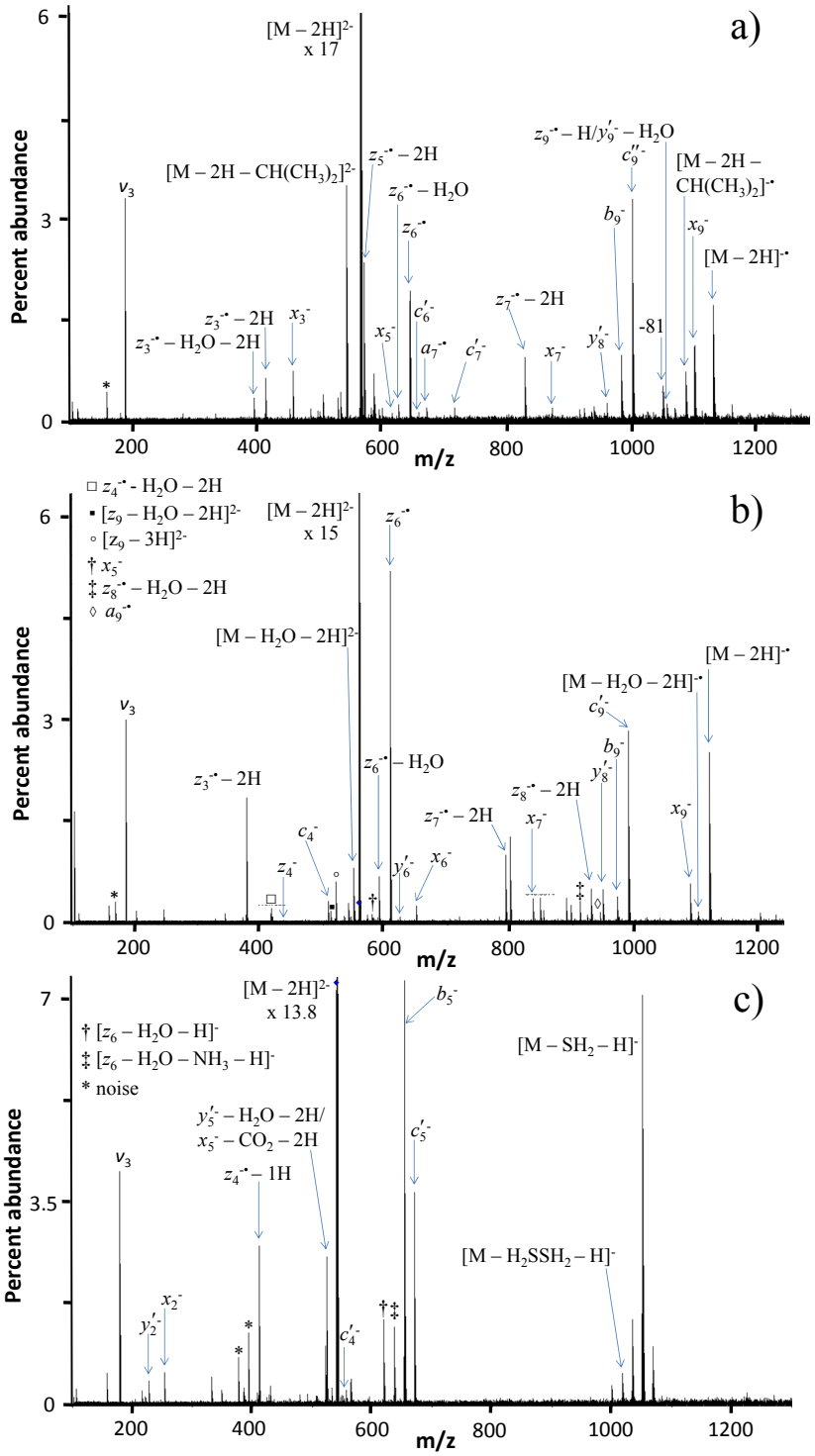

Figure 4.1 a–c. EDD spectra of doubly deprotonated neuromedin B (a), neuromedin C (b) and DTT-reduced vasopressin (c). Electronic noise is indicated by * and the 3rd harmonic is indicated by v_3.

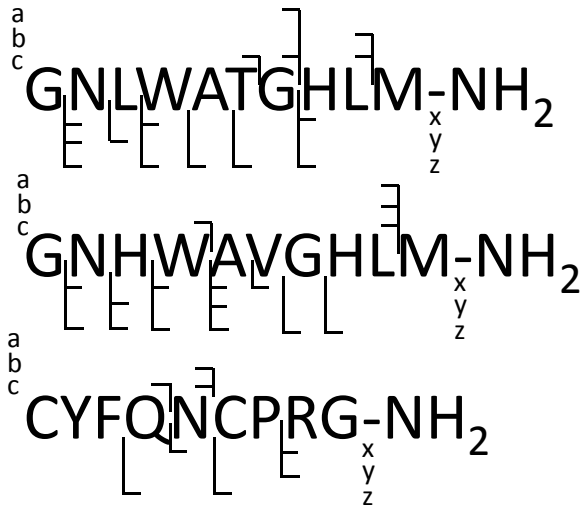

Figure 4.2. Summary of EDD product ions observed from doubly-deprotonated neuromedin B (top), neuromedin C (middle), and reduced vasopressin (bottom). N-terminal ions consist of *a*/*b*/*c*-ions, and C-terminal ions consist of *x*/*y*/*z*-ions with horizontal lines indicating the presence of each ion.

EDD of DTT-reduced vasopressin (Figure 4.1c) did not produce as extensive fragmentation as the neuromedin peptides; however, backbone fragmentation was realized. In a previous report of unreduced vasopressin,[32] mostly fragmentation of the disulfide bond was observed. It is likely that, for the unreduced species, electron detachment occurs from the disulfide bond[32] ($IE_{R\text{-}SS\text{-}R} \simeq 8.46 - 9.1$[33]), potentially precluding backbone fragmentation. In the spectrum above, the expected charge-reduced peak is not observed but neutral loss peaks originating from the oxidized precursor ion species are seen. Neutral loss of 34 and 68 Da could correspond to loss of SH_2 and H_2S-SH_2, respectively; however, other low abundance neutral losses could not be identified. Overall, the aforementioned non-acidic peptides fragmented extensively along the backbone; however, most peptides do contain carboxylic acids that may hamper structural characterization with EDD.

4.3.2 EDD of ANSA-Derivatized Desulfonated Caerulein

Several peptides, including caerulein and its desulfonated form as well as hirudin and cholecystokinin with and without sulfonate, were ANSA-derivatized, but only derivatized desulfonated caerulein was detected in subsequent MS analyses following LC purification. Desulfonated caerulein contains two acidic sites corresponding to two aspartic acid residues because the C-terminus is amidated. Figure 4.3 a–c compares EDD of non-derivatized (a), singly-derivatized (b) and doubly-derivatized (c) desulfonated caerulein. EDD of non-derivatized non-sulfonated caerulein produces $a^{\bullet}$ and *x* as well as *c*-ions with significant CO_2 loss accounting for 67% of the total product ion signal. EDD of singly-derivatized caerulein results in much less CO_2 loss (45% of the total product ion signal) but also much less backbone fragmentation. When both the carboxylic acids were blocked with ANSA, CO_2 loss was completely eliminated but very few product ions were observed. It is also important to note that sulfonate loss (from the ANSA group) in the

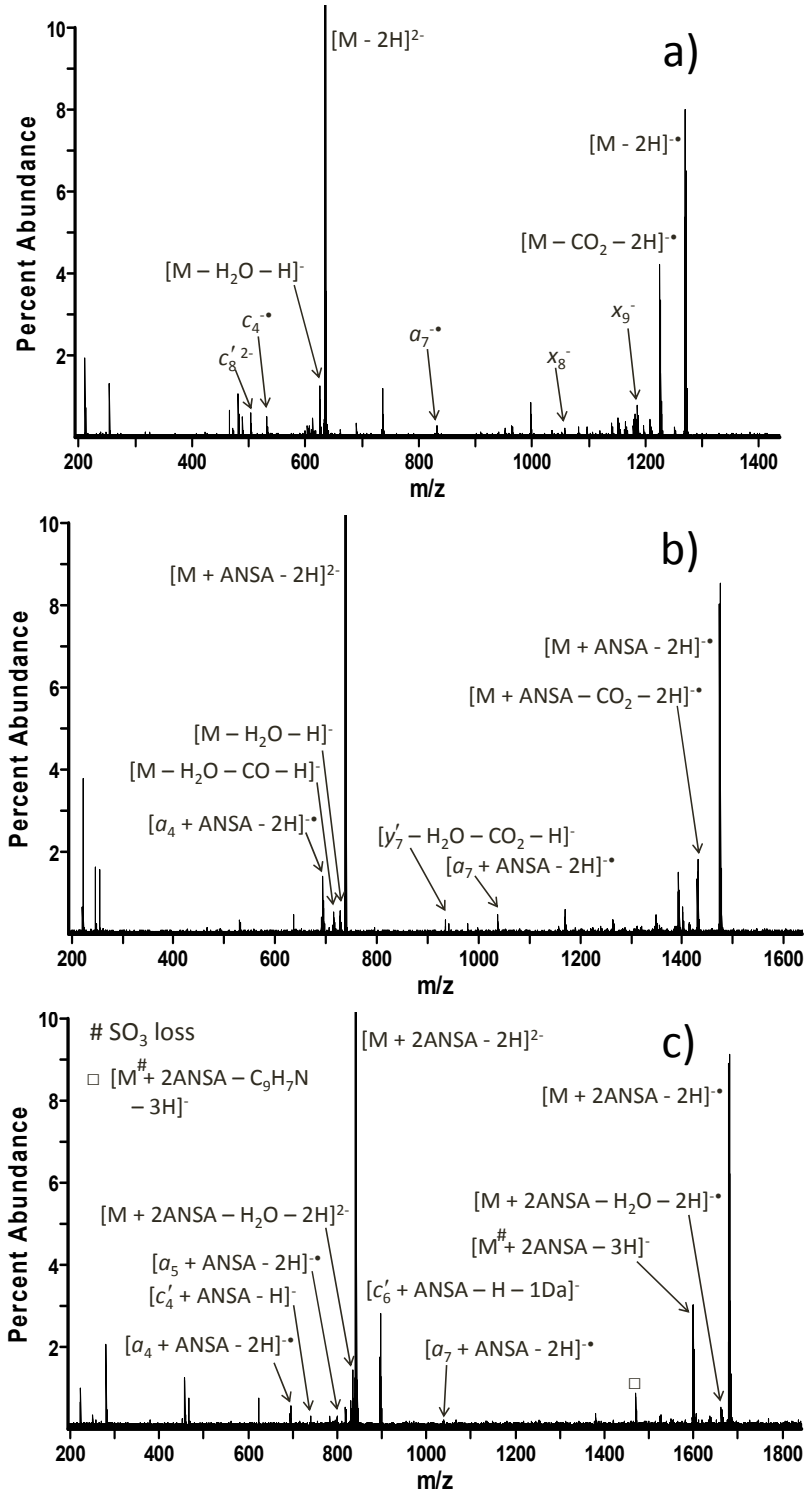

Figure 4.3 a–c. EDD spectra of non-derivatized (a), singly-derivatized (b) and doubly-derivatized (c) desulfonated caerulein. Sulfonate loss (from ANSA) is indicated by #.

doubly-derivatized peptide appears to have replaced carboxylate loss. It is possible that the most energetically-favorable fragmentation is CO_2 loss followed by SO_3 loss prior to C_α-C backbone fragmentation. Based on the observed abundant SO_3 neutral loss, lack of reproducible products, and poor synthetic yield, the ANSA derivatization strategy was not further pursued.

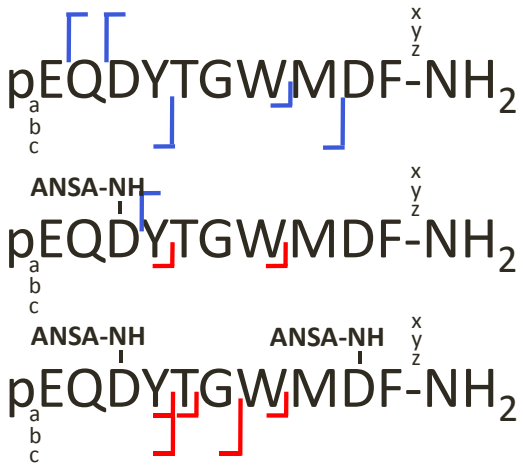

Figure 4.4. Summary of EDD product ions observed from non-derivatized (top), singly-derivatized (middle) and doubly-derivatized (bottom) desulfonated caerulein. Blue lines indicate ions observed without ANSA while red lines indicate ions that contain ANSA.

4.3.3 EDD of acetylated peptides

Acetylation may alter the gas-phase structure of peptide ions. Specifically, N-acetylation may change hydrogen bonding/salt bridge formation in gaseous peptide ions and thus alter EDD fragmentation behavior. Figures 4.5, 4.7, 4.9 and 4.11 a–b compare EDD of the non-acetylated (a) and acetylated (b) forms of desulfonated cholecystokinin, sulfonated cholecystokinin, angiotensin I and neurokinin B, respectively, while Figures 4.6, 4.8, 4.10 and 4.12 summarize the EDD product ions observed for each peptide. In Figure 4.5, a similar amount of CO_2 neutral loss is seen for the non-acetylated and acetylated species; however, significantly more unique neutral loss events are observed

following EDD of acetylated CCK. As for the other neutral losses, it may be possible that these are due to a different gas-phase structure, such as disruption of salt bridge interactions.

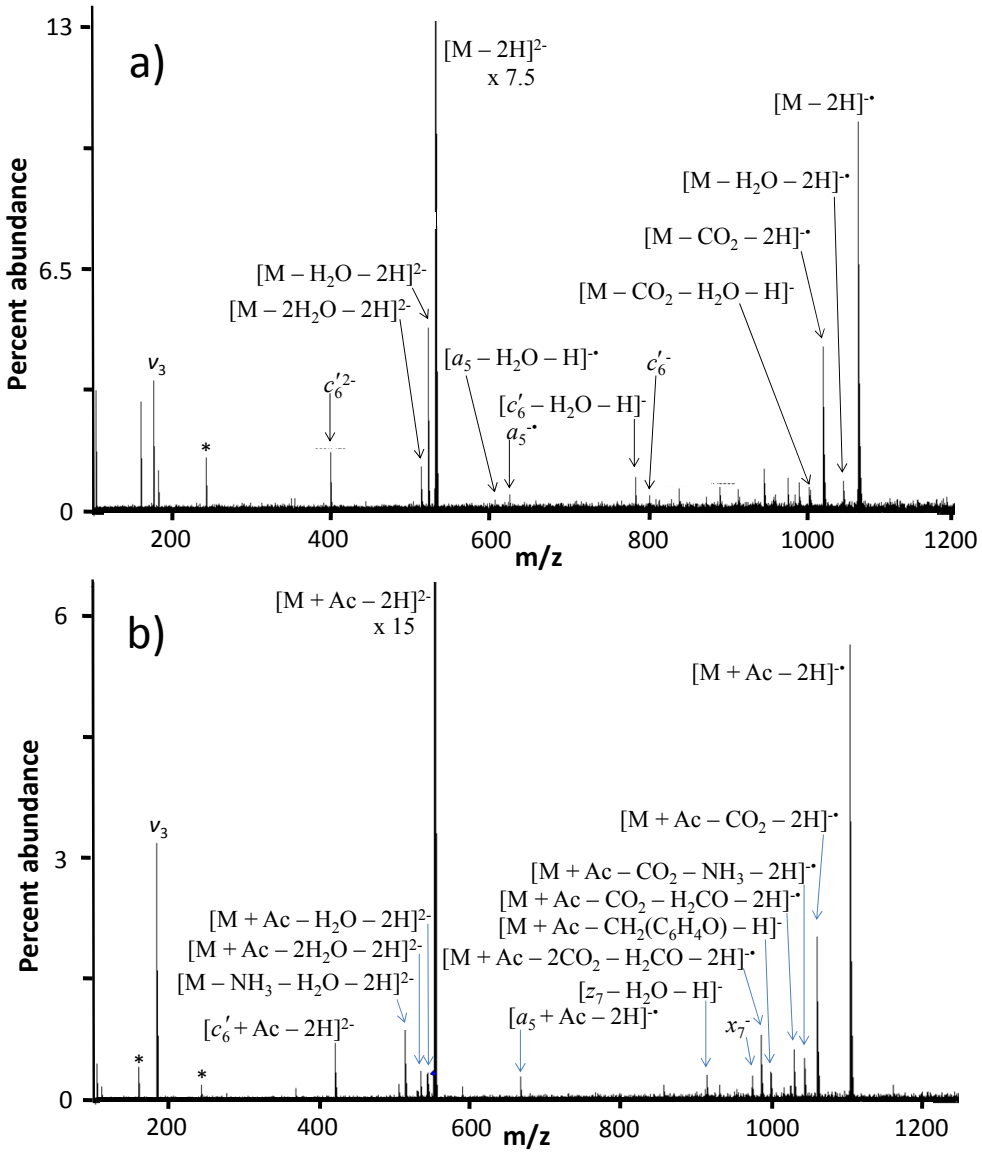

Figure 4.5 a–b. EDD spectra of non-acetylated (a) and acetylated (b) desulfonated cholecystokinin.[34] Electronic noise is indicated by * and the 3rd harmonic is indicated by v_3.

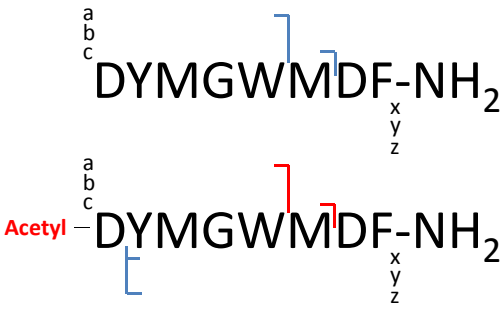

Figure 4.6. Summary of EDD product ions observed from non-acetylated (top) and acetylated (bottom) desulfonated cholecystokinin. Blue lines indicate ions observed without acetylation while red lines indicate ions that contain the acetylated N-terminus.

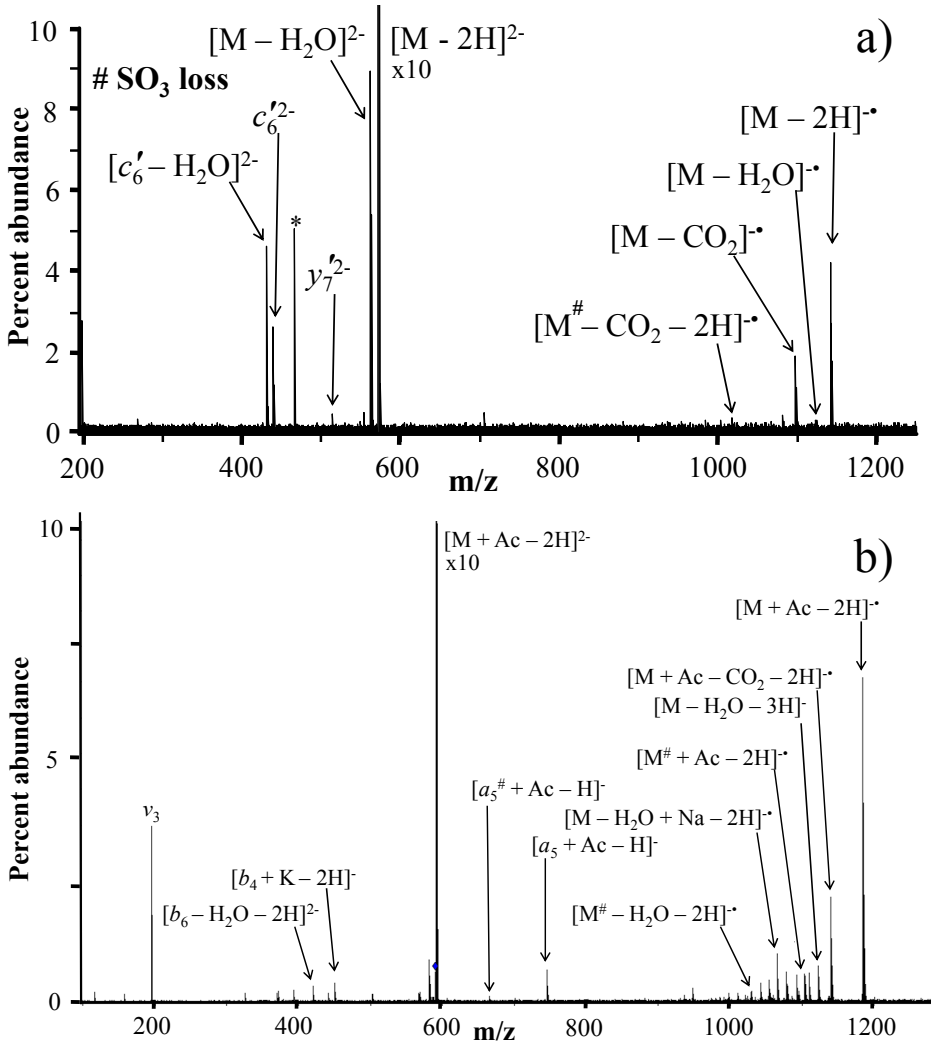

Figure 4.7 a–b. EDD spectra of non-acetylated (a) and acetylated (b) sulfonated cholecystokinin with sulfonate loss indicated by # and the 3rd harmonic indicated by v_3.

Comparison of EDD of non-acetylated (a) and acetylated (b) sulfonated cholecystokinin (CCKS), shown in Figure 4.7 a–b and Figure 4.8, suggests that neutral

loss is increased following acetylation, similar to the results for CCK. In the CCKS

Figure 4.8. Summary of EDD product ions observed from non-acetylated (top) and acetylated (bottom) sulfonated cholecystokinin. Blue lines indicate ions observed without acetylation. No observed ions contained the acetylated N-terminus.

spectra, we also observed sodium (Na^+) and potassium (K^+) adduct peaks, which are common in mass spectrometry due to sample or solution impurity as well as ESI source contamination. For this particular peptide, the acetyl group was not retained on any product ion. The reason behind this behavior is currently unclear but may be due to radical-driven acetyl loss, which has been seen in ECD of acetylated glycans.[35]

Figure 4.9 a–b show EDD spectra of non-acetylated (a) and acetylated (b) angiotensin I. Clearly, EDD of angiotensin I produces more backbone fragmentation events than those observed from CCK or CCKS. Fragmentation efficiency is roughly the same for non-acetylated and acetylated angiotensin; however, we observed an acetylation of either the histidine or possibly arginine side chain. We conclude that either of these residues is indeed the site of acetylation due to the presence of an *x*-ion which contains the acetyl group (Figure 4.9a). Both side chains are quite basic and have been acetylated in previous work in our group using identical acetylation protocols (Ning Wang, unpublished result).

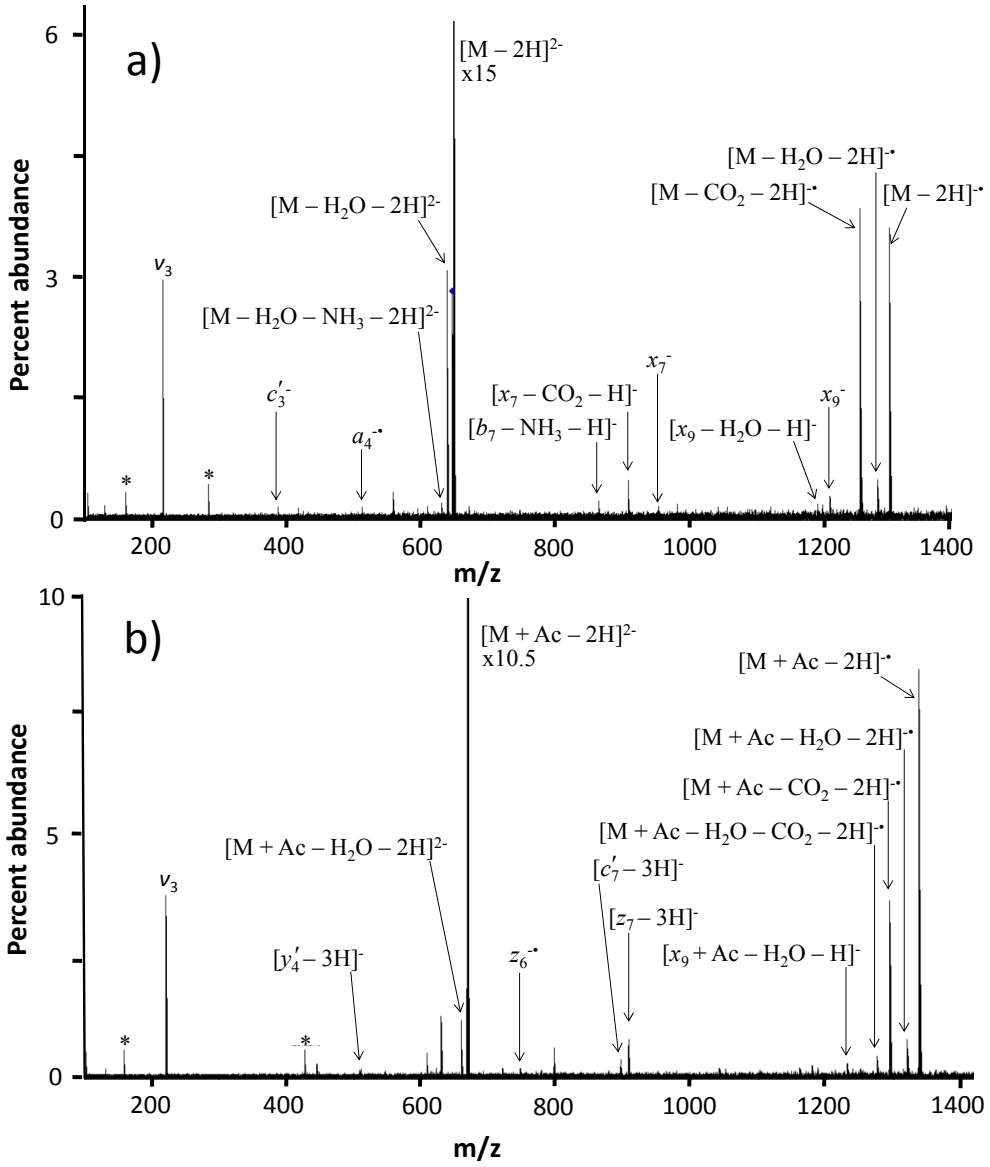

Figure 4.9 a–b. EDD spectra of non-acetylated (a) and acetylated (b) angiotensin I with electronic noise indicated by * and the 3rd harmonic indicated by v_3.

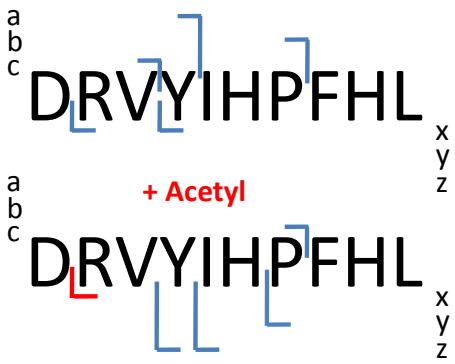

Figure 4.10. Summary of EDD product ions observed from non-acetylated (top) and acetylated (bottom) angiotensin I. Blue lines indicate ions observed without acetylation while red lines indicate ions observed with acetylation. The site of acetylation was not determined definitively and was indicated by "+ Acetyl."

Figure 4.11 a–b shows EDD spectra of non-acetylated (a) and acetylated (b) neurokinin B. Similar to unmodified angiotensin, non-acetylated neurokinin B exhibits rich fragmentation with both abundant N- and C-terminal product ions. EDD of acetylated neurokinin B illustrates two important findings: 1) All N-terminal product ions contain the acetylated N-terminal residue, which was not observed with all other peptides examined here; and 2) C-terminal product ions are significantly reduced after acetylation. One possible explanation for this observation is that acetylation is somehow influencing the site of deprotonation and subsequently the site of electron detachment and preferred fragmentation. Two viable sites for deprotonation for this petpide include the side chain of each aspartic acid residue. Because this peptide is C-terminally amidated, the most acidic sites will be the carboxylic acids followed by backbone amide nitrogens. Due to the extensive backbone fragmentation, deprotonation and subsequent electron detachment from a backbone amide nitrogen appears to occur.

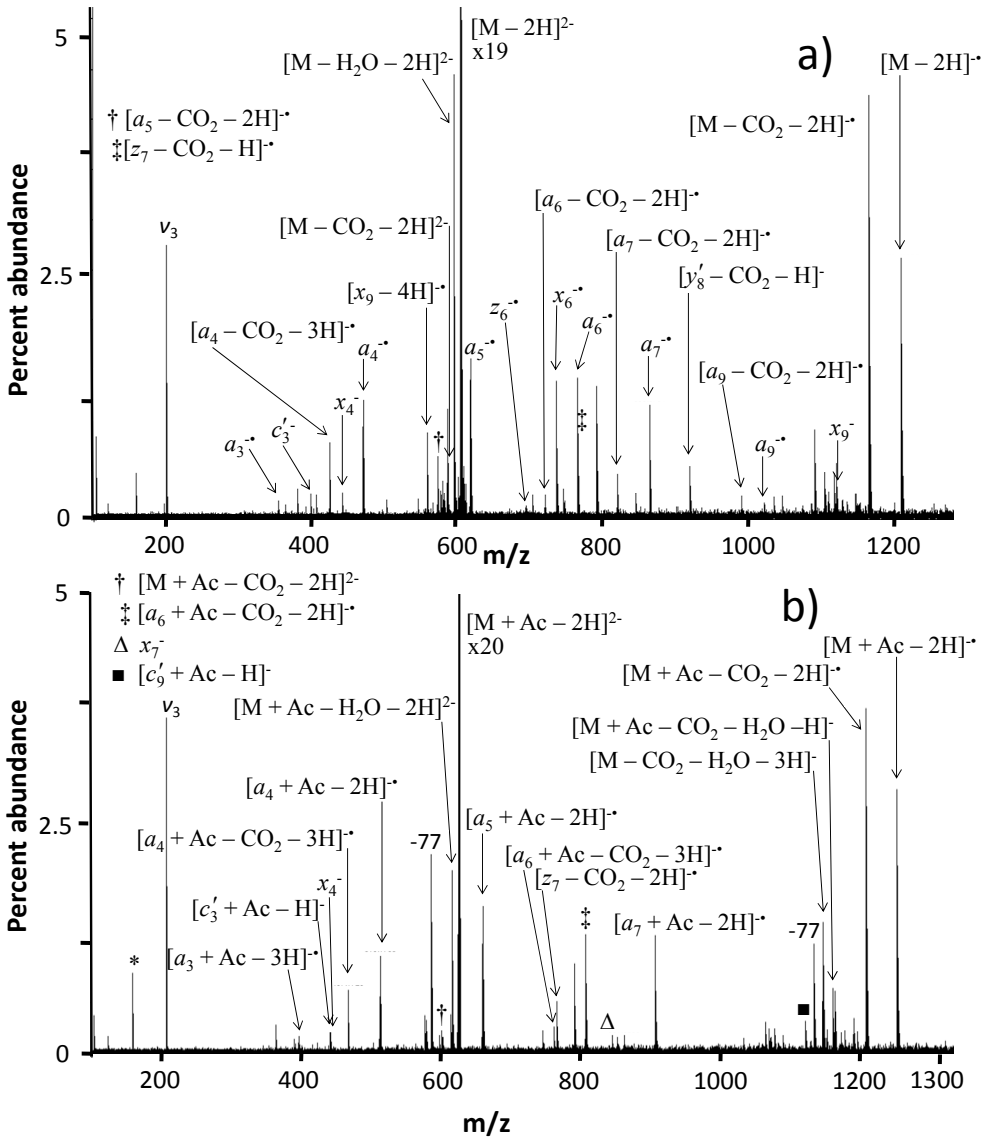

Figure 4.11 a–b. EDD spectra of non-acetylated (a) and acetylated (b) neurokinin B with electronic noise indicated by * and the 3rd harmonic indicated by ν_3.

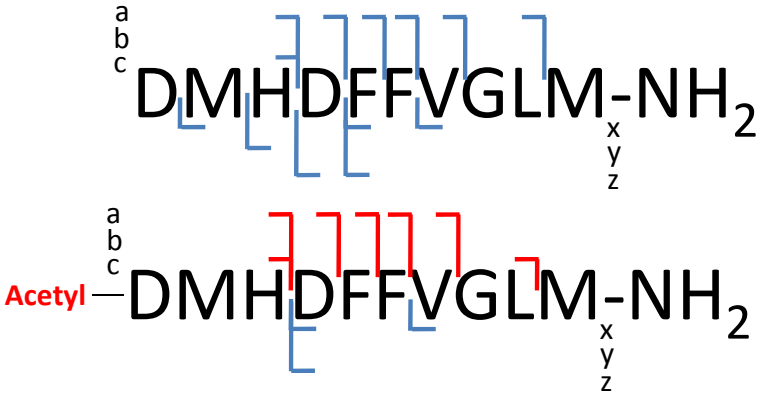

Figure 4.12. Summary of EDD product ions observed from non-acetylated (top) and acetylated (bottom) neurokinin B. Blue lines indicate ions observed without acetylation while red lines indicate ions observed with acetylation.

4.3.4 EDD of Anion-Adducted Peptides

Anion adduction was performed with ammonium salts of both chloride and bromide. It has been suggested previously that matching the gas-phase basicity of a proton-containing site with an anion for adduction leads to the formation of a stable gas-phase adduct.[*27] The proposed interaction mechanism is shown in Figure 4.13. Liu and Cole argue that protonated amine groups ($GPB_{R\text{-}NH2}$ = 860-910 kJ/mol for primary through tertiary alkyl amines[36]) are less likely to be involved in anion adduction compared to neutral carboxylic acids ($GPB_{R\text{-}COO^-}$ = 1418.5±9.6 – 1428.7±8.4 kJ/mol, where R = straight-chain hydrocarbon) due to a mismatch in the GPB of the protonated amine and the anion adduction species. For instance, if a base (A^-) is adducted to a protonated amine ($NH_2\cdots H^+\cdots A^-$) rather than to a carboxylic acid ($COO^-\cdots H^+\cdots A^-$), it is

[*] This notation seems counterintuitive to the mirrored acidity-basicity model of acids and their conjugate bases. It is important to note that the authors explain that the matching GPBs are that of the anion adduct and the *deprotonated* conjugate base of the carboxylic acid where adduction occurs.

more likely to lose HA from the protonated amine because the resulting neutral amine group has a much lower GPB than the deprotonated carboxylate and, thus, it requires less

$$NH_2 - Peptide - COO^- \bullet\bullet\bullet\bullet H^+ \bullet\bullet\bullet\bullet A^-$$

Figure 4.13. Proposed gas-phase interaction mechanism of an anion (A-) with a carboxylic acid. Adapted from Liu and Cole.[27]

energy to remove the proton plus adducted base complex (HA) from a protonated amine.

Specifically, chloride and bromide were chosen because their gas phase basicities (GPBs, 1373.6 $\pm$ 8.4 kJ/mol and 1331.4 $\pm$ 4.6 kJ/mol, respectively) closely match that of a proton-bearing carboxylic acid and these anions are therefore able to form highly stable complexes with carboxylic acids in the gas phase. Liu and Cole have shown that anions of medium-to-high GPB such as chloride and bromide can form more highly-charged adducts (z = -2 – -3) than anions of lower GPB based on experimental evidence collected for nine different anions with GPBs ranging from 1265 – 1530 kJ/mol.[27] These authors report that chloride, with the higher GPB of the two halides, has a more favorable interaction with slightly less acidic carboxylic acid sites, which should have a higher GPB than a deprotonated carboxylate since GPB mirrors gas-phase acidity. Matching GPBs allows the anion to form a stable adduct and additionally facilitates retention of the adducted anion following collisional activation. These authors also found that HSO_4^- of lower GPB than Br^- and Cl^- was more prone to depart from a carboxylic acid adduction site than the higher GPB anions.

Figure 4.14 a–c compares the EDD spectra of doubly-deprotonated (a) leutinizing hormone releasing hormone (LHRH) to the singly deprotonated, single chloride-adducted

precursor ion ($[M + Cl^- - H]^{2-}$) and the doubly bromide-adducted precursor ion ($[M + 2Br^-]^{2-}$) in (b) and (c), respectively, while Figure 4.15 summarizes the EDD product ions observed for these peptides.

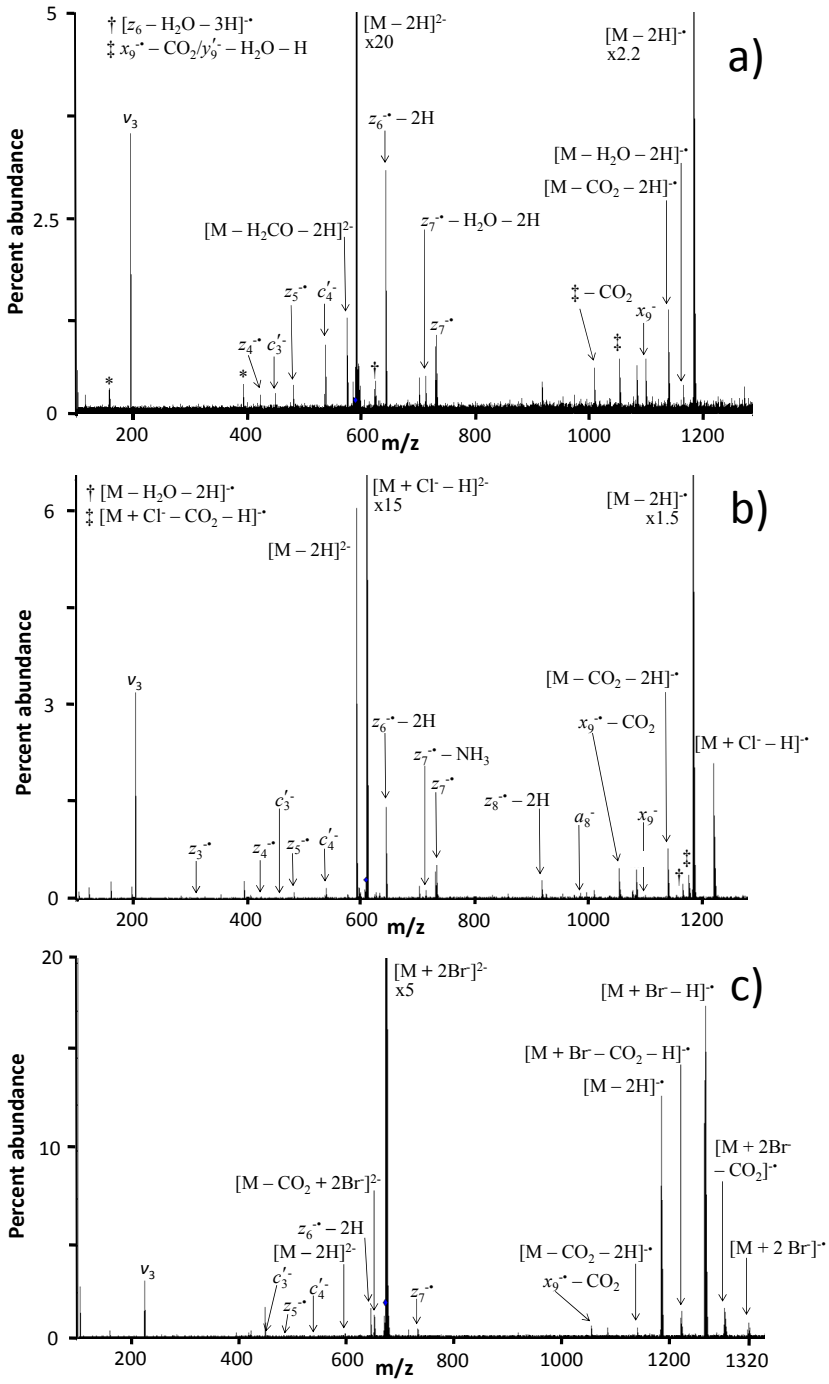

Figure 4.14 a–c. EDD spectra of doubly-deprotonated (a), singly-deprotonated and singly chloride-adducted (b), and doubly bromide-adducted LHRH. Electronic noise is indicated by * while the 3rd harmonic is indicated by v_3.[34]

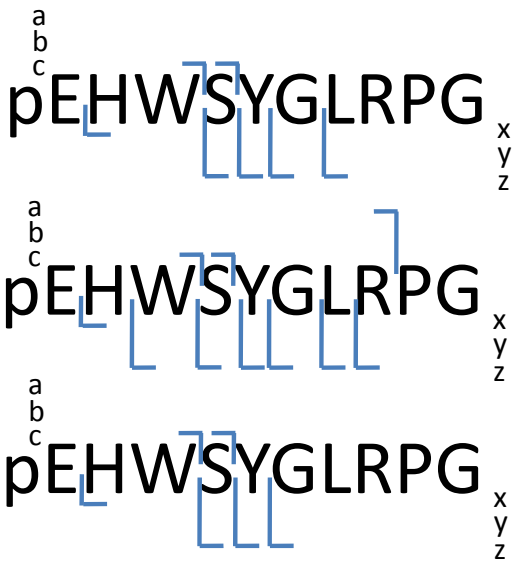

Figure 4.15. Summary of EDD product ions observed from doubly-deprotonated (top), singly-deprotonated and singly chloride-adducted (middle), and doubly bromide-adducted LHRH. Blue lines indicate ions observed without an anion adduct. No product ions were observed with chloride or bromide adducts.

It is interesting to note that fragmentation of doubly-deprotonated and doubly bromide-adducted LHRH provided nearly identical structural information. However, EDD of chloride-adducted LHRH produced additional unique *z*-ions and resulted in significantly improved sequence coverage (89%) compared to the other LHRH fragmentation spectra (56% and 44% for doubly-deprotonated LHRH and doubly bromide-adducted LHRH, respectively). Unfortunately, there are no product ions that contain the adducted anions; therefore, we cannot unambiguously identify the site(s) of anion adduction. We expect that the most likely site of chloride and bromide anion adduction is the C-terminal carboxylic acid. Our results support this idea for chloride adduction due to the decrease in CO_2 neutral loss following EDD but not for bromide adduction. Carbon dioxide loss from the charge-reduced precursor ion relative to the charge-reduced species is 13% for doubly-deprotonated LHRH while this ratio is 8% for

singly-deprotonated, singly chloride-adducted LHRH, and 17% for doubly bromide-adducted LHRH. As discussed above, we did not observe any product ions containing the anion adduct. Because chloride has a higher GPB, it is possible that only chloride is lost during electronic activation and leaves behind a carboxylic acid that cannot easily dissociate by CO_2 loss. On the other hand, bromide with a lower GPB is more likely to depart as HBr, leaving behind a peptide carboxylate that has a very small activation barrier to overcome in order to lose CO_2.

In Figures 4.16 a–c and 4.17, it is seen that Met-OH substance P behaves similarly in EDD compared to leutinizing hormone releasing hormone. Enhanced sequence coverage, supported by additional C-terminal product ions, was observed for chloride- but not bromide-adducted substance P. Even though the total number of fragmentation events for non-adducted and chloride-adducted substance P is the same, we observe more unique sequence information following EDD of the chloride-adducted precursor, suggesting that chloride adduction may promote different fragmentation pathways.

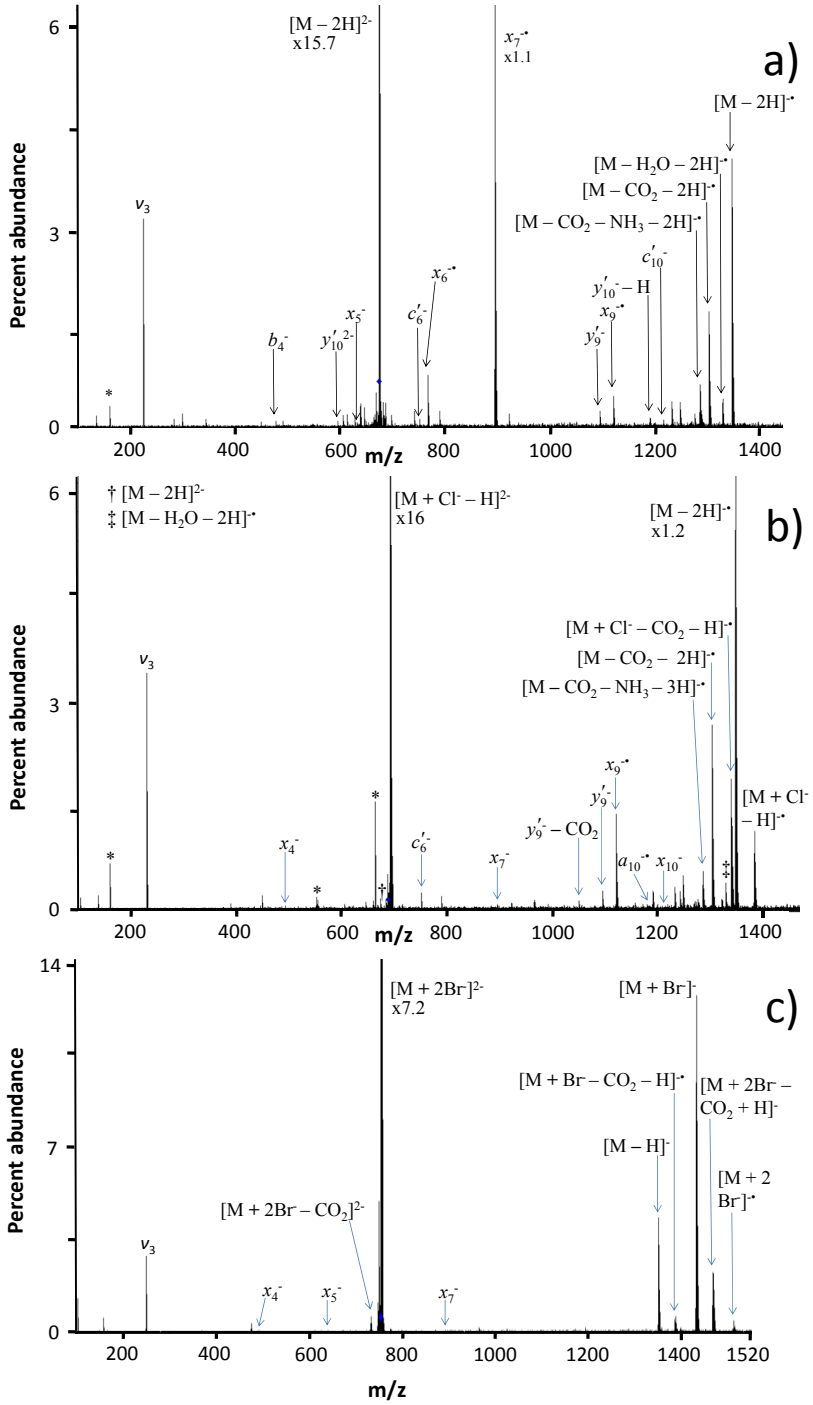

Figure 4.16 a–c. EDD spectra of doubly-deprotonated (a), singly-deprotonated and singly chloride-adducted (b), and doubly bromide-adducted Met-OH substance P. Electronic noise is indicated by * while the 3rd harmonic is indicated by v_3.

Figure 4.17. Summary of EDD product ions observed from doubly-deprotonated (top), singly-deprotonated and singly chloride-adducted (middle), and doubly bromide-adducted Met-OH substance P. Blue lines indicate ions observed without an anion adduct.

An interesting finding is the presence of several $x_n^{-\bullet}$ radical ions in EDD of doubly-deprotonated substance P. As discussed above, radical *x*-ions are usually not observed in favor of even-electron *x*-ions due to an energy barrier of ~74.2 kJ/mol. However, it appears that chloride and bromide adduction may significantly hinder these fragmentation pathways as evidenced most notably from the disappearance of $x_7^{-\bullet}$ in both anion-adducted EDD spectra. It is possible that a nearby adducted anion influences the local electronic environment near the proline-glutamine bond, thus precluding fragmentation at this site.

Carbon dioxide loss from the charge-reduced precursor ion relative to the charge-reduced species is considerably higher for substance P compared to CO_2 loss in EDD of leutinizing hormone (76% for doubly-deprotonated SubP, 69% for singly-deprotonated,

singly chloride-adducted SubP, and 22% for doubly bromide-adducted SubP). Bromide adduction resulted in the least CO_2 neutral loss; however, this reduction should be cautiously ascertained due to the reduced overall fragmentation efficiency observed in this spectrum. Despite a large ratio of CO_2 loss relative to the charge-reduced species for chloride adducted ions, the most dominant product ion corresponds to loss of H^+Cl^- from the charge-reduced ion. This loss suggests that the GPB of the chloride anion and the proton-containing interaction site were not ideally matched and resulted in an unstable complex.

Perhaps the most intriguing results are the EDD fragmentation spectra of doubly-deprotonated (a), singly-deprotonated, singly chloride-adducted (b), and doubly bromide-adducted (c) angiotensin I shown in Figure 4.18 a–c. EDD of doubly-deprotonated angiotensin I resulted in significant CO_2 neutral loss with few product ions observed, corresponding to 44% sequence coverage. Interestingly, despite the abundant neutral losses observed in EDD of singly-deprotonated, singly chloride-adducted angiotensin (Figure 4.18 b), a rich series of ions resulting from backbone fragmentation produces 100% sequence coverage for this peptide. Though several m/z values matched that of chloride-adducted product ions within 15 ppm error, we could not confidently assign these due to the absence of the chloride isotopic signature. EDD of doubly bromide-adducted angiotensin I produced similar poor sequence coverage (33%) as compared to the doubly-deprotonated precursor ion, and there is abundant neutral loss from the charge-reduced species. However, in this particular case, the expected charge-reduced ion $[M + 2Br^-]^{-\bullet}$ is not observed while the charge-reduced ions corresponding to one and two HBr neutral losses are the most dominant product ions in the spectrum. As suggested

previously, it is possible that the GPB of the bromide anion and the two interaction sites were not ideally matched, causing facile loss of HBr from both interaction sites. Because bromide has a lower GPB than chloride,[27] it may be more likely to observe hydrogen bromide loss concurrently as opposed to loss of the bromide anion only. Surprisingly, we would have expected to see much more abundant CO_2 loss following the loss of HBr, which leaves a labile carboxylate if the interaction site was the C-terminus or the side

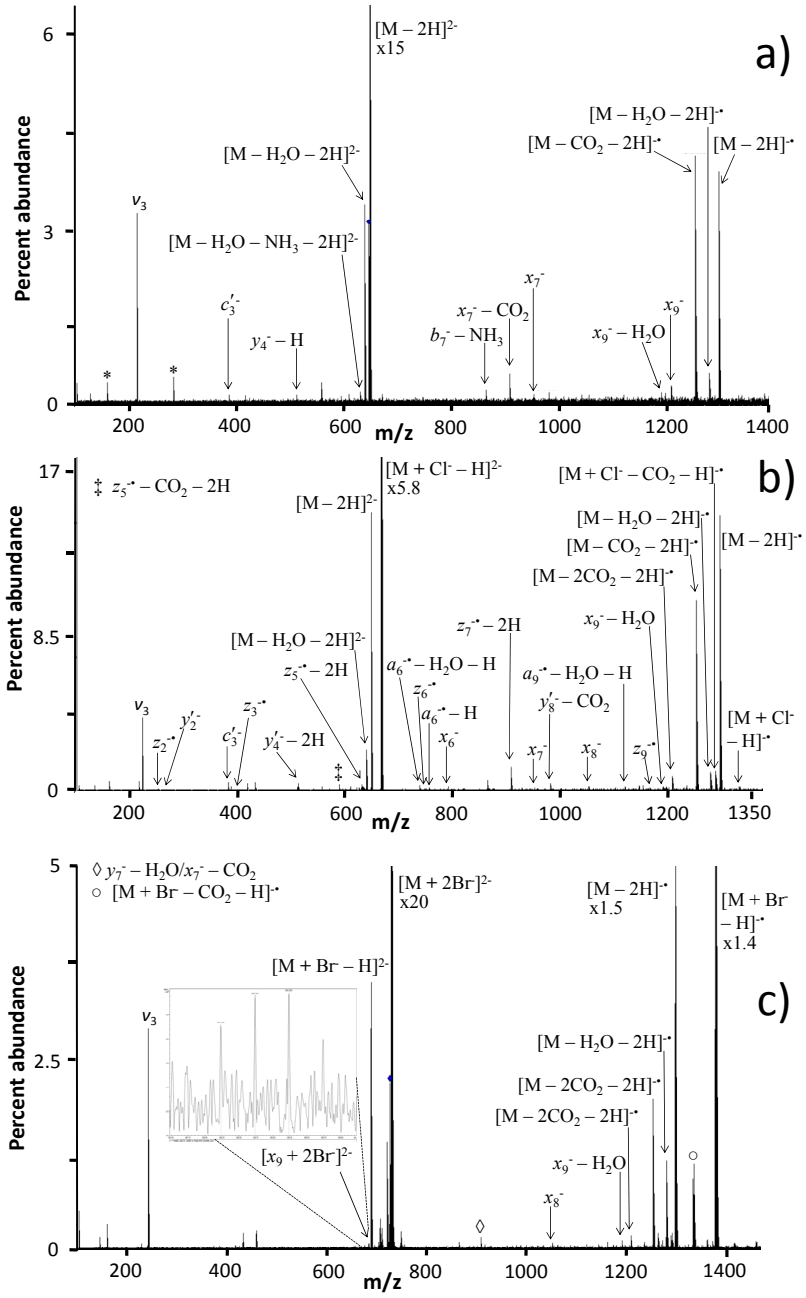

Figure 4.18 a–c. EDD spectra of doubly-deprotonated (a), singly-deprotonated and singly chloride-adducted (b), and doubly bromide-adducted (c) angiotensin I. The inset in (c) shows the isotopic distribution for the $[x_9 + 2Br^-]^{2-}$ ion. Electronic noise is indicated by * while the 3rd harmonic is indicated by v_3.

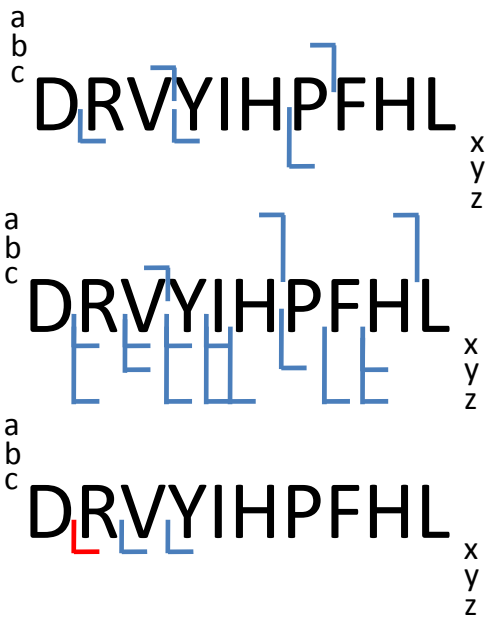

Figure 4.19. Summary of EDD product ions observed from doubly-deprotonated (top), singly-deprotonated and singly chloride-adducted (middle), and doubly bromide-adducted (bottom) angiotensin I. Blue lines indicate ions observed without an anion adduct, and red lines indicate ions observed with chloride or bromide adduction.

chain of the aspartic acid residue. Because there are very few product ions observed in this spectrum, it is likely that much of the excess energy following electron detachment was funneled into neutral loss events. It is interesting to note that, while we see the same trends for sequence coverage (improved coverage for chloride-adducted species but reduced coverage for bromide-adducted species) and types of ions observed (more C-terminal than N-terminal ions), we observe a doubly bromide-adducted product ion following EDD of angiotensin I (see inset of Figure 4.18c). Despite the low signal-to-noise, we can assign this adduct ion based on accurate mass as well as the characteristic isotopic distribution pattern expected for bromide attachment. Because the identified x_9 ion contains both bromides but only one carboxylic acid, we must consider adduct

interactions at sites other than the carboxylic acids previously hypothesized by Liu and Cole.[27] Instead of the N-terminal carboxylic acid from the aspartic acid side chain, the anion may interact with a lower GPB site, perhaps the protonated side chain of a basic residue such as arginine. Although we did not calculate the likelihood of this interaction, we can speculate that the surrounding residues, which include one basic arginine residue, two basic histidine residues, and a turn-inducing proline residue, may affect not only the tertiary gas-phase structure but also the apparent GPB due to inductive effects.[27]

There could be a number of explanations for how the EDD sequence coverage improved dramatically with anion adduction. First, there was a slight reduction in overall CO_2 loss in EDD of chloride-adducted angiotensin I compared to the EDD spectrum of the doubly-deprotonated species. Less CO_2 loss may allow other fragmentation pathways to be realized, resulting in the extensive fragmentation observed. Alternatively, chloride adduction could have altered the gas-phase tertiary structure of the peptide, allowing the peptide to fragment more extensively. Regardless of the reason behind these results, we can clearly see that EDD fragmentation was enhanced in several cases by adding halides to the electrospray solvent prior to MS analysis.

4.4 Conclusion

We have presented evidence for the improvement of EDD-generated primary structural information upon direct and indirect chemical modification of carboxylic acids, which commonly result in facile CO_2 loss in EDD. EDD of non-acidic peptides showed that sequence coverage improves markedly when CO_2 loss is eliminated. We attempted to expand this idea by chemically modifying carboxylic acids with ANSA, only to find

that the number of fragmentation events decreased substantially and neutral loss of the ANSA sulfonate group was observed in place of CO_2 neutral loss. Acetylation of free amines may alter gas-phase peptide ion structures, leading to altered EDD fragmentation behavior. Our results show that, in some cases, acetylation alters typical fragmentation pathways, as evidenced by the reduced number of C-terminal product ions observed for acetylated neurokinin B. Lastly, adduction of bromide to various peptides resulted in decreased fragmentation efficiency while adduction of chloride provided improved fragmentation efficiency and sequence coverage. Interestingly, a single fragment was observed with bromide adduction to angiotensin I. Although we cannot conclude definitively the changes that occur to the gas-phase structure upon anion adduction, we have shown with multiple peptides that additional backbone fragmentation, and thus sequence information, can be garnered from this approach.

Future directions involve expansion of this study to examine a wider variety of analytes, such as more highly acidic peptides with acidic post-translational modifications, e.g., phosphorylation and sulfonation as well as basic peptides that are difficult to multiply charge in negative ion mode MS.

4.5 References

1. B. A. Budnik, K. F. Haselmann, R. A. Zubarev, Electron detachment dissociation of peptide di-anions: an electron-hole recombination phenomenon. *Chem. Phys. Lett.* **2001**, *342*, 299-302.
2. R. A. Zubarev, Reactions of polypeptide ions with electrons in the gas phase. *Mass Spectrom. Rev.* **2003**, *22*, 57-77.
3. B. A. Budnik, R. A. Zubarev, $MH2^{+\cdot}$ ion production from protonated polypeptides by electron impact: observation and determination of ionization energies and a cross-section. *Chem. Phys. Lett.* **2000**, *316*, 19-23.
4. R. A. Zubarev, Reactions of polypeptide ions with electrons in the gas phase. *Mass Spectrometry Reviews* **2003**, *22*, 57-77.

5. F. Kjeldsen, O. A. Silivra, I. A. Ivonin, K. F. Haselmann, M. Gorshkov, R. A. Zubarev, C-alpha-C backbone fragmentation dominates in electron detachment dissociation of gas-phase polypeptide polyanions. *Chem.-Eur. J.* **2005**, *11*, 1803-1812.
6. J. Yang, J. Mo, J. T. Adamson, K. Hakansson, Characterization of oligodeoxynucleotides by electron detachment dissociation Fourier transform ion cyclotron resonance mass spectrometry. *Anal. Chem.* **2005**, *77*, 1876-1882.
7. J. Yang, K. Hakansson, Fragmentation of oligoribonucleotides from gas-phase ion-electron reactions. *J. Am. Soc. Mass Spectrom.* **2006**, *17*, 1369-1375.
8. J. J. Wolff, T. N. Laremore, A. M. Busch, R. J. Linhardt, I. J. Amster, Electron detachment dissociation of dermatan sulfate oligosaccharides. *J. Am. Soc. Mass Spectrom.* **2008**, *19*, 294-304.
9. J. J. Wolff, L. Chi, R. J. Linhardt, I. J. Amster, Distinguishing glucuronic from iduronic acid in glycosaminoglycan tetrasaccharides by using electron detachment dissociation. *Anal. Chem.* **2007**, *79*, 2015-2022.
10. H. K. Kweon, K. Hakansson, Metal oxide-based enrichment combined with gas-phase ion-electron reactions for improved mass spectrometric characterization of protein phosphorylation. *J. Proteome Res.* **2008**, *7*, 749-755.
11. L.-S. Wang, C.-F. Ding, X.-B. Wang, J. B. Nicholas, Probing the potential barriers and intramolecular electrostatic interactions in free doubly charged anions. *Phys. Rev. Lett.* **1998**, *81*, 2667-2670.
12. H.-K. Woo, X.-B. Wang, B. Kiran, L.-S. Wang, Temperature-dependent photoelectron spectroscopy of methyl benzoate anions: observation of steric effect in o-methyl benzoate. *J. Phys. Chem. A* **2005**, *109*, 11395-11400.
13. I. Anusiewicz, M. Jasionowski, P. Skurski, J. Simons, Backbone and side-chain cleavages in electron detachment dissociation (EDD). *J. Phys. Chem. A* **2005**, *109*, 11332-11337.
14. R. A. Zubarev, K. F. Haselmann, B. A. Budnik, F. Kjeldsen, F. Jensen, Towards an understanding of the mechanism of electron-capture dissociation: a historical perspective and modern ideas. *Eur. J. Mass Spectrom.* **2002**, *8*, 337-349.
15. A. T. Iavarone, K. Paech, E. R. Williams, Effects of charge state and cationizing agent on the electron capture dissociation of a peptide. *Anal. Chem.* **2004**, *76*, 2231-2238.
16. H. C. Liu, K. Hakansson, Divalent metal ion-peptide interactions probed by electron capture dissociation of trications. *J. Am. Soc. Mass Spectrom.* **2006**, *17*, 1731-1741.
17. H. Liu, K. Hakansson, Electron capture dissociation of tyrosine O-sulfated peptides complexed with divalent metal cations. *Anal. Chem.* **2006**, *78*, 7570-7576.
18. J. Chamot-Rooke, G. van der Rest, A. Dalleu, S. Bay, J. Lemoine, The combination of electron capture dissociation and fixed charge derivatization increases sequence coverage for O-glycosylated and O-phosphorylated peptides. *J. Am. Soc. Mass Spectrom.* **2007**, *18*, 1405-1413.
19. X. Chen, Y. M. E. Fung, W. Y. K. Chan, P. S. Wong, H. S. Yeung, T.-W. D. Chan, Transition metal ions: charge carriers that mediate the electron capture dissociation pathways of peptides. *J. Am. Soc. Mass Spectrom.* **2011**, *22*, 2232-2245.
20. Y. M. E. Fung, H. Liu, T.-W. D. Chan, Electron capture dissociation of peptides metalated with alkaline-earth metal ions. *J. Am. Soc. Mass Spectrom.* **2006**, *17*, 757-771.

21. R. Fussenegger, B. M. Rode, Effect of Metal-Ion Bonding to Amides on Character of C-N Bond of Ligand Molecule. *Chem. Phys. Lett.* **1976**, *44*, 95-99.
22. H. Sigel, R. B. Martin, Coordinating Properties of the Amide Bond--Stability and Structure of Metal-Ion Complexes of Peptides and Related Ligands. *Chem. Rev.* **1982**, *82*, 385-426.
23. R. Mihalca, A. J. Kleinnijenhuis, L. A. McDonnell, A. J. R. Heck, R. M. A. Heeren, Electron capture dissociation at low temperatures reveals selective dissociations. *J. Am. Soc. Mass Spectrom.* **2004**, *15*, 1869-1873.
24. E. W. Robinson, R. D. Leib, E. R. Williams, The role of conformation on electron capture dissociation of ubiquitin. *J. Am. Soc. Mass Spectrom.* **2006**, *17*, 1469-1479.
25. L. Han, S.-Y. Hyung, J. J. S. Mayers, B. T. Ruotolo, Bound anions differentially stabilize multiprotein complexes in the absence of bulk solvent. *J. Am. Chem. Soc.* **2011**, *133*, 11358-11367.
26. T. G. Flick, S. I. Merenbloom, E. R. Williams, Anion effects on sodium ion and acid molecule adduction to protein ions in electrospray ionization mass spectrometry. *J. Am. Soc. Mass Spectrom.* **2011**, *22*, 1968-1977.
27. X. Liu, R. B. Cole, A new model for multiply charged adduct formation between peptides and anions in electrospray mass spectrometry. *J. Am. Soc. Mass Spectrom.* **2011**, *22*, 2125-2136.
28. J. R. Kornacki, J. T. Adamson, K. Hakansson, Electron detachment dissociation of chloride-adducted oligosaccharides. *Manuscript in revision*.
29. I. Lindh, W. J. Griffiths, T. Bergman, J. Sjovall, Charge-remote fragmentation of peptides derivatized with 4-aminonaphthalenesulphonic acid. *Rapid Commun. Mass Spectrom.* **1994**, *8*, 797-803.
30. A. Kalli, K. Hakansson, Electron capture dissociation of highly charged proteolytic peptides from Lys N, Lys C and Glu C digestion. *Mol. BioSyst.* **2010**, *6*, 1668-1681.
31. M. M. Savitski, M. L. Nielsen, R. A. Zubarev, Side-chain losses in electron capture dissociation to improve peptide identification. *Anal. Chem.* **2007**, *79*, 2296-2302.
32. A. Kalli, K. Håkansson, Preferential cleavage of S-S and C-S bonds in electron detachment dissociation and infrared multiphoton dissociation of disulfide-linked peptide anions. *Int. J. Mass Spectrom.* **2007**, *263*, 71-81.
33. J. J. Butler, T. Baer, S. A. Evans, Energetics and structures of organosulfur ions - Ch3ssch3+, Ch3ss+, C2h5s+, and Ch2sh+. *J. Am. Chem. Soc.* **1983**, *105*, 3451-3455.
34. Y. M. E. Fung, C. M. Adams, R. A. Zubarev, Electron ionization dissociation of singly and multiply charged peptides. *J. Am. Chem. Soc.* **2009**, *131*, 9977-9985.
35. M. Mormann, H. Paulsen, J. Peter-Katalinic, Electron capture dissociation of O-glycosylated peptides: radical site-induced fragmentation of glycosidic bonds. *Eur. J. Mass Spectrom.* **2005**, *11*, 497-511.
36. W. Yang, W. J. Mortier, The use of global and local molecular parameters for the analysis of gas-phase basicity of amines. *J. Am. Chem. Soc.* **1986**, *108*, 5708-5711.

CHAPTER V

CONCLUSIONS AND FUTURE DIRECTIONS

5.1 Conclusions

In this dissertation, we have presented a metal-oxide based strategy for enrichment of sulfopeptides from digestion mixtures, a combination of different vibrational and electronic activation methods for the unambiguous site determination of *O*-tyrosine sulfonates in acidic peptides, and a variety of approaches for improving electron detachment dissociation of acidic peptides.

Metal oxides such as titanium and zirconium dioxide have been used in previous work in our laboratory to enrich acidic phosphopeptides.[1-2] Experimental work from Dobson and McQuillan[3-4] showed that acidic analytes, specifically poly-oxyanions can interact with the surface of metal oxides. This interaction depends highly upon the method of metal oxide preparation as well as the pH of the oxyanion interaction. We have shown that careful control of the binding and elution pH maintains a high selectivity of sulfonate interaction compared to competing interaction from carboxylic acids. Specifically, the binding pH must be held close to the pKa of sulfonates ($pK_a^{R\text{-}OSO_3H} \simeq 2$) and lower than the pKa value of carboxylic acids ($pK_a^{R\text{-}COOH} \simeq 4\text{-}5$) while the elution pH should be held high enough to replace sulfonates with hydroxyls at the metal oxide surface, affecting a transition from Lewis acidity to basicity. Also, we found that there is

a minimum binding amount for a given surface area of titanium dioxide. A minimum of 200 pmol was determined to be the ideal loading amount for the 50 μg titanium dioxide-coated micropipette tips that we used for this work.

Due to inductive effects throughout the peptide, it is possible to observe a lower pK_a than the one stated above for carboxylic acids, leading to non-selective interactions. We have attempted to address this problem by acetylation and methylation of carboxylic acids contained in the sulfopeptide:digestion mixtures prior to metal-oxide enrichment; however, stoichiometric conversion of carboxylic acids was not realized (data not presented) perhaps due to the number of carboxylic acids present in a protein digest. Furthermore, if all carboxylic acids are blocked by acetyl or methyl groups, the ionization efficiency will decrease substantially, leading to less MS signal in negative ion mode.

To circumvent this problem of reduced synthetic yield, liquid chromatographic (LC) separation of the peptide mixture into fractions could reduce the number of peptides per fraction to be acetylated or methylated prior to titanium-dioxide enrichment. Ideally, however, the entire enrichment protocol from start to finish would be best realized if it was performed with minimal sample handling and chemical derivatization in order to create a high-throughput method for analysis of biological samples. This idea requires a combination of reversed-phase and titanium-dioxide based chromatographic separations prior to detection by mass spectrometry. An analytical platform of multi-dimensional LC separations using a combination of reversed-phase and titanium-dioxide chromatographic columns for enrichment of phosphopeptides combined with mass spectrometry detection has, in fact, been reported in recent literature.[5-6] Because sulfopeptides are particularly labile in positive ion mode MS, online LC-MS analysis must be performed in solvents

that can facilitate negative ion mode MS detection. Optimization of the enrichment conditions as well as LC separation and MS analysis conditions must also be considered.

Another future direction would be to perform on- or off-line metal oxide sulfopeptide enrichment from biological samples which could contain as little as picomole to femtomole amounts of sulfonated peptides. To the best of our knowledge, there are few accounts of quantification of endogenous sulfopeptides.[7-9] All three of these accounts measure the plasma concentration of cholecystokinin. It has been suggested by several authors that cholecystokinin and gastrin II play critical roles in cell proliferation in various cancers.[10-12] These ideas have been published from 1994 to most recently in 2011, yet there is no known concerted effort in regards to attacking this problem. Tyrosine-*O*-sulfonation has also been found in human and mouse retina,[13] but its absence can negatively affect morphogenesis and synaptic function in the mouse retina.[14] These authors suggest that tyrosine-*O*-sulfonation may have broader implications in neuronal development. To date, there are no known efforts to examine early neuronal development by use of differentiated neuronal stems cells (Dr. Wieland Huttner, personal communication). Fortunately for us at the University of Michigan, we have several excellent stem cell and embryonic stem cell researchers. Specifically, Dr. O'Shea from the Cell and Developmental Biology Department works with embryonic stem cells before and after their initial stages of differentiation into neuronal stem cells. Prior collaborative work with Dr. O'Shea (via Dr. David Lubman) has allowed me to examine the proteomic profile of embryonic stem cells and differentiated neuronal stem cells. However, at the time, we were investigating the occurrence of phosphorylation and

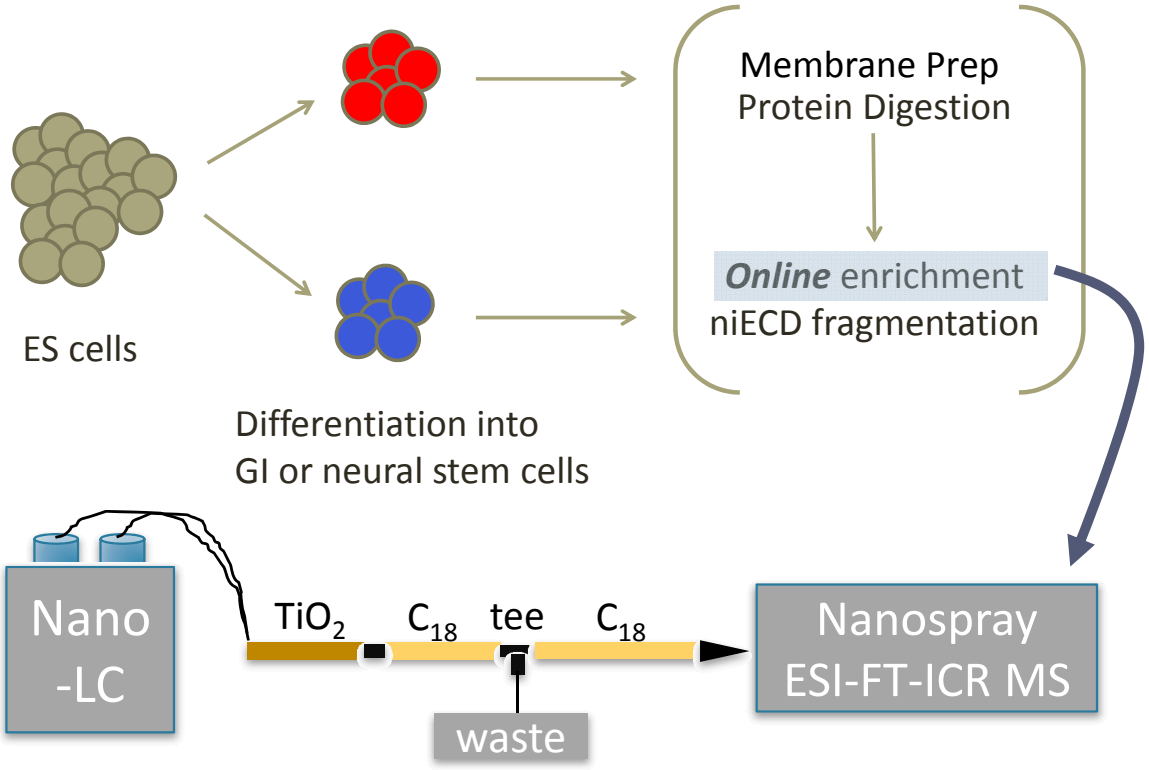

Figure 5.1. Proposed online nano-LC-MS/MS approach for high-throughput analysis of sulfopeptides. GI is the abbreviation for gastrointestinal while ES cells is the abbreviation for embryonic stem cells.

were not aware of the potential for sulfopeptide identification. We propose that differentiated neural and/or gastrointestinal cells may secrete sulfopeptides, which could be obtained from either a membrane prep or directly from the extracellular matrix. The offline TiO_2 enrichment could be converted to an online approach as mentioned above by conducting pH gradient separations on a microcapillary fused-silica column packed with a very small amount (< 50µg) of TiO_2 particles. The LC fraction corresponding to the pH of elution for sulfopeptides (pH ~10) could be selectively collected following either two stages of reversed-phase LC as shown in Figure 5.1 (where after the first separation, unwanted fractions can be diverted to waste) or by anion exchange chromatography

followed by reversed-phase LC separation. This multidimensional separation approach could then be coupled to tandem mass spectrometry techniques such as negative ion electron capture dissociation for primary structural characterization. Pairing the analysis of early-stage neuronally-differentiated stem cells with the online LC-MS/MS platform for enrichment of sulfopeptides would be the ultimate vision of this research effort.

In addition to improving enrichment, we have shown that the site of *O*-tyrosine sulfonation can be determined using vibrational and electronic activation methods. Furthermore, nearly full sequence coverage can be achieved by either a single method or by a combination of complementary methods. We have shown that for achieving high levels of both sequence coverage and sulfonate retention in CAD, a high charge state up to 4- may be required. However, this approach is not a guaranteed protocol for all peptides as we saw when comparing hirudin and gastrin II CAD in the 4- charge state. Furthermore, smaller peptides such as leucine-enkephalin cannot be observed as quadruply-deprotonated species in ESI-MS. In EDD, we observed similar trends: higher charge states facilitate improved overall fragmentation with more sulfonate retention and less neutral loss. For peptides that were not observed at a signal abundance great enough for EDD in charge states greater than 2- (caerulein, cionin, cholecystokinin), we observed poor fragmentation efficiency. In NETD of gastrin II, fragmentation improved upon increasing charge state from 2- to 4-; however, only C- and N-terminal flanking residues were fragmented from the ends of the peptide, yielding no information regarding the sulfonate site and the internal peptide sequence. This lack of backbone fragmentation may be due to secondary structural constraints, precluding efficient dissociation of the peptide fragments. Vibrational activation prior to NETD could facilitate unfolding of the

gaseous peptide; however, we believe that the sulfonate residue would be cleaved in such a process. NETD of hirudin in the 2- charge state yielded five *x*-ions, representing the core of the peptide backbone combined with one complementary *a*-ion to provide sulfonate localization. On the other hand, NETD of caerulein and cholecystokinin in the 2- charge state yielded very little structural information through backbone cleavage but completely retained the sulfonate residue. In contrast to higher charge states yielding improved backbone fragmentation, niECD of singly- and doubly-deprotonated precursor ions provided extensive backbone cleavage and complete sulfonate retention (with the exception of cionin, 1-). Because electrons are captured by negatively-charged precursor ions, the resulting charge-increased species can yield product ions of higher charge state than the precursor ion, leading to improved ICR detection and a wider pool of possible product ions. The observed c' and $z^{\bullet}$ ions are highly complementary to product ions observed in the aforementioned techniques, indicating that niECD provides a unique method to the electronic activation "toolbox" for analyzing acidic precursor ions.

There is still much to be investigated in regard to sulfopeptide characterization with vibrational and electronic activation methods. In this thesis, only six sulfopeptides were examined. A wider variety of tyrosine-*O*-sulfopeptides, as well as serine- and threonine-sulfonated peptides,[15] with different structural motifs could also be analyzed in the future. Initially, peptide concentrations were kept relatively low (0.5-5 μM) to ensure proper spray without significant ion suppression. In the future, precursor ions which were difficult to isolate such as triply-deprotonated hirudin should be analyzed at slightly higher concentrations in order to further investigate fragmentation behavior at higher charge states, especially in CAD, EDD, and NETD. To investigate the fragmentation

behavior as a function of charge state for the aforementioned techniques, an analysis of the parent ion signal abundance versus the lab frame of reference energy for each technique should be conducted. For example, we anticipate that the CAD breakdown curves as a function of charge state would show that higher charge states require much less CAD energy to fragment compared to lower charge states. Additionally, vibrational activation prior to NETD or EDD of highly-charged precursors such as gastrin II and hirudin can be investigated to prove or disprove our belief that sulfonate loss would occur following vibrational activation. It is possible that the gas-phase structure could provide intermolecular stabilization of the sulfonate residue and yield additional backbone cleavages not observed without prior vibrational activation. Lastly, the gas-phase structure of sulfopeptide ions as a function of charge state should be investigated using ion mobility mass spectrometry (IMS). We believe that structural analysis of precursor ions will change drastically as a function of how many negative charges are located on the peptide ion. Specifically, we anticipate that a relatively elongated structure would arise from a higher charge-state peptide as opposed to a more compact structure that would arise from a lower charge-state peptide. As discussed in Chapter 3, sulfonated human gastrin II as a 4- ion did not exhibit many fragmentation events, resulting in low sequence coverage in CAD and NETD. Structural analysis using IMS could provide insight for explaining why this higher charge-state peptide did not produce sufficient fragmentation events as predicted by the charge-state dependence for CAD and NETD fragmentation.

As the work with sulfopeptide characterization progressed, we noticed that EDD and NETD were subject to abundant neutral loss of CO_2, which could preclude backbone

fragmentation if energy is lost through exothermic release of CO_2. Because CO_2 is structurally inherent to acidic peptides which contain carboxylic acids, we needed to develop methods to block the facile loss of CO_2 while enabling deprotonation to occur at other acidic sites. Initially, we investigated EDD of non-acidic peptides to see if other neutral losses could potentially preclude efficient backbone fragmentation. We found that neutral loss of water did not prevent extensive fragmentation as we observed *a*, *b*, *c*, *x*, *y*, and *z*-ions from EDD of neuromedin B and C. EDD of disulfide bond-reduced vasopressin exhibited abundant neutral loss of SH_2; however, there were more backbone fragmentation events observed than in previously published work for EDD of similar single disulfide-bonded peptides.[16] Chemical derivatization was performed of peptide carboxylic acids with 4-aminonaphthalene sulfonic acid (ANSA), which contains an amine to facilitate condensation between the carboxylic acid and the amine as well as a sulfonic acid ($R\text{-}SO_3^-$) to replace the negative charge lost by the carboxylate following derivatization. The addition of one and two ANSA groups to desulfonated caerulein (which contains two carboxylic acids) did significantly reduce and eliminate CO_2 loss for the first and second ANSA additions, respectively; however, backbone cleavages were also reduced. Acetylation blocks free amines, resulting in different gas-phase structures that produced *a*, *b*, *c*, *x*, *y*, and *z*-ions. Fragmentation efficiency was improved for all precursors analyzed (with the exception of neurokinin B), but CO_2 neutral loss was not reduced. Anion adduction of chloride or bromide to acidic peptides appears to be the most promising for reducing CO_2 loss while maintaining backbone fragmentation compared to the aforementioned methods. In most cases, EDD of singly-deprotonated, singly chloride-adducted precursor ions resulted in improved sequence coverage but with

no chloride-adducted product ions observed. On the other hand, EDD of doubly bromide-adducted precursor ions did not improve fragmentation efficiency and also lead to more CO_2 neutral loss than EDD of the chloride-adducted species with the exception of chloride-adducted angiotensin I. Surprisingly, this particular precursor ion exhibited abundant CO_2 loss yet provided more extensive fragmentation than EDD of both the non-adducted and the bromide-adducted precursor ions.

Along these same lines, other anions such as nitrate (NO_3^-), dihydrogen phosphate ($H_2PO_4^-$), and fluoride (F^-) should be evaluated as potential candidates for anion adduction. The gas-phase basicities (GPBs) of these anions are 1330, 1350, 1530 kJ/mol, respectively, which are near the suggested value for a carboxylic acid (1430 kJ/mol).[17] As we have shown, the anion with the closest match to the GPB of the carboxylic acid to which the anion will presumably bind produces the best fragmentation results for a given peptide. With this in mind, we believe that dihydrogen phosphate or fluoride would provide the best GPB match to carboxylic acids; however, it is possible that fluoride is not a reasonable candidate due to its weak acid character as well as its tendency to be highly solvated in the liquid phase.

An additional avenue for preventing CO_2 loss would be to synthetically modify the carboxylic acid residues with O-allyl or O-benzyl groups. This permanent modification would force deprotonation at a backbone amide or other acidic site on the peptide, rendering CO_2 loss improbable and perhaps enhancing backbone fragmentation, assuming that deprotonation occurs on the peptide backbone. We have been pursuing this idea recently with limited success in the first round of analysis, but we anticipate that this project can be finished at a later date.

5.2 References

1. H. K. Kweon, K. Hakansson, Selective zirconium dioxide-based enrichment of phosphorylated peptides for mass spectrometric analysis. *Anal. Chem.* **2006**, *78*, 1743-1749.
2. H. K. Kweon, K. Hakansson, Metal oxide-based enrichment combined with gas-phase ion-electron reactions for improved mass spectrometric characterization of protein phosphorylation. *J. Proteome Res.* **2008**, *7*, 749-755.
3. H. Dobson, A. J. McQuillan, In situ infrared spectroscopic analysis of the adsorption of aliphatic carboxylic acids to TiO_2, ZrO_2, Al_2O_3, Ta_2O_5 from aqueous solutions. *Spectrochim. Acta A* **1999**, *55*, 1395-1405.
4. K. D. Dobson, A. J. McQuillan, In situ infrared spectroscopic analysis of the adsorption of aromatic carboxylic acids to TiO_2, ZrO_2, Al_2O_3, and Ta_2O_5 from aqueous solutions. *Spectrochim. Acta A* **2000**, *56*, 557-565.
5. M. W. H. Pinkse, P. M. Uitto, M. J. Hilhorst, B. Ooms, A. J. R. Heck, Selective isolation at the femtomole level of phosphopeptides from proteolytic digests using 2D-nano LC-ESI-MS/MS and titanium oxide precolumns. *Anal. Chem.* **2004**, *76*, 3935-3943.
6. M. W. H. Pinkse, S. Mohammed, J. W. Gouw, B. van Breukelen, H. R. Vos, A. J. R. Heck, Highly robust, automated, and sensitive online TiO_2-based phosphoproteomics applied to study endogenous phosphorylation in *Drosophila melanogaster*. *J Proteome Res* **2008**, *7*, 687-697.
7. J. F. Rehfeld, Accurate measurement of cholecystokinin in plasma. *Clin. Chem.* **1998**, *44*, 991-1001.
8. S. A. Young, S. Julka, G. Bartley, J. Gilbert, B. Wendelburg, S.-C. Hung, W. H. K. Anderson, W. Yokoyama, Quantification of the sulfated cholecystokinin CCK-8 in hamster plasma using immunoprecipitation liquid chromatography-mass spectrometry/mass spectrometry. *Anal. Chem.* **2009**, *81*, 9120-9128.
9. S. Young, S. Julka, G. Bartley, J. Gilbert, B. Wendelburg, S.-C. Hung, K. Anderson, W. Yokoyama, in *58th ASMS Conference on Mass Spectrometry and Allied Topics*. American Society for Mass Spectrometry: Salt Lake City, Utah, **2010**.
10. J. F. Rehfeld, W. W. van Solinge, The tumor biology of gastrin and cholecystokinin. *Adv. Canc. Res.* **1994**, *63*, 295-347.
11. E. Rozengurt, J. H. Walsh, Gastrin, CCK, signaling, and cancer. *Ann. Rev. Physiol.* **2001**, *63*, 49-76.
12. G. L. Matters, C. McGovern, J. F. Harms, K. Markovic, K. Anson, C. Jayakumar, M. Martenis, C. Awad, J. P. Smith, Role of endogenous cholecystokinin on growth of human pancreatic cancer. *Int. J. Oncol.* **2011**, *38*, 593-601.
13. Y. Kanan, A. Hoffhines, A. Rauhauser, A. Murray, M. R. Al-Ubaidi, Protein tyrosine-*O*-sulfation in the retina. *Exp. Eye Res.* **2009**, *89*, 559-567.
14. D. M. Sherry, A. R. Murray, Y. Kanan, K. L. Arbogast, R. A. Hamilton, S. J. Fliesler, M. E. Burns, K. L. Moore, M. R. Al-Ubaidi, Lack of protein-tyrosine sulfation disrupts photoreceptor outer segment morphogenesis, retinal function and retinal anatomy. *Eur. J. Neurosci.* **2010**, *32*, 1461-1472.

15. K. F. Medzihradszky, Z. Darula, E. Perlson, M. Fainzilber, R. J. Chalkley, H. Ball, D. Greenbaum, M. Bogyo, D. R. Tyson, R. A. Bradshaw, A. L. Burlingame, O-sulfonation of serine and threonine: mass spectrometric detection and characterization of a new posttranslational modification in diverse proteins throughout the eukaryotes. *Mol. Cell. Proteomics* **2004**, *3*, 429-440.
16. A. Kalli, K. Håkansson, Preferential cleavage of S-S and C-S bonds in electron detachment dissociation and infrared multiphoton dissociation of disulfide-linked peptide anions. *Int. J. Mass Spectrom.* **2007**, *263*, 71-81.
17. X. Liu, R. B. Cole, A new model for multiply charged adduct formation between peptides and anions in electrospray mass spectrometry. *J. Am. Soc. Mass Spectrom.* **2011**, *22*, 2125-2136.